Republic of Iraq
Ministry of Higher Education and Scientific Research
University of Kerbala
College of Engineering
Civil Engineering Department

Evaluating Performance of Portable Dynamic Cone Penetrometer in Characterizing Subgrade Reaction Modulus of Sandy Soil

A Thesis

Submitted to the College of Engineering of the University of Kerbala in Partial Fulfillment of the Requirements for the Degree of Master of Science in Civil Engineering

By
Laith Ali Salem

(B.Sc. in Civil Eng./University of Kerbala 2017)

Supervised by

Assistant Professor Dr. Alaa M Shaban

Assistant Professor Dr. Raid R.A. Almuhanna

2022 A.D. 1443 H.D.

بِسْمِ اللهِ الرَّحْمَنِ الرَّحِيم

إِنَّ الْأَبْرَارَ لَفِي نَعِيمٍ ﴿22﴾ عَلَى الْأَرَائِكِ يَنظُرُونَ ﴿23﴾

تَعْرِفُ فِي وُجُوهِهِمْ نَضْرَةَ النَّعِيمِ ﴿24﴾ يُسْقَوْنَ مِن رَّحِيقٍ

مَّخْتُومٍ ﴿25﴾ خِتَامُهُ مِسْكٌ وَفِي ذَلِكَ فَلْيَتَنَافَسِ الْمُتَنَافِسُونَ

﴿26﴾

صَدَقَ اللهُ العَلِيُّ العَظيم

﴿سورة المطففين، الآيات 22 - 26﴾

Abstract

The rigid pavement is a system consists of different layers that are capable to resist traffic loading. The traffic loading is transmitted through the pavement layers then finally reaches to the subgrade that works as supporting platform for the pavement. The subgrade reaction modulus (ks), which characterizes the reaction of soil layers when subjected to loads, has been calculated by using the plate load test (PLT). The PLT requires a specialized engineering team, high cost and time to conduct the test. This study presents an experimental and theoretical work to predict the subgrade reaction modulus of sand soils through developing simple and reliable statistical models based on dynamic measurements obtained from performing the in-place dynamic cone penetrometer test.

To achieve the aim of this work, three testing techniques were carried out including: dynamic cone penetrometer (DCP), plate load test (PLT) and sand replacement test (SRM). These tests were implemented to assess geotechnical engineering characteristics of subgrade sand soils collected from three roadway projects located at Karbala, Iraq. To evaluate the effect of compaction process on subgrades' performance, three compaction levels were considered in preparing laboratory testing model using three number of compactor passes (NOP).

Soil parameters obtained from the DCP were California bearing ratio (CBR), penetration index (DCPI) and bearing capacity (q), while those determined from performing the PLT test include: subgrade reaction modulus, maximum settlement, and Young's elastic modulus. Finally, the SRM were carried out to assess: moisture content, dry density, and degree of compaction.

The results of experimental work showed that the highest value of degree of compaction is (98.85%) for (18 NOP) and the lowest value is (87.43%) in for (10

NOP), the values of ks ranged from 135 to 230 kPa/mm, DCPI value varied from 14.5 to 26 mm/blow, CBR ranged from 8 to 13.5%, q ranged from 105.45 to 149.42 kPa. These results were statistically analyzed and related with each other to find the best fit regression model to predict ks.

The statistical models are classified into three groups:1st group: models based on DCP Measurements, 2nd group: models based on basic soil properties, and 3rd group: models based on DCP and basic soil properties. The statistical analysis results exhibited that the ks can be predicted based on DCP measurements and physical properties measurements (DC, C_c, C_u) with significant R-squared equals to 88%. The finding of statistical analysis proved that DCP devices can be used as a non-destructive tool for field assessing the subgrade reaction modulus quickly and accurately.

Certification

We certify that this thesis titled "**Evaluating Performance of Portable Dynamic Cone Penetrometer in Characterizing Subgrade Reaction Modulus of Sandy Soil**" which is being submitted by "**Laith Ali Salem Abbas,**" was prepared under our supervision at the University of Kerbala in partial fulfillment of the requirements for the degree of Master of Science in Civil Engineering "**Infrastructure Engineering**"

Signature:

Assistant Prof. Dr. Alaa M Shaban

Date: 23 / 6 / 2022

Signature:

Assistant. Prof. Dr. Raid R.A. Almuhanna

Date: 23 / 6 / 2022

Linguistic Certification

I hereby certify that this thesis entitled "**Evaluating Performance of Portable Dynamic Cone Penetrometer in Characterizing Subgrade Reaction Modulus of Sandy Soil**" has been proofread and edited under my linguistic supervision, and was amended to meet proper English language.

Signature: 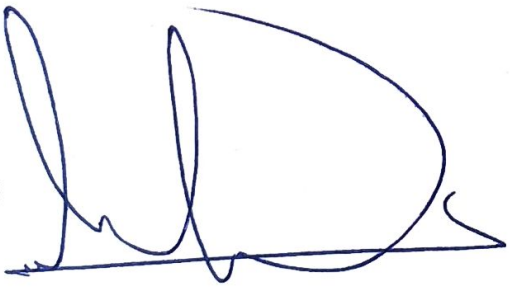

Linguistic Supervisor: Dr. Mahdi Abbas Mahdi Al-Naddaf.

Date: 23 / 6 / 2022

EXAMININATION COMMITTEE CERTIFICATION

We certify that this thesis entitled "**Evaluating Performance of Portable Dynamic Cone Penetrometer in Characterizing Subgrade Reaction Modulus of Sandy Soil**" and as an examining committee, we examined Engineer "**Laith Ali Salem**" in its content and in what is connected with it, and that in our opinion it is adequate as a thesis for degree of Master of Science in Civil Engineering (Infrastructure Engineering).

Supervisor

Signature:

Name: Assist. Prof. Dr. Alaa M Shaban

Date: 23 / 6 / 2022

Supervisor

Signature:

Name: Assist. Prof. Dr. Raid R.A. Almuhanna

Date: 23 / 6 / 2022

Member

Signature:

Name: Assist. Prof. Dr. Ayman Jamil Kazem

Date: 24 / 6 / 2022

Member

Signature:

Name: Assist. Prof. Dr. Fatima Fahim Hussein

Date: 25 / 6 / 2022

Chairman

Signature: J. Al-Obaedi

Name: Prof. Dr. Jala Taqi Shaker

Date: 25 / 6 / 2022

Signature:

Name: Assist. Prof. Dr. Sajjad Amir Hamzah

Head of Department of Civil Engineering

Date: 25 / 6 / 2022

Signature: L. Sh. Ras

Name: Prof. Dr. Laith Sh. Rasheed

Dean of the Engineering College

Date: 4 / 7 / 2022

Dedication

To the designer of the human civilization that is established on the unity of almighty **Allah** (SWT). To the redeemer of human volition and thought. To the seal of the prophets and the master of all beings, the **Holy Prophet Muhammad** (Peace be upon him and his Household).

I dedicate this work to **my kind family**, **my dear father**, **my beloved mother**, and **sisters** for their love, care, and support during this stage. Thank you, all my beloved family, for your huge support; otherwise, work would not have taken place; thanks, with all my heart.

To **my supervisors** for their valuable advice, support and patience throughout this period. Without their enormous knowledge, I would not have made this possible.

Laith Ali Salem

2022

Acknowledgments

In the name of ALLAH (SWT), the most compassionate and merciful, I have to thank and praise our God, who gave me health and the necessary strength to carry out the present research. I am extremely grateful to my supervisors "**Assistant Professor Dr. Alaa M Shaban** and **Assistant Prof. Dr. Raid R.A. Almuhanna"** for their help, encouragement, support, and patience throughout this period. Without their enormous knowledge, I would not have made this possible and always made the time and effort to respond to my queries. Appreciations also to Eng. Sinaa and Eng. Mannar, the staff of highway materials and soil materials laboratories in the College of Engineering at University of Kerbala.

I would like to thank my closest friends who helps me during the experimental works, especially "**Eng.AlhussainFattehalla",** who supported me and help me throughout the project's work, "**Eng. Sajad Hameed"** to their help and support.

I always will be grateful to **Al-Quds land company** represented by "**Eng. Hameed Majid"** and "**Eng. Ahmed Shaker"** for the facilities and support they have given me during the work.

Table of Contents

List of Figures

List of Tables

List of abbreviations

AASHTO	American Association of State Highway and Transportation Officials
ANOVA	Analysis of variance
ASTM	American Society for Testing and Materials
CBR	California Bearing Ratio
Cc	Coefficient of Curvature.
CF	The ratio between subgrade reaction modulus before and after correction
Cu	Coefficient of Uniformity
Dc	Degree of Compaction
DCP	Dynamic Cone Penetration Test
DCPI	Dynamic cone penetration index
Dr	Relative density
Es	Young's modulus of soil
FWD	Falling weight deflectometer
he	Equivalent thickness
ks	Subgrade Reaction Modulus
LL	Liquid Limit
LWD	Light weight deflectometer
NOP	Number of passes
OMC	Optimum moisture content
P	Contact pressure
ϕ'	Soil friction angle
p_max	loading plate's maximum settlement under static load
PI	Plasticity index
PL	Plastic limit
PLT	Plate load test
s_max	loading plate's maximum settlement under static load
SPSS	Statistical Package for Social Science
SRM	Sand replacement
SSE	Squares residual or error sum
SSR	Sum of Squares Regression
SST	Total of sum squares
UCS	Unconfined compressive strength
USCS	Unified Soil Classification
V	Poison's ratio

Chapter one

Introduction

1.1 Background

The primary objective of the subgrade is to be able to transfer loads from the top paving layers without failures. The subgrade is arranged in the form of earth layers that are made up of particles of various shapes and sizes that achieves stability through the process of compaction. The performance of rigid pavement is determined by a number of parameters that can characterize the strength of the soil, such as subgrade reaction modulus (ks), degree of compaction , bearing resistance (CBR) and other soil characteristics (Eka et al., 2012).

The subgrade reaction modulus (ks), which characterizes the reaction of soil layers when subjected to loads, is often utilized in the structural design of foundations and pavements. The subgrade reaction modulus is the relation between soil pressure and deflection, which is typically determined by using a plate load test (Atarigiya et al., 2019). Subgrade reaction modulus calculated by using plate load test describes the relationship between loads – displacements, This test requires a specialized engineering team, as well as its process is expensive and laborious(Ziaie and Alibolandi, 2012) .

In recent years, researchers such as (Konard and Lachance, 2000)**,**(Chukka and Chakravarthi, 2012) **,**(Nguyen and Mohajerani, 2015) have preferred to design the pavement systems based on equipment that perform non-destructive testing measurements by applying dynamic loads that assist in determining the engineering characteristics of the soil. One of the equipment used for this purpose is the dynamic cone penetrometer (DCP).

1.2 Research Problem

A set of soil engineering properties are required to perform analysis or structural design of pavement systems. One of these engineering properties is the subgrade reaction modulus (ks). ks is defined as the stress per unit deformation of the soil. This parameter is determined using the plate load test according to (AASHTO T 222, 2007) . There are various restriction and requirements related with using the PLT test in field. The test's limitations can prevent ideal performance of the test that is directly affected in the accuracy of the (ks) value. These difficulties can be summarized in four basic matters:

1. The PLT is checked on specific parts of the road and this does not give a clear indication of its value for all parts of the road. This leads to a reduction in the testing frequency of conducting the examination on the parts of the road.
2. Because of the large diameter size of the plate used for this examination, it is difficult to carry it out in small places.
3. In the load settlement curve generated from the test, the failure load is typically not clearly defined, thus personal interpretation of an engineer might not precise enough.
4. This test requires a specialized engineering team, in addition to that, it requires a high cost and time.

1.3 Research Aim and Objectives

This study aims to predict the subgrade reaction modulus of sand soils through developing simple and reliable statistical models based on dynamic measurements obtained from performing in-place dynamic cone penetrometer (DCP).

To achieve the research aim, a set of objectives have been conducted as follows:

1- Collecting subgrade soils from three different roadway project located in Kerbela.
2- Evaluating collected subgrade soil and identifying their engineering characteristics.
3- Utilizing dynamic cone penetrometer and plate load test to determine subgrade reaction modulus and strength properties by obtaining DCP dynamic measurements such as: dynamic cone penetration index, California bearing resistance and bearing capacity.
4- Correlating dynamic measurements obtained from the DCP test with the subgrade reaction modulus obtained from the PLT test.

1.4 Scope of Work

1- Examine subgrade sand soils (A-3) for different locations at an optimum water content and different compaction level to assess the modulus of subgrade reaction.
2- The primary physical and chemical characteristics of selected subgrade soils were assessed, as well as laboratory testing procedures.
3- The test procedures were carried out in accordance with specified requirements, and the findings of this research were evaluated using a statistical software.
4- All experiments were carried out in the labs of the University of Kerbala. Testing devices, such as the loading frame has been locally manufactured which consists of steel box and data collection system. This produced equipment was recognized as the first equipment created by the University of Kerbala to supply a same condition for sites experiments.

1.5 Thesis Layout

The research study is presented in the form of six chapters arranged as follows:

1. **Chapter One**: presents a summarized overview of the significance of subgrade and the definition of subgrade reaction modulus, and also describes the aim and objectives of the research, its research problem, and a simple explanation of the work structure.
2. **Chapter Two:** gives a summary of the subgrade reaction modulus as well as hypotheses to explain previous studies on the plate load and dynamic cone penetrometer. It provides a brief overview for previous correlation research comparing PLT to other tests
3. **Chapter Three:** describes the research methodology, soil types and locations for this research, explain chemical and physical test for the subgrade, testing equipment, and the laboratory tests used to examine the selected subgrade.
4. **Chapter Four:** displays the results of laboratory tests, which include three testing methods, PLT test, DCP and SRM tests for selected types of soil.
5. **Chapter Five:** presents the statistical analysis of the data, as well as a theoretical models built with statistical software
6. **Chapter Six:** summarizes the theoretically and experimentally research findings, and recommendations for further research.

Chapter Two

Literature Review

2.1 Introduction

The rigid pavement system consists of different layers that are capable to resist traffic loading. The traffic loading is transmitted through the pavement layers then finally reaches to the subgrade that works as supporting platform for the pavement as shown in Figure (1).

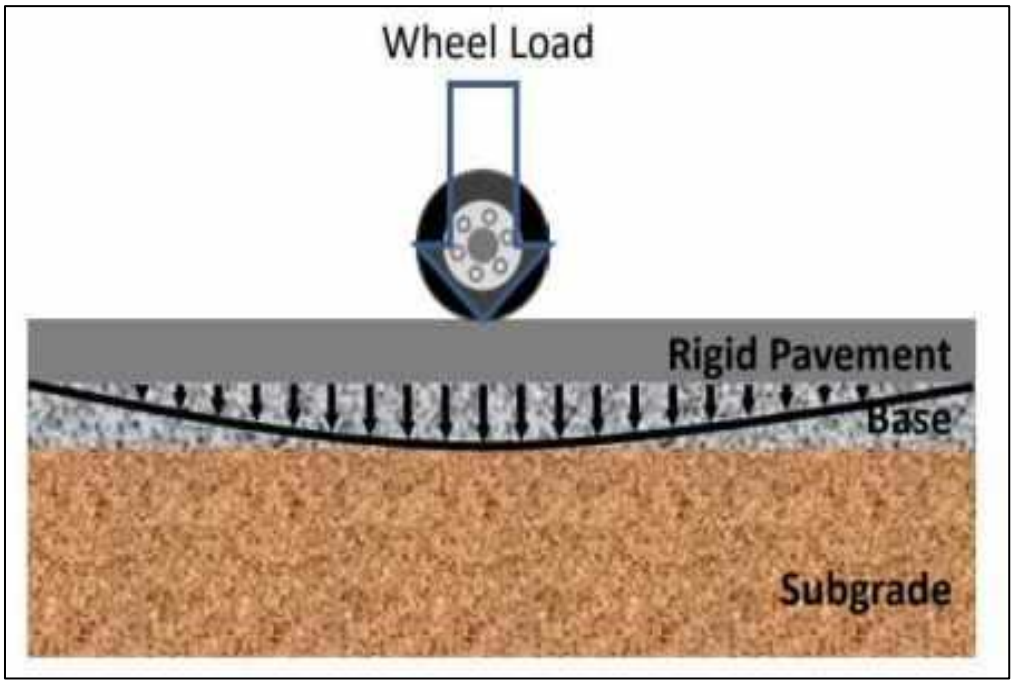

Figure (2.1) Loading transmitted in a pavement system(Islam et al., 2020)

Characterizing subgrade soils' behavior under wheel loadings is necessary before the pavement design process. Rational and empirical pavement design procedures are depending on many factors one of which that represents subgrade soil properties under various loading conditions. The design load capacity of a subgrade to resist deformation under stresses is being used to calculate strength or stiffness. Overall, a more resistant subgrade could be capable of carrying more load before reaching a critical value of permeant deformation (Ziaie and Alibolandi, 2012).

The rigid pavement design is based on a strength criterion known as a subgrade reaction modulus. This parameter is defined as an applied pressure per unit of displacement. The value of the subgrade reaction modulus is based on plate load test or statistical correlation with soil characteristics (Diner, 2011). This chapter presents a background information about strength and stiffness characteristic of the subgrade then summarizes theoretical and numerical models for determining various subgrade strength proprieties.

2.2 Characterization of Subgrade Soil in Pavement Engineering

The excellent pavement performance depends on strength and stiffness of subgrade. The strength is the stresses needed to rupture the material and the stiffness is the ability for returning material to original size and shape after releasing stresses. The characterization of subgrade represents by, its ability to resist repeated traffic loading, which is called subgrade resilient modulus. The subgrade resilient modulus (Mr) is the ratio between the repeated axial dynamic load to the recovery axial strain after large number of load cycles under triaxial test (Khasawneh, 2019).

$$Mr = \frac{\sigma_d}{\varepsilon a} \tag{2.1}$$

where $\sigma_d = \sigma_1 - \sigma_3$ (where σ_1)reflects the amount axial stress, also known as the major principal stress, (σ_3) represents radial stress, also known as the minor principal stress) and εa represents the elastic strain.

The value of (Mr) could be calculated backwards from deflection measurements or estimated directly from laboratory testing. The primary objective of laboratory testing is to simulate field conditions such as confinement , water content, and soil type (Ghorbani et al., 2020)**.**

The characteristics and quality of unbound materials used in pavement is affected on dimension and thickness of pavement layer. A bearing resistance factor (called (California bearing ratio) provides stiffness indication for subgrade and unbound pavement layers(Islam et al., 2020). In the pavement design process, the mechanical properties of unbounded pavement materials are the parameters that must be determined in the design. Subgrades are defined based on their resistance to deformation under a variety of repeated loading status. (Ping and Sheng, 2011).

2.3 Subgrade Reaction Modulus(ks)

The most essential parameter that is used for structural analysis and design of rigid pavements is the subgrade reaction modulus(ks), which represents the relation between soil pressure and deflection. It is used to check out how much support the layers under the rigid pavement surface have

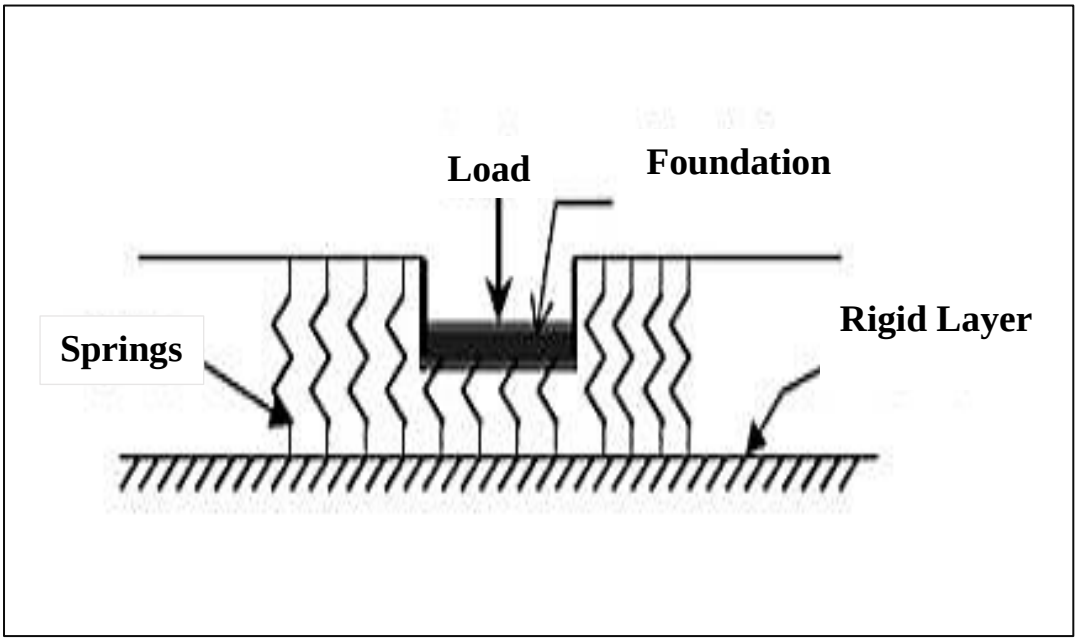

Figure(2.2) Basic concept for determining subgrade reaction modulus (Kim, 2018)

The subgrade reaction modulus is determined using plate load test (PLT) in which the reaction pressure for the soil under a rigid plate of standard diameter per unit settlement is determined(Kim and Park, 2011). Figure (2.2) shows basic concept for determining subgrade reaction modulus.

The mathematical theories have been built to explain the behavior of the lower layers to reach the most logical value for the (ks), the following subsection presents the most common models to determine ks:

2.3.1 Winkler Foundation Model

The Winkler model (1867) was described the soil medium as a series of similar, but mutually separate, closely independent systems. Springs were described as isolated, linearly elastic elements. The deformation of foundations according to this characterization, only the loaded area is affected by applied loads as shown in Figure (2.3).

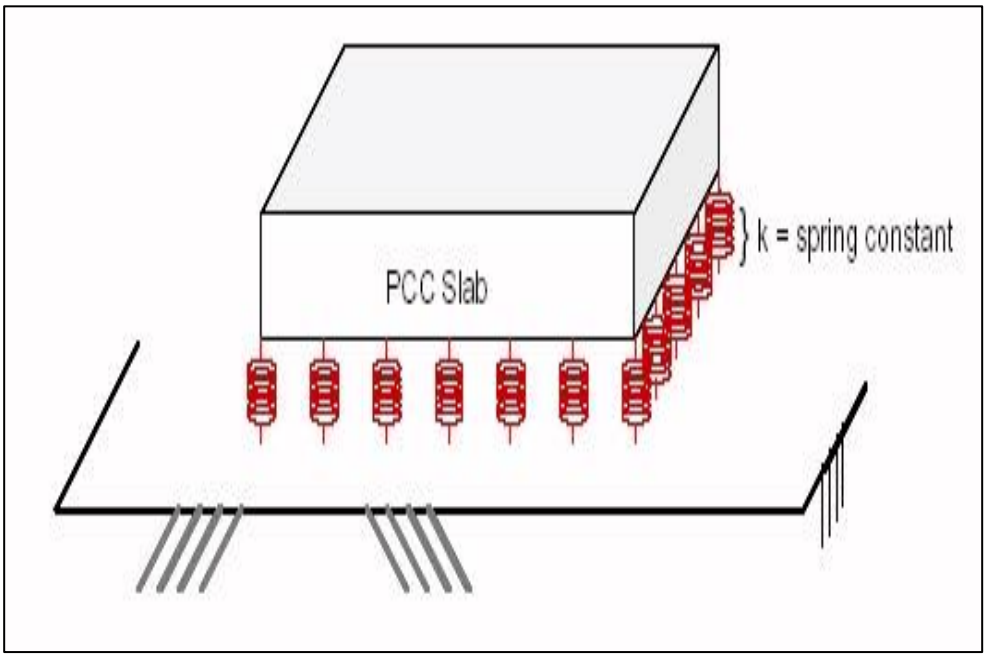

Figure (2.3) Winkler Model (Rajpurohit et al., 2014)

2.3.2 Elastic Continuum Model

Continuum elastic theory is a model to characterize the soil behavior in a three-dimensional medium, it had been assumed that soil properties were affected by two factors, namely: the elastic modulus and Poisson's ratio. Boussinesq ,1885 developed a derivation to calculate the value of subgrade reaction modulus (ks) according to Hooke's law in which it was assumed that the weight of the soil is neglected and the middle of the soil extends in all directions (Aron et al., 2012)

$$\nu = \pi pD/4Es\ (1-\nu^2) \quad (2.2)$$

$$ks = 4Es\ \pi D/(1-\nu^2) \quad (2.3)$$

Where: p: Contact pressure (kPa)

ν: Poison’s ratio.

Es: Young’s modulus of soil (MPa)

D: diameter of plate (mm).

2.4 Subgrade Reaction Modulus Test

The ultimate bearing capacity and the displacement for a soil that is resulting from an applied vertical load is the main point for evaluating the soil when designing pavements and foundations. The soil bearing capacity and displacement can be determined using the plate loading test. PLT is one of the oldest and most popular in-site tests to calculate the ability of soil to resist loading and the vertical displacement expected from the forces through time (Atarigiya et al., 2019).

The parameters normally determined from the (PLT) are: the subgrade reaction (ks), the elastic modulus (Es), and the allowable bearing pressures (qall). These parameters can be evaluated from load-deformation plots obtained from the testing data. A plot of typical PLT load-deformation curve is shown in Figure (2.4). In all soils, fills and rocks, the plate load test may be conducted. Generally, coarse-grained and composite soils as stiff to firm, fine-grained soils are acceptable.

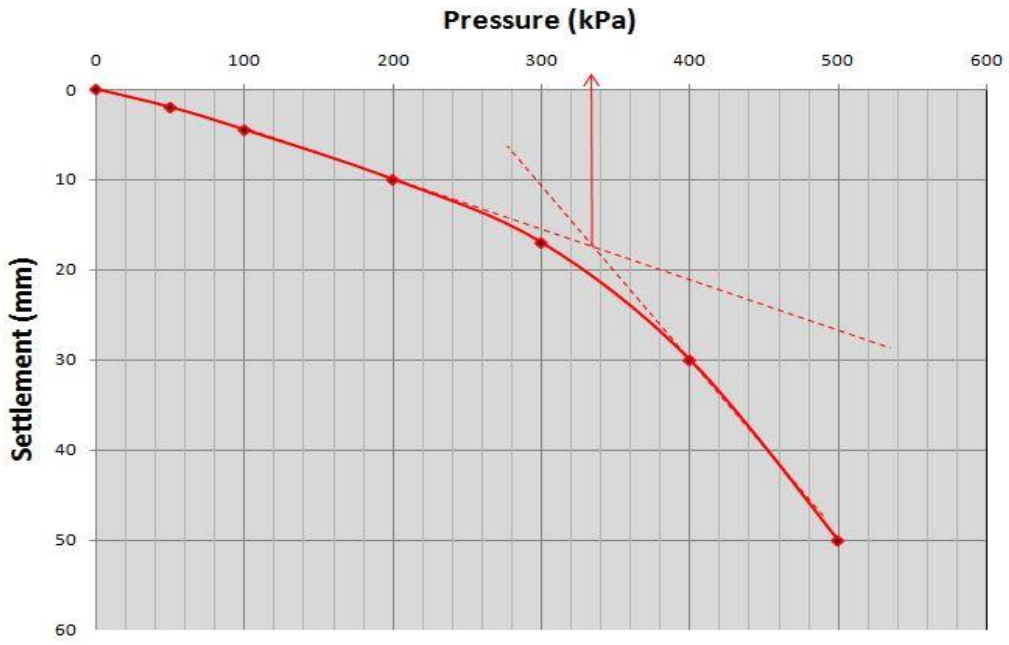

Figure (2.4) Basic calculation of plate load test(Atarigiya et al., 2019)

When perform plate load test on subgrade layers to calculate the value of subgrade reaction modulus, several factors can affect the value of subgrade reaction modulus.

These factors are discussed as follow:

1.Moisture content

The main objective of compacting granular materials is to increase the density of the material by removing the air between the aggregate particles, using mechanical energy. The degree of compaction of granular materials can thus be measured in terms of the dry unit weight or density of the material. Aggregate materials are

obtaining a higher dry density if they are compacted in a wet or moist state, when compared to a dry material. This is due to the lubrication effect of the water between the aggregate, which minimizes friction and abrasion of the material (Lee and Jeong, 2016).

The moisture content after compaction will not being in the optimum value at all position, so that the subgrade reaction modulus should be correct in a saturated condition. The following equation was recommended by the (US Army Engineer Waterways Experiment Station, 1945) and (CRD-C 655, 1995) for empirically determining the modulus of subgrade reaction at saturated:

$$ks = \frac{ku \,.\, ps}{pd} \tag{2.4}$$

Where:

ks: Modulus of subgrade reaction for the saturated soil in (kPa/mm)

ku: Modulus of soil reaction for the soil at natural moisture in (kPa/mm)

ps: The unit pressure in kPa used to determine the value of ku

pd: The unit pressure in kPa used to a saturated consolidation test

2.Size of Loading Plate

The size of loading plate effects on the zone of influence, which is a zone of subgrade soils likely to be affected by applied loading on the subgrade surface area. The plate load size is influence on stress - settlement curve shows that, there is an increasing on settlement with increasing plate load dimension (Arau´jo et al., 2017)**.** The depth of influence can estimate up to twice of the width for the bearing plate. Plate load tests of variety of shapes and sizes can be used to determine the subgrade reaction modulus (ks), as summarized in table (2.1).

Table (2.1) Common size and shape of the loading plate

Reference	Shape of the loading plate	Dimensions
Terzaghi (1955)	Square	L = 305 mm
ASTM D1195 and D 1196 (1993)	Circular	D: 305 to 762 mm
British standards code (B.S 5930) (1997)	Circular or square of equivalent area	D: 300 to 1000 mm
Peck et al. (1997)	Square	L=305 mm
Ping and Yang. (1998)	Circular	D: 705, 950 and 1050 mm
Egyptian code (2001)	Circular or square of equivalent area	D: 300, 450 and 706 mm
Reza. and Masoud (2008)	Circular or square of equivalent area	D: 300 and 1000 mm

2.5 Empirical Models for Predicting ks

In the following sub-sections, statistical relationships will be presented and discussed to determined (ks) in terms of other variables as follow:

2.5.1 ks-CBR Correlation Models

(ks-CBR) correlations for determining the subgrade reaction modulus for coarse dense soils obtained from the statistical analysis performed by the Packard (1986) and Federal Aviation Administration (2009). The results of these statistical analysis are illustrated in the following equation respectively:

$$ks = 53.438CBR^{0.5719} \quad (2.6)$$

$$ks = (1500CBR/26)^{0.7788} \quad (2.7)$$

(Tuleubekov and Brill, 2014) developed another empirical relationship to calculate the subgrade reaction modulus for sand soils, use the formula below:

$$ks = 28.6926\ CBR^{0.7788} \quad (2.7)$$

Where:

ks: subgrade reaction modulus (kPa/mm)

CBR: California Bearing Ratio (%)

These correlations estimate the subgrade reaction for a given CBR value, which help designers to design thickness of rigid pavements.

2.5.2 ks-Mr Correlation Models

Several studies have tried to find a relationship between (ks) and (Mr). These correlations are experimental research to predict the load deformation and resilient module properties of granular subgrade soils. The in-situ properties of subgrade soils were evaluated thorough field static load bearing test program, as shown in table (2.2)

Table (2.2) Correlations Between ks and Mr

Reference	Correlation Equation
UFC (2001)	$Ks = (Mr/26)^{-1.284}$
(Ping and Sheng, 2011)	$Ks = 2.25\ Mr$
Barker and Alexander (2012)	$Ks = 0.74\ Mr/E^{-0.284}$

E: Elastic modulus of subgrade (MPa)

ks: subgrade reaction modulus (MPa$/m^3$).

Mr: Resilient modulus (MPa)

2.5.3 ks-E Correlation Models

Soil elastic modulus (E) is a soil parameter and a measure of soil stiffness. In the range of elastic soil behavior, it is defined as the ratio of stress along an axis to strain along that axis. The elastic modulus is frequently used in soil settlement estimation and elastic deformation analysis(Kim and Park, 2011).

Soil elastic modulus can be estimated using laboratory or in-situ tests, or by correlating with other soil properties. Table (2.3) shows Correlation Between subgrade reaction modulus and E.

Table (2.3) Correlation between ks and E

Reference	Correlation Equation
AASHTO (1986)	$ks=E/0.492$
Ullidtz (1987)	$ks=0.54\ E/he$
Khazanovich et al (2001)	ks= 0.296 E
Setiadji and Fwa (2008)	ks=0.259 E−6.512

ks: Modulus of subgrade reaction (MPa$/m^3$).

E: Elastic modulus of subgrade (MPa).

he: Equivalent thickness (mm).

2.6 Dynamic Cone Penetrometer (DCP)

2.6.1: Historical Development of DCP

the dynamic cone penetrometer (DCP) is a portable, rapid, in situ test used to evaluate the strength pavement layers. The DCP measures soil penetration resistance and correlate it with California bearing capacity (CBR). The design of DCP test was penetrate soils to a depth of 1 m using a hammer with an 8 kg weight and a 20 mm

diameter and 60-degree cone. In order to force DCP test into the soil, two people are usually required (Hamid, 2015).Figure (2.5) shows the dynamic cone penetrometer parts.

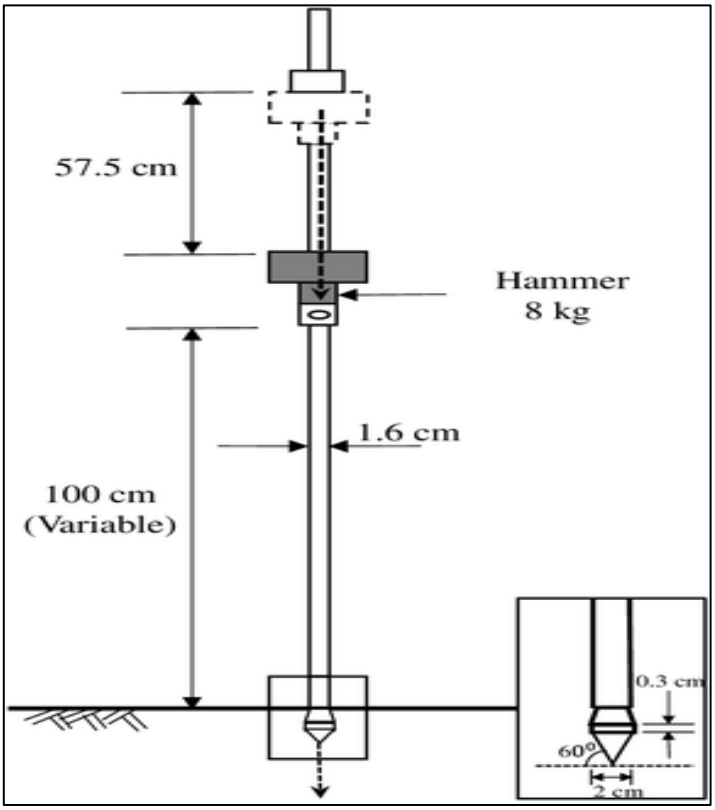

Figure (2.5) Dynamic cone penetrometer parts(ASTM D6951, 2003)

The device has gone through several development stages since it has been used to improve performance and accuracy in performing the examination. These modifications to the device can be summarized as follow:

1**. Scala, A.J. (1956):** The drop height of hammer was 508 mm, the hammer weight was 9 kg, and the cone angle was 30 degrees. Scala's penetrometer was used with an extension to a depth of 1.8 m.

2. **Sowers, G.F.; and Hedges, C.S. (1966):** introduced a DCP device with 6.8 kg hammer, falling 508 mm on the driving rod.

3. **Van Vuuren, D.J. (1969):** It was made of a 10 kg hammer sliding on a 16 mm rod dropping from 460 mm height. The cone was 20 mm in diameter

Since 1973, An 8 kg hammer dropped from a height of 575 mm with a 60-degree cone with a diameter of 20 mm was utilized in South Africa.

2.6.2: Theoretical Basis of DCP

The penetration test is an in-situ test that is performed in a borehole. The test will determine the resistance of the underlying soil to the penetration. It can also be used to calculate the unconfined compressive strength of cohesive soils(Nguyen and Mohajerani, 2015).

The basic concept for dynamic cone penetrometer work can be described as a relationship between penetration(mm) and number of blows (mm/blows). This relationship presents in the value of dynamic cone penetration index (DCPI). The DCPI is a measurement of strength for the subgrade, Mathematically, it is the cumulative penetration (mm) divided by number of blows(blows).

$$DCPI = \frac{Cumulative\ penetration\ (mm)}{Number\ of\ blows(blows)} \tag{2.8}$$

Researchers and pavement agencies were tried to correlate the DCPI with CBR and other soil properties. (Kleyn,1975) was found an equation relate the DCPI with CBR as follow:

$$CBR = \left(\frac{292}{DCPI^{1.12}}\right) \tag{2.9}$$

Where: CBR = California bearing capacity (%)

DCPI = dynamic cone penetrometer index(mm/blows)

2.6.3: Factors Affecting DCP Measurements

Factors affecting the DCP test will be discussed as follow:

1. Water content

Studies were conducted to determine the effect of water content on DCP readings. The study was conducted on soils containing different percentages of water content. The results show that small changes in water content led to significant decreasing on dynamic cone penetration index (DCPI)(Kofi and Yao , 2015).

2. Alignment of DCP rods

The bottom and top rods of the DCP should be straight and the cone should be seated freely in the position on the test material. After the first setting blows any inclination in the DCP rods lead to incorrect depth reading according to number of blows. (ASTM D6951, 2003)

3. Lifting height of hammer

The hammer should be lifting to the upper of top roads and release by gravity. During the test, if the hammer doesn't raise to the standard height, the penetration energy will decrease leads to in correct readings. (ASTM D6951, 2003)

2.7 Correlations between DCP and Soils Properties

Determination of soil properties was being a challenge for geotechnical and pavement engineers. The researchers were trying to find simple alternative method that calculate these parameters. The dynamic cone penetrometer is one of non-destructive tests that its testing measurements correlate with soil properties.

The dynamic cone penetration test (DCP) was widely applied for field examination and soil layer evaluation. DCP testing may be used to characterize soil properties in different methods. The capability of the dynamic cone penetrometer (DCP) device to give a continuous record of relative soil strength with depth. The

DCP device is characterized by its low cost and ease of use, as well as its ability to give accurate findings and quick property evaluation(Chukka & Chakravarthi, 2012).The following subsections provide a summary of the DCP's soil parameter correlations and relationships.

2.7.1 DCP correlation with CBR

DCP-CBR correlations have been created for materials in the laboratory and in the field. the minimal penetration depth necessary in DCP to determine the strength of surface layers and developed links between DCP index and CBR, the depth ranging from highly flexible clay to poorly graded sand is 2.5 to 28 cm. It was also confirmed that DCPI can be used to assess the thickness and position of a weak soil layer in a pavement.(Gupta and Krawinkler, 1999) and (Truebe et al., 1995) developed the following correlations between DCPI and CBR:

$$\text{Log (CBR)} = 1.4 - 0.55 \log DCPI \quad (2.10)$$

$$\text{CBR} = 320/DCPI^{0.943} \quad (2.11)$$

where: CBR: California bearing capacity (%)

DCPI: dynamic cone penetrometer index (mm/blows)

(Shaban , 2018) developed a statistical model to predict the CBR by utilizing two in-place, portable, non-destructive devices. These devices were the modified pressure meter test and DCP. The result of this research showed that there is a strong correlation between CBR and limit pressure (PL) for the same subgrade with R^2 = 0.92 %:

$$\text{CBR} = 0.0344(\text{PL}) - 5.50 \quad (2.12)$$

Where: CBR: California bearing capacity (%)

PL= limit pressure (kPa)

Also Figure (2.6) clarifies other correlations for prediction of CBR Using (DCP)(Al-Refeai and Al-Suhaibani, 1997)

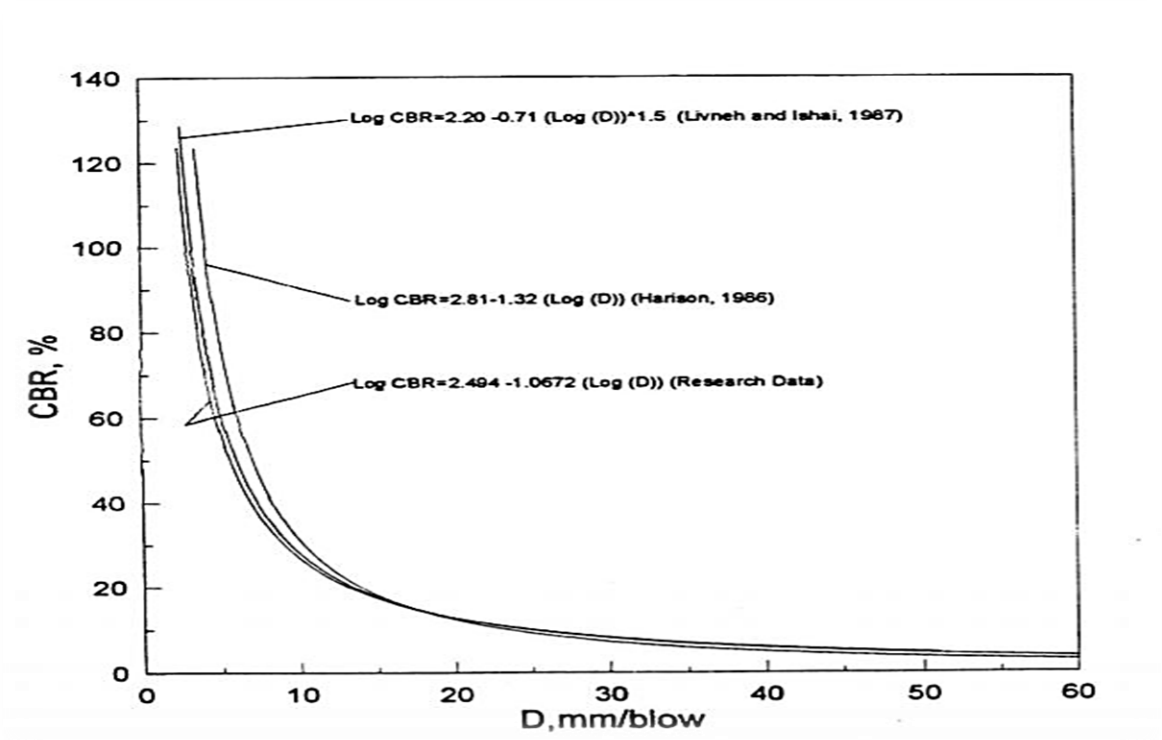

Figure (2.6) DCP correlations with CBR(Al-Refeai & Al-Suhaibani, 1997)

2.7.2 DCP correlation with shear strength

Several studies have suggested a connection between relative density and friction angle. The shear strength has a major influence on dynamic cone penetration test results, as an increase in relative density causes an increase in sand friction angle, which causes a reduction in the (DCPI).

(Ayers, 2015) developed correlations between (DCPI) and soil shear strength based on laboratory DCP and triaxial tests, applying DCPI index for granular material as a simple and easy in-situ testing technique for different confining stress.

(Konard and Lachance, 2008) established equations based on results of laboratory work to describe the link between dynamic cone penetration index, relative density and soil friction angle.

$$\phi' \text{ (deg)} = 52.16/ (DCPI^{0.13}) \quad (2.13)$$

$$\phi' \text{ (deg)} = 26.31 + 0.21(\text{Dr}) \quad (2.14)$$

where:

ϕ' (deg): Soil friction angle

DCPI: Dynamic cone penetrometer index(mm/blows)

Dr: Relative density (%)

2.7.3 DCP correlation with Mr

Several transportation agencies have applied the dynamic cone penetration test to evaluate the compacted subgrades. (Rahim and George, 2002) showed a relationship between DCPI and resilient modulus in sand and fine-grained soils. The experimental study found that in fine-grained soils, increasing the moisture content above the optimal levels significantly raised DCPI, also developed a correlation between resilient modulus by two different equations for fine-grained soils and coarse-grained receptively.

$$Mr = a_0(DCPI)^{a1}\left[\gamma_{dr}^{a2} + \left(\frac{LL}{wC}\right)^{a_3}\right] \quad (2.15)$$

$$Mr = b_0\left[\frac{DCpI}{log\ Cu}\right]^{b_1}\{\gamma d_r^{b_2} + W_{Cr}^{b_3}\} \quad (2.16)$$

Where:

Mr: Laboratory resilient modulus (MPa)

DCPI: Penetration Index

γd: Dry density (kN/m^3)

wc: Moisture content (%)

LL: Liquid limit

PI: Plasticity index

Cu: Uniformity coefficient

These equations can predict the value of MR based on a set of soil properties such as dry density, moisture content, liquid limit, plasticity index.

2.7.4 DCP correlation with ks

Based on laboratory and field studies for DCP, plate load loading tests (Abu-Farsakh et al., 2005) showed that the DCP test could be used to evaluate subgrade and pavement layers. The creation of empirical connections between DCP data and the PLT elastic modulus, resilient modulus, and the CBR, the DCP test was an effective technique for compaction control.

Figures (2.7) shows various models generated by combining PLT modulus with DCPI. The regression models generated by combining field and laboratory data are more similar to the field models than to the laboratory models. Figure (2.7) also show a comparison of the expected DCP-PLT relationships with the model presented by (Konard and Lachance, 2000)**.** The models generated from the combined data are more closely related to the correlation proposed by (Konard and Lachance, 2000) confirming that the models obtained from the combined data are more accurate.

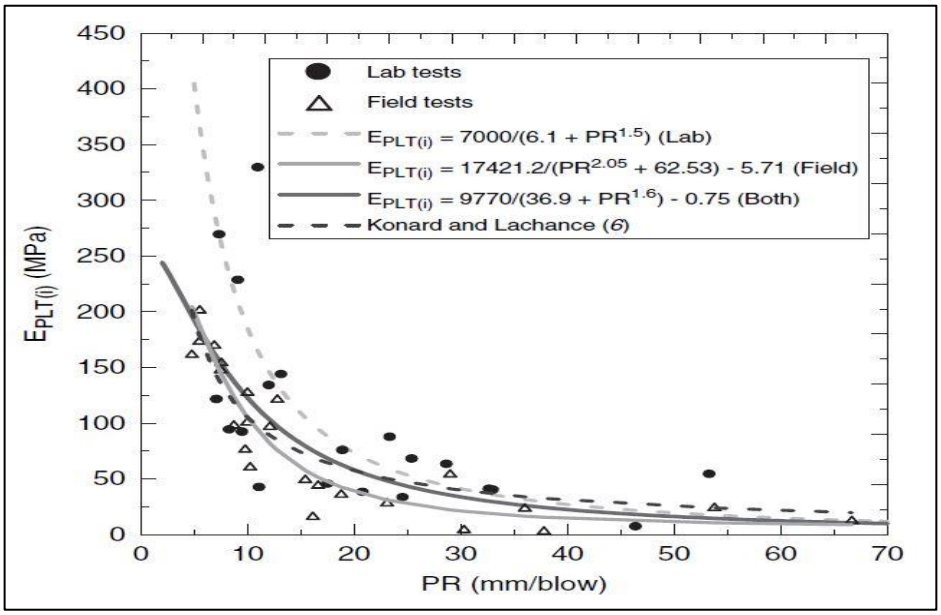

Figure (2.7) DCP correlation with plate load test

EPLT(i) = initial tangent elastic modulus, MPa
PR= Penetration Index (mm/blows)

2.8 summary

The relationship between soil pressure and deflection is represented by the (ks) which represents the strength of the layers under a rigid pavement. (PLT) can be used to determine the degree of stress in the subgrade. The performance of the pavement is determined by the strength and stiffness of the subgrade. The strength of a material is measured by the stresses required to rupture, whereas the stiffness is the ability of a material to return to its original size and shape after releasing stresses.

The dynamic cone penetration test (DCP) was widely utilized for field examination and evaluating of soil layers. DCP testing may be used to describe soil characteristics in a number of different ways. The (DCP) is characterized by its inexpensive speed and efficiency of use, as well as its ability to provide accurate findings.

Extensive studies were performed to create a relationship between ks value and various test equipment, as well as to correlate bearing resistance to soil characteristics. The relationships developed by (Konard and Lachance, 2000) between in-situ ks and DCP was proposed in order to advance current knowledge of subgrade reaction modulus values prediction using advanced techniques.

.

Chapter Three
Experimental Work

3.1General

The experimental program includes a set of laboratory tests to evaluate the subgrade reaction modulus of subgrade, which requires evaluating and identifying physical properties of selected local subgrade soils. This chapter describes the experimental work done throughout the scope of the research project. It describes the materials utilized, the test techniques employed, and the procedure of plate load test (PLT), dynamic cone penetrometer (DCP), and sand replacement method (SRM).

3.2 Selection of Subgrade

Three types of subgrade soils were collected from three sites in Karbala city: (1) Al-Tahadi, (2) Al-Fares and (3) Al-Intifada. According to the Unified Soil Classification System (USCS), soils have been classified as a poorly graded sand soil (SP), These soils have been categorized as (A-3) according to the classification system of American Association of State Highway and Transportation Officials (AASHTO). These sites were selected because they were roadway projects under development which allow the subgrade to be studied during this research. Figure (3.1) shows the location of these soils.

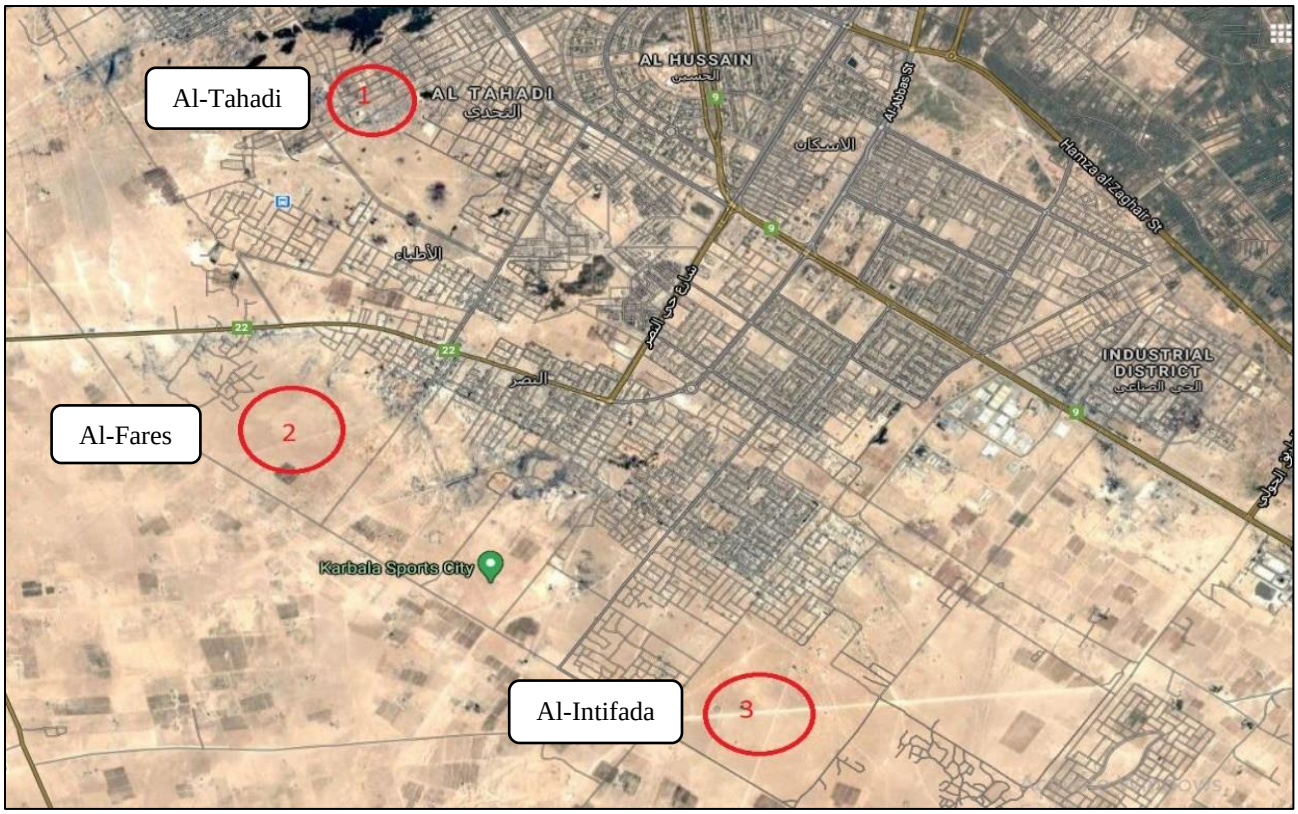

Figure (3.1) Location of Selected Sites in Karbala city

3.3 Soil Characteristics

Each soil type was exposed to a variety of laboratory tests to determine the fundamental soil characteristics, including sieve analysis, Atterberg limits, standard and modified Proctor tests, and laboratory CBR. These tests were performed in accordance with ASTM and AASHTO guidelines. Table (3.1) shows lists results of physical and chemical tests. Figures (3.2), (3.3), (3.4) and (3.5) illustrate grain-size distribution, Procter test curve and CBR test curve, respectively

Table (3.1) Results of physical and chemical tests.

Property	Site			Specification
	Al-Fares	Al-Tahadi	Al-Intifadah	
AASHTO Classification	A-3	A-3	A-3	AASHTO M 145
USCS Classification	Sand Poorly graded (SP)	Sand Poorly graded (SP)	Sand Poorly graded (SP)	ASTM D 2487
Max. Dry Density (g/cm^3)	2.105	1.83	1.975	ASTM D 1557
OMC%	8	7.5	7.8	ASTM D 1557
(D10),(D30),(D60)	0.12, 0.20, 0.40	0.19, 0.33, 0.58	0.19, 0.27, 0.54	ASTM D2487
Specific Gravity (GS)	2.6	2.61	2.6	ASTM D 854
Uniformity Coefficient (Cu)	3.21	2.81	2.97	ASTM D 2487
Curvature Coefficient (Cc)	0.84	0.71	0.95	ASTM D 2487
LL	NL	NL	NL	ASTM D 4318
PL	NP	NP	NP	ASTM D 4318
CBR Soaked	21	20	20	ASTM D 1883
CBR Unsoaked	62	68	55	ASTM D 1883
SO_3	2.72	3.8	2.91	B.S Part 3, 1990
Gypsum	8.185	6.268	5.862	B.S Part 3, 1990

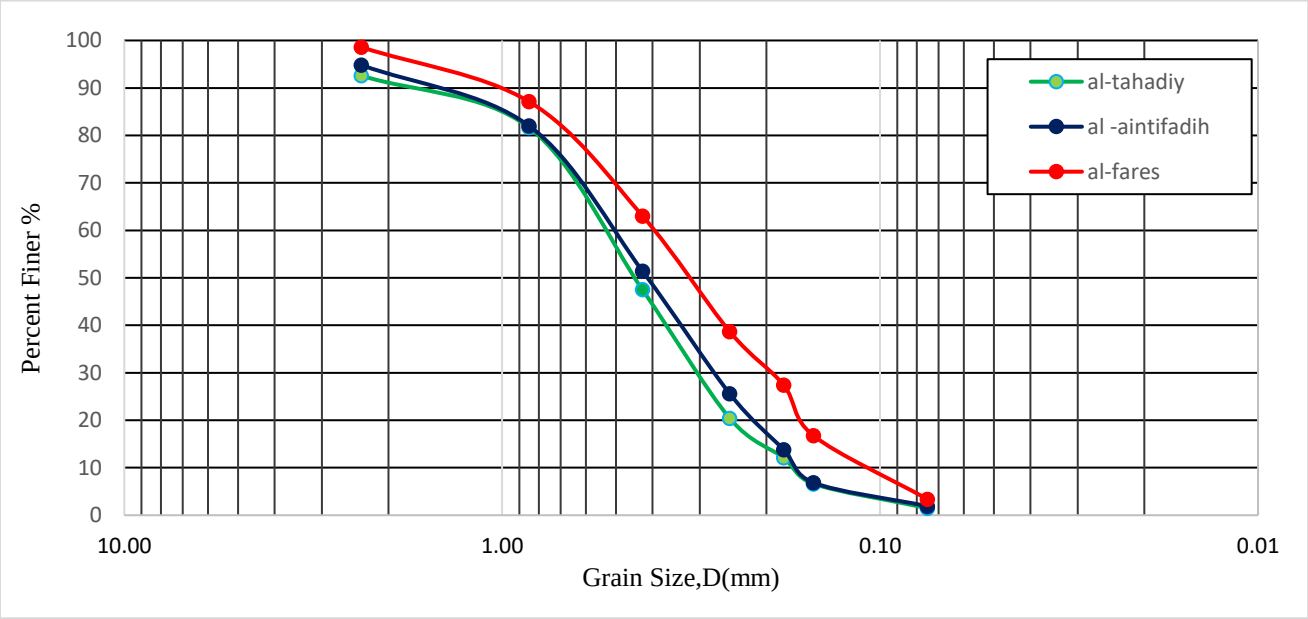

Figure (3.2) Distribution of practical size of Subgrades

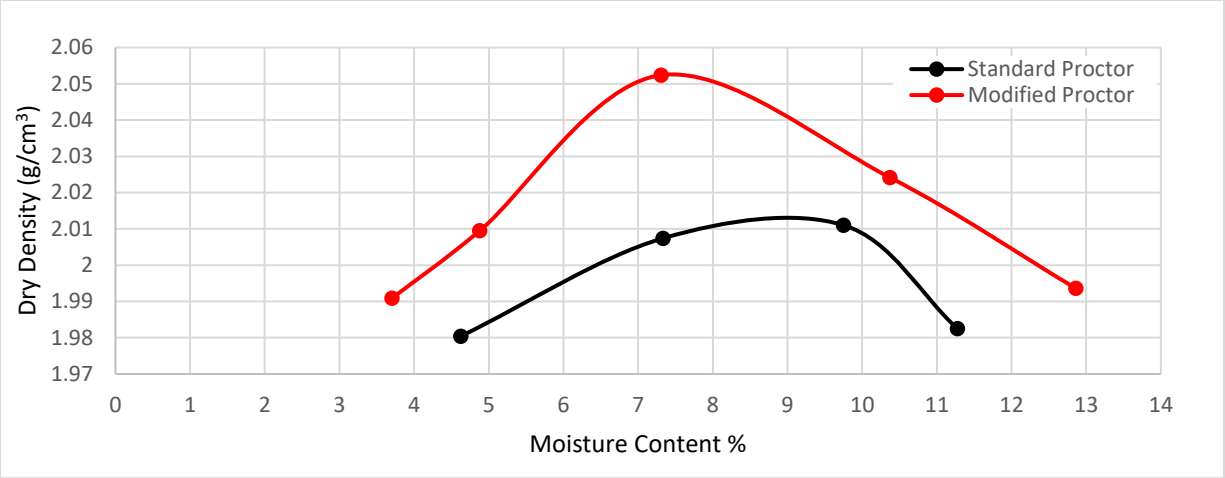

(a)

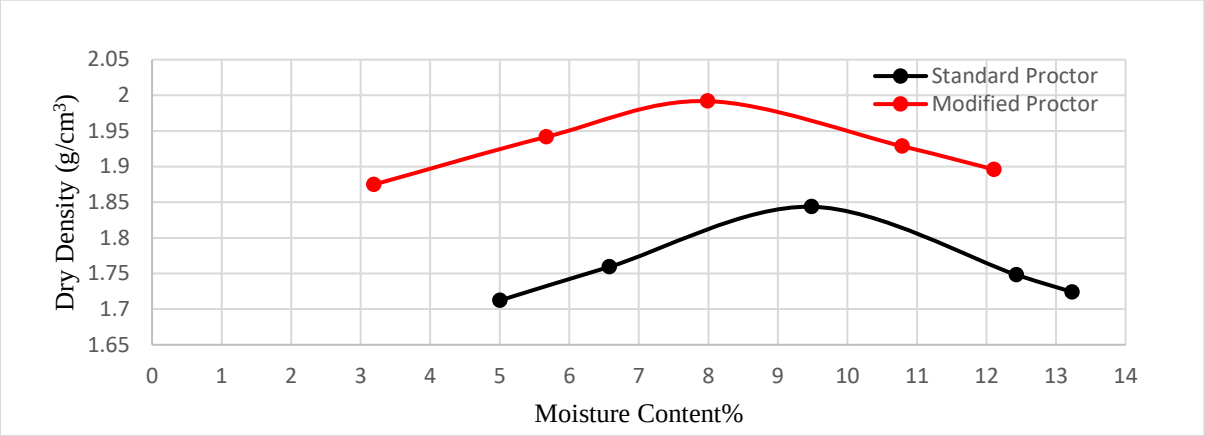

(b)

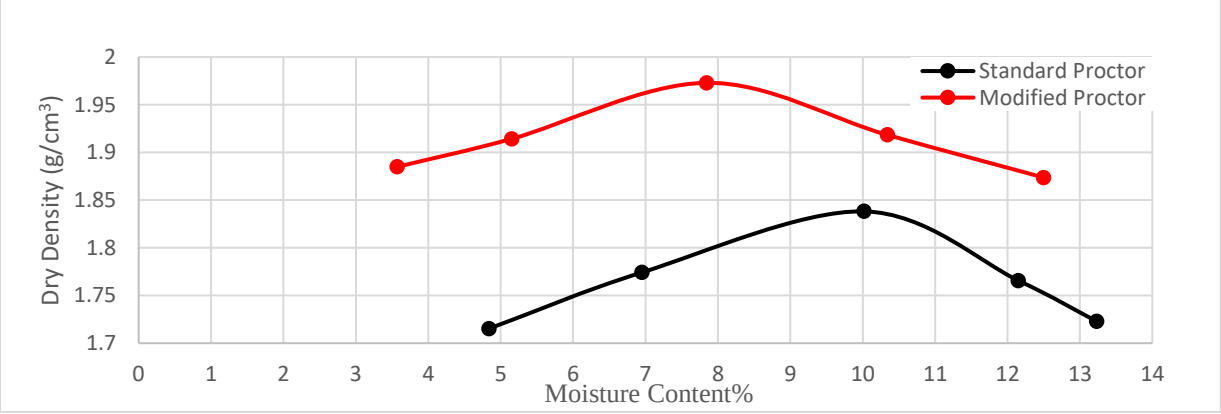

(c)

Figure (3.3) Curves of Proctor test (a) Al-Tahadi, (b) Al-Fares and (C) Al-Intifada

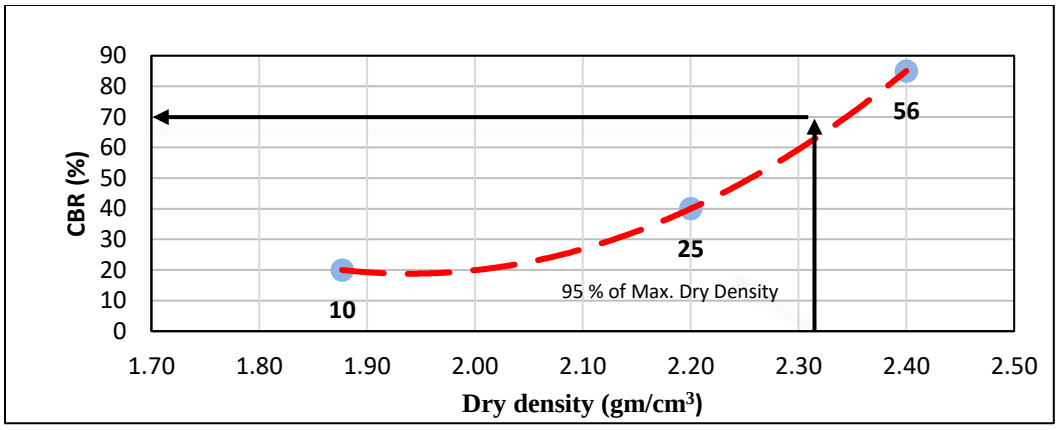

(a) CBR Unsoaked for Al-Tahadi

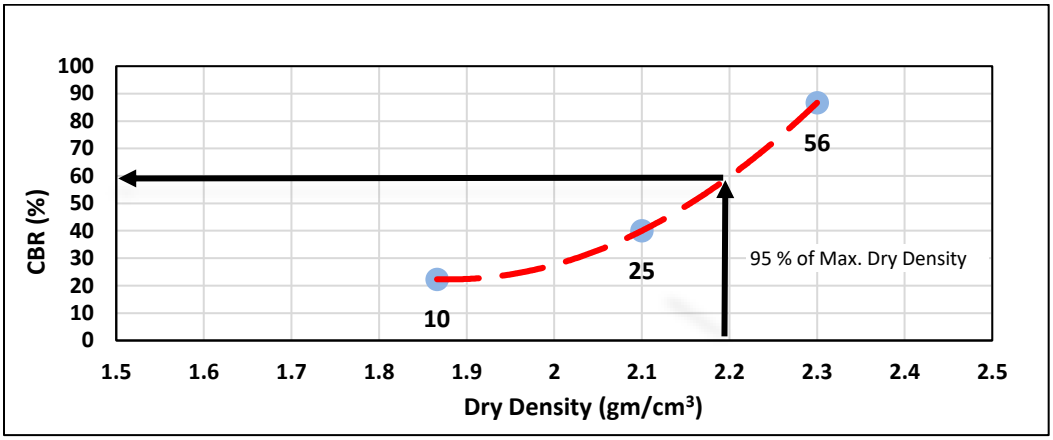

(b) CBR Unsoaked for Al- Al-Fares

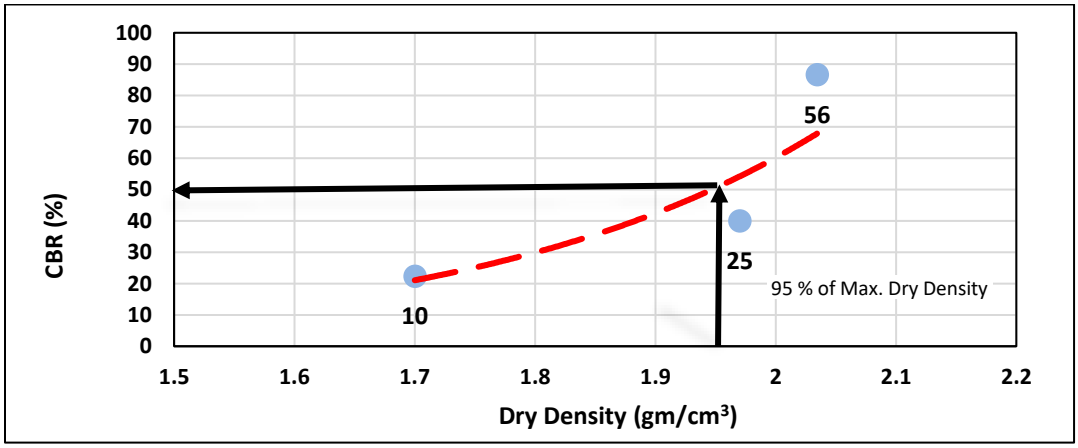

(e) CBR Unsoaked for Al-Intifada

Figure (3.4) Unsoaked CBR Test (a) Al-Tahadi , (b) Al-Fares and (c) Al-Intifada

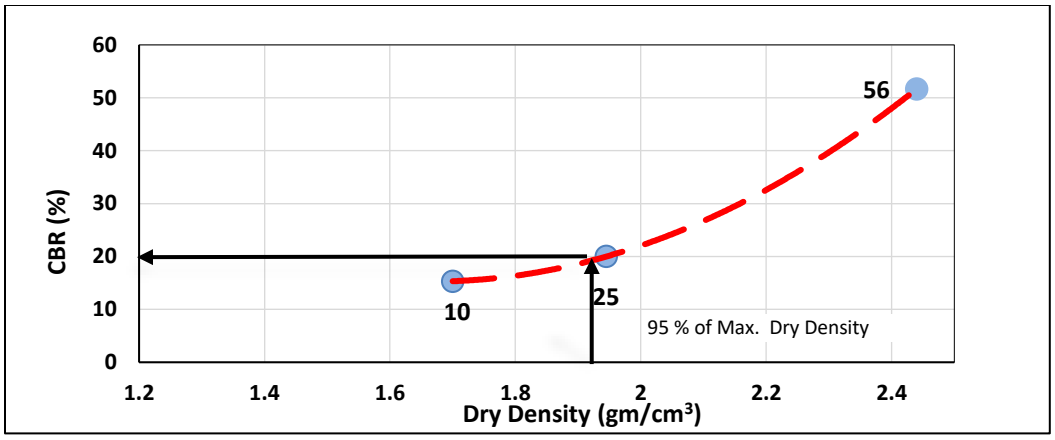

(a) CBR Soaked for Al-Tahadi

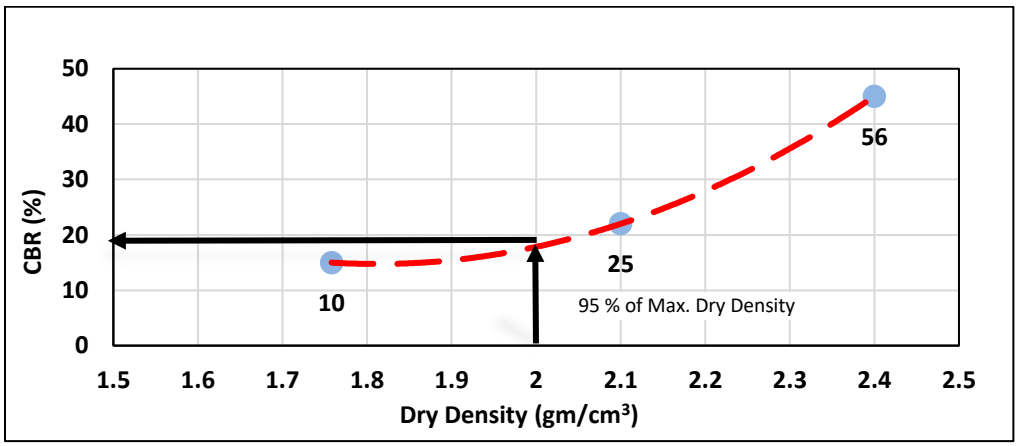

(b) CBR Soaked for Al-Fares

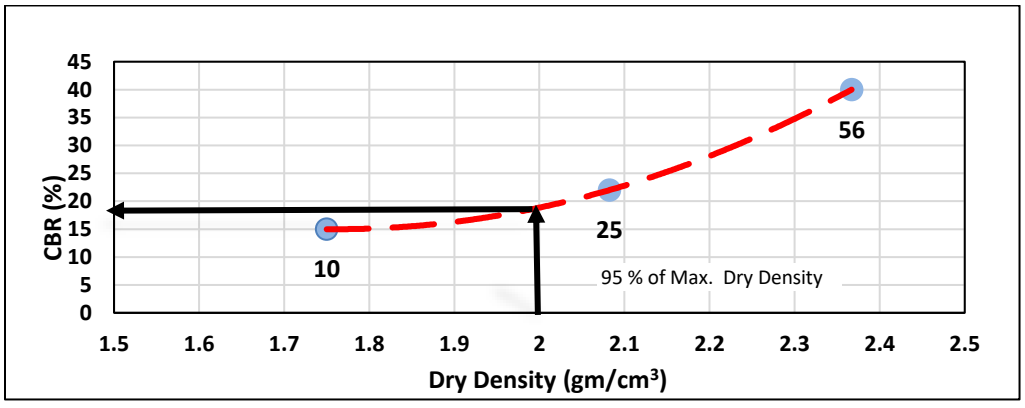

(c) CBR Soaked for Al-Intifada

Figure (3.5) Soaked CBR Test (a) Al-Tahadi, (b) Al-Fares and (c) Al-Intifada

3.3 Soil Preparation

Two testing devices (PLT and DCP) were used to assess the structural efficiency of the subgrade layers. Furthermore, measurements of density and water content data were obtained while performing the SRM.

The soil was treated with a drum mixer shown in Figure (3.6) of 0.25 m^3 at optimum the moisture content. In order to make it easier to transfer the sample to the mixer and ensure proper mixing, 150 kg of subgrade was separated into 25 kg containers for each mixture. In the testing steel box, the subgrades have been compacted into layers (20 cm for layer) up (0.6 m) height which is greater than PLT's influence depth. Total sample volume for each try was equivalent to 1.728 m^3

For each soil type, three compaction levels were used, depending on the number of compactor passes (NOP) performed to each layer. The compaction effort was divided into three categories: ten numbers of passing (10-NOP), fourteen numbers of passes (14-NOP), and eighteen numbers of passes (18-NOP). The goal of utilizing three compaction levels was to achieve a variety of density for each soil type and determine the extent to which compaction affected the test findings. A steel plate compacter was used to achieve the compacted effort (model: petrol engine with power 6.0 Kw, weight 160 kg, and frequency 4000 VPM), the compressed attempt is shown in Fig (3.6).

(a) (b)

Figure (3.6) (a) Electrical Mixer, (b) steel plate compacter

The following testing sequence was chosen: three PLT, six DCP, six sand replacement. Figure (3.7) presents a schematic representation of the test arrangement and locations.

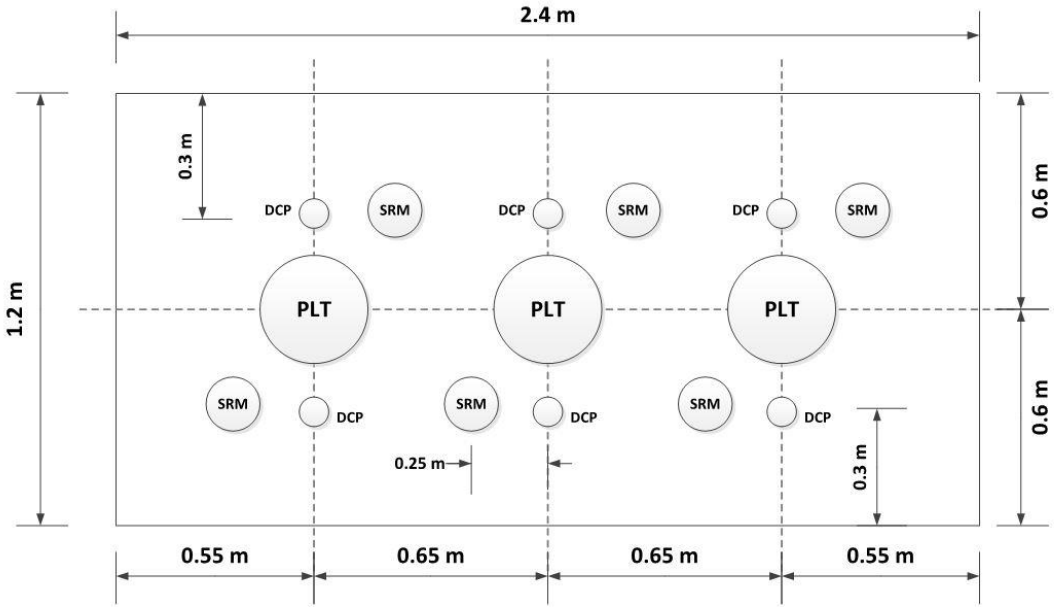

Figure (3.7) Schematic representation of the test arrangement and locations.

3.4 Research Methodology

The main intent of the research is to evaluate (A-3) subgrade soils available in Karbala from different sites. A series of laboratory tests were performed to determine the chemical and physical properties of the subgrade soil used. The soil is compacted within the steel frame before being approved then tested using a dynamic cone penetrometer, plate load test, and sand replacement test. Figure (3.8) shows diagram representation of research methodology and Tables (3.1) summarizes the total number of laboratory tests.

The experimental work is made up of 213 sets of laboratory tests divided into two phases as follows: The first: 78 physical and chemical properties. The second: 135 laboratory setups, including DCP, PLT, SRM.

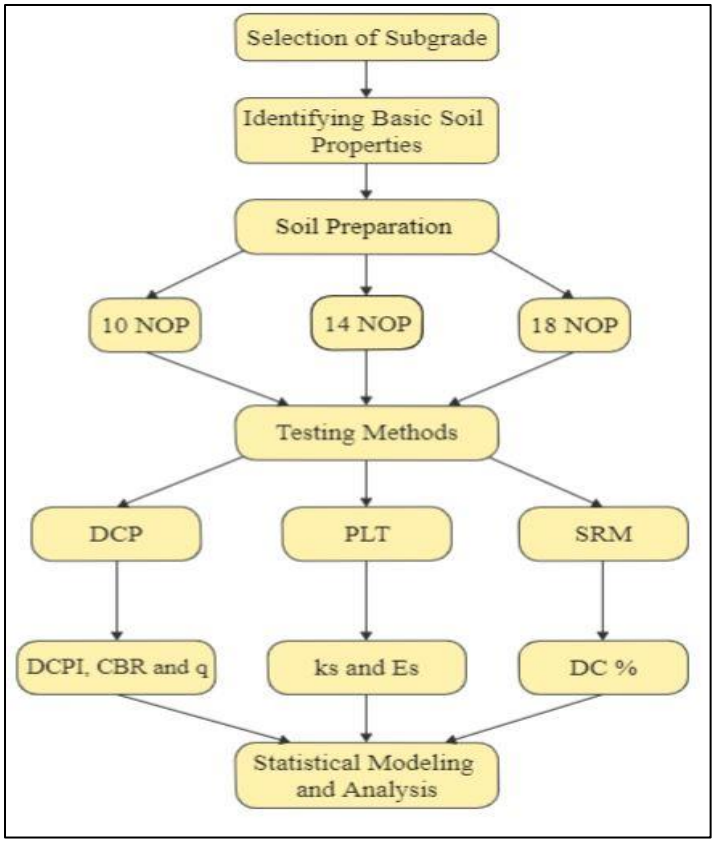

Figure (3.8) Diagram representation of research methodology

Tables (3.2) Total number of laboratory tests.

Tests Type		SUBGRADE SOIL			Total number	
		Al-Intifada	Al-Fares	Al-Tahadi		
		Physical Properties				
CBR	Soaked	8	8	8	24	78
	Unsoaked	8	8	8	24	
Proctor	Standard	2	2	2	6	
	Modified	2	2	2	6	
Grain Size Distribution		1	1	1	3	
Specific Gravity		3	3	3	9	
Chemical Test		2	2	2	6	
Laboratory Test						
DCP		18	18	18	54	135
PLT		9	9	9	27	
SRM		18	18	18	54	

3.5 Loading Frame Setup

The field experimental program was aimed to determine the subgrade reaction modulus by using in-situ plate load test and strength of unbound pavement layers subgrades by computing dry density and California bearing resistance, and dynamic stiffness characteristics. To model in-situ subgrade conditions, a steel box with dimensions (length = 2.4m, height = 1.25m, width = 1.2m) was utilized as shown in Figure (3.9). The steel box's purpose is to represent the subgrade layer in performing compaction and other testing. The height of the steel box was determined based on the depth of influence of the plate load test. The total deformation influence is 2B from the plate load diameter (D=300 mm.), therefore the zone of influence depth is 0.6m.

(a) steel box

(b) loading frame

Figure (3.9) Laboratory testing setup

3.6 Testing Methods

3.6.1 Static Plate Loading test (PLT)

The plate loading test was carried out in accordance with the standard testing technique outlined in (ASTM D1196, 2004) and (AASHTO T222, 2007). A 300 mm diameter circular steel plate was located below the load cell and jack assembly, as shown in Figure (3.10). The steps for carrying out PLT as follows:

1- To get the average deflection of the loading plate, two dial gauges with sensitivity of 0.01mm/min and one 75 mm LVDT were placed at an angle of 120^0 from each other at the edge of the loading plate (25 mm from the circumference) as shown in Figure (3.10).
2- A seating load of 0.5 ton was given to dial gauges and LVDT to create a deflection of no less than 0.25 mm. The sitting load was removed when the

dial and LVDT readings came to rest. To begin the loading, the dial gauges were set to zero. The load was then applied in stages with uniform increments.

Figure (3.10) Plate load test

3- The number of increments should be sufficient to allow for the collection of a suitable number of load-deflection points (i.e., at least six points should be collected during the test). Following each increment, the load should be maintained until a deflection increase of no more than 0.03 mm/min occurs for three consecutive minutes.

4- A load-deformation curve was produced from the data collected through the technique described above by graphing the load for each increase in (kPa) against the average deflections. The average deflection is the average of two dial and LVDT measurements taken between zero and the end of each load increment. If the curve is not roughly a straight line going through the origin, it must be corrected by drawing a straight line between the unit loads of 69 and 207 kPa as shown in Figure (3.11)

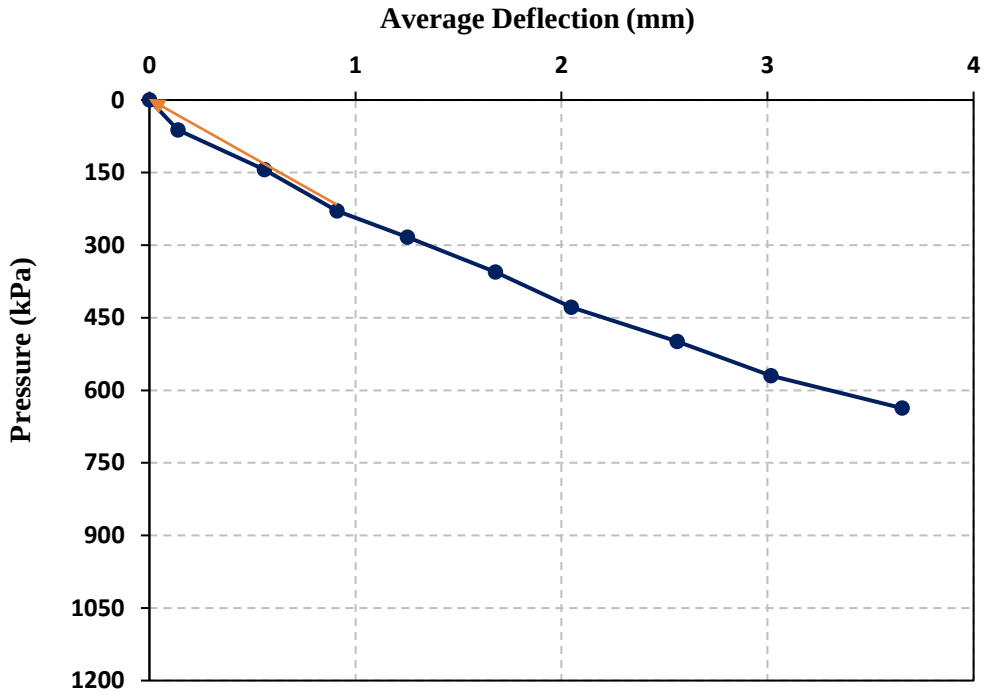

Figure (3.11) Typical load-deformation Curve

3.6.2 Dynamic Cone Penetrometer test (DCP)

The test technique entails measuring the penetration according to (ASTM D 6951, 2009). The Dynamic Cone Penetrometer with an 8-kg hammer (8-kg) was utilized on compacting soil to evaluate subgrade soil for pavement applications. Figure (3.12) shows diagram of DCP device. Basic concept of using dynamic cone penetrometer is held in a vertical or plumb position by the handle, and the hammer is lifted and released from the usual drop height. The recorder measures and records overall penetration or penetration per blow for a specific number of blows

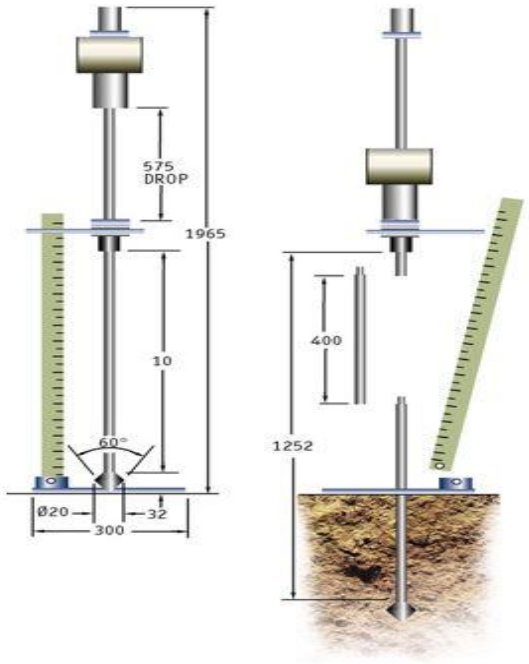

Figure (3.12) DCP equipment graphic (ASTM D 6951, 2009).

The following is a quick description of the testing process utilized throughout this project:

1. Inspect the equipment for fatigue and damaged components, and ensure that all linkages are securely secured.

2. The operator maintains the gadget upright by gripping the handle on the top shaft.

3. The operator raises and releases the hammer from the anvil to the handle when a partner calculates the distance between the bottom of the anvil and the ground.

4. The second person records the new height at the bottom of the anvil. To remove the DCP from the formed during the process cavity, use an extraction jack. If the tip is available, a simple tap with the hammer on the handle is sufficient. Figure (3.13) and (3.14) shows DCP in research lab and its typical results, respectively.

Figure (3.13) DCP in laboratory test setup

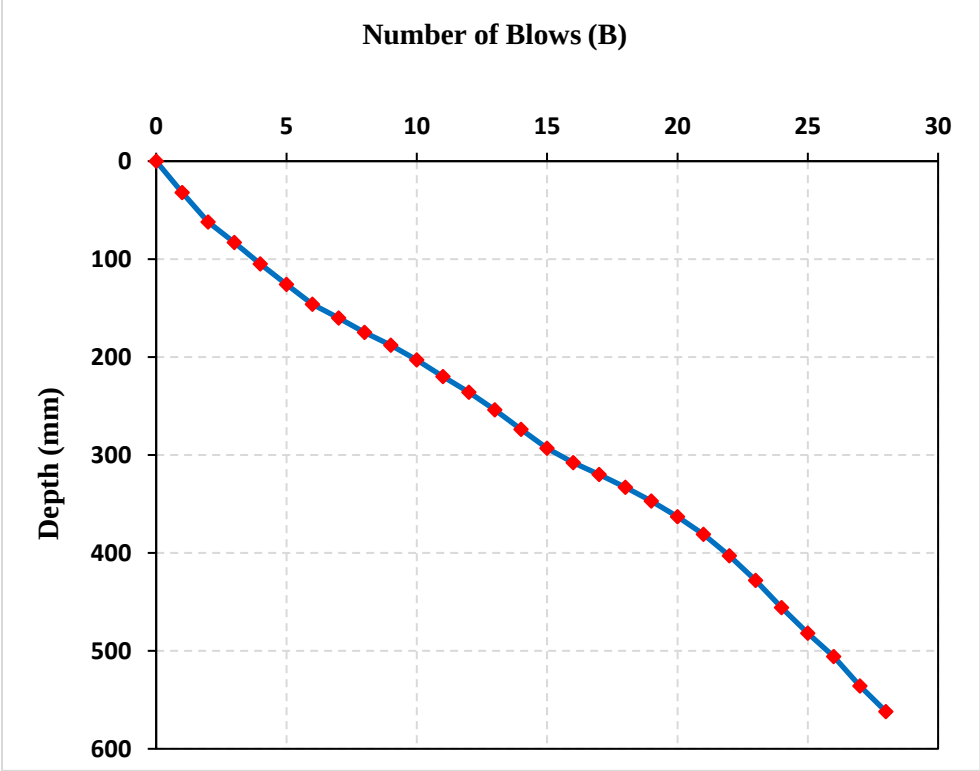

Figure (3.14) Typical results of DCP

3.6.3 Sand replacement test (SRM)

This test is used to measure the density of the field as well as the moisture content of the soil according to (ASTM D1556, 2015). In the soil to be tested, a test hole is excavated by hand, and all soil get from the hole is picked up in a container. The volume of the hole is calculated by filling it with free-flowing sand of known density. The in-place wet density of the soil is calculated by dividing the removed material's wet mass by the volume of the hole.

The SRM is suitable for natural, saturated, or highly flexible soils that may bend or press through test hole excavation, however it is suitable for soils containing significant amounts of rock or coarse particles that exceed 1.5 in (38 mm). Figure (3.15) shows sand replacement method test

Figure (3.15) Sand replacement method test

3.7 Summary

This chapter discusses methods of investigation, selection of a site, soil subgrade types for research, production of loading systems and methods of testing of materials. This study presents an evaluation of various fields tests and correlations between them in order to identify a suitable and reasonable correlation to estimate subgrade reaction modulus by using dynamic cone penetrometer, plate load test and chemical and physical test of soil.

Chapter Four

Results of Experimental Work

4.1 General

The results of laboratory tests are presented in this chapter which were carried out on (A-3) soils collected from different sites located in Karbala city. The total number of experimental tests is 135 (27 of which have been performed under static load, 54 for dynamic cone penetrometer and 54 for determining field densities and the moisture content). A summary and discussion of these results will be presented in the following sections:

4.2 Results of SRM

The sand replacement method (SRM) depending to (ASTM D1556, 2000) was performed in this experimental investigation. Table (4.1) shows degree of compaction and dry density results for the subgrades using different NOP (i.e., number of passes).

The density was determined based on three levels of number of passes (10,14 and 18). The results showed that increasing number of passes causes an increase in the degree of compaction and dry density. The SRM testing method is directly affected by the amount of water content, size of hole, technique of collecting a disturbed soil sample from the hole, effort of compaction. For these reasons there is a difference in degree of compaction and dry density for the same number of passes (Chukka & Chakravarthi, 2012). The Al-Intifada soil was most affected by the compaction process, which showed an increase in the value of Dc% by 5% for 18 NOP compared to 10 NOP.

Table (4.1) Degree of compaction and dry density results of the subgrades with different NOP

Site	NOP	Testing point	Wet Density (gm/cm^3)	Dry Density (gm/cm^3)	Wc %	Max. Dry Density(gm/cm^3)	Dc %
Al-Tahadi	10	A	2.0	1.8	7.0	2.105	87.4
		B	2.0	1.9	6.9	2.105	88.5
		C	2.0	1.9	6.1	2.105	88.8
	Average		2.0	1.9	6.6	2.105	88.2
	STD		0.011	0.015	0.478	0.000	0.703
	14	A	2.1	1.9	7.2	2.105	92.1
		B	2.1	2.0	6.9	2.105	92.8
		C	2.1	2.0	7.0	2.105	93.5
	Average		2.1	2.0	7.0	2.105	92.8
	STD		0.014	0.015	0.146	0.000	0.718
	18	A	2.2	2.0	7.0	2.105	95.8
		B	2.1	2.0	7.1	2.105	95.0
		C	2.1	2.0	7.0	2.105	94.8
	Average		2.146	2.005	7.051	2.105	95.237
	STD		0.012	0.011	0.081	0.000	0.537
Al-Fares	10	A	1.9	1.8	7.8	1.970	90.9
		B	2.0	1.8	8.3	1.970	91.9
		C	2.0	1.8	7.4	1.970	93.4
	Average		2.0	1.8	7.8	1.970	92.0
	STD		0.024	0.025	0.477	0.000	1.279
	14	A	2.0	1.9	7.9	1.970	95.4
		B	2.0	1.9	8.7	1.970	95.2
		C	2.0	1.9	8.3	1.970	94.9
	Average		2.0	1.9	8.3	1.970	95.2
	STD		0.007	0.005	0.445	0.000	0.274
	18	A	2.1	1.9	8.5	1.970	97.7
		B	2.1	1.9	7.9	1.970	96.5
		C	2.1	1.9	7.4	1.970	97.0
	Average		2.064	1.912	7.963	1.970	97.063
	STD		0.021	0.012	0.556	0.000	0.610
Al-Intifada	10	A	1.9	1.8	7.9	1.975	91.0
		B	2.0	1.8	8.7	1.975	92.8
		C	2.0	1.8	8.3	1.975	91.4
	Average		2.0	1.8	8.3	1.975	91.8
	STD		0.028	0.018	0.445	0.000	0.931
	14	A	2.0	1.9	7.8	1.975	94.4
		B	2.0	1.9	8.3	1.975	94.6
		C	2.0	1.9	7.4	1.975	95.0
	Average		2.0	1.9	7.8	1.975	94.7
	STD		0.008	0.005	0.477	0.000	0.275
	18	A	2.1	1.9	8.5	1.975	97.1
		B	2.1	2.0	7.9	1.975	98.9
		C	2.1	1.9	7.4	1.975	96.7
	Average		2.1	1.9	8.0	1.975	97.5
	STD		0.028	0.023	0.556	0.000	1.167

The results in Table (4.1) indicates that the highest value of degree of compaction is (98.859) in Al-Intifada for (18 NOP) and the lowest value is (87.431) in Al-Tahadi for (10 NOP). The increase in degree of compaction ratio is because of reduction in voids volume. As shown in Figure (4.4), The soil of the Al-fares and Al-Intifada is more responsive and influenced by a rise in NOP, as it provides higher Dc values. This is related to the Al-Tahadi soil's low dry density value in comparison to Al-Fares and Al-Intifada, which is directly related to the degree of compaction.

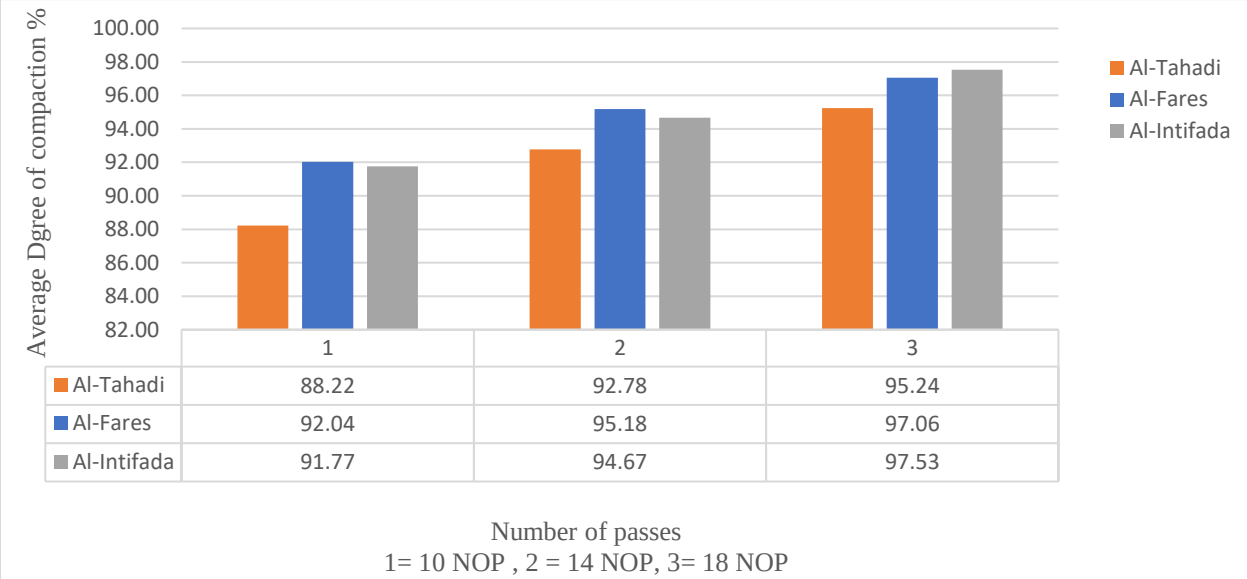

	1	2	3
Al-Tahadi	88.22	92.78	95.24
Al-Fares	92.04	95.18	97.06
Al-Intifada	91.77	94.67	97.53

Figure (4.1) Effect of NOP on Degree of Compaction

4.3 Results of PLT

The plate load test (PLT) was carried out incrementally according to the standard testing procedure defined in (AASHTO T222, 2007), with a maximum applied load of 50 to 70 kN (5-7 tons). Twenty-seven PLT experiments were carried out on subgrades with varying levels of compaction. The following parameters were calculated from the load-deflection curve of PLT:

- p_{max} : is the max contact pressure produced by the ratio of applied load to the area of loading plate.

- CF: is the ratio of the load-deformation curve's subgrade reaction modulus before and after correction.

- s_{max}: the loading plate's maximum settlement under static load.

- ks: subgrade reaction modulus in (kPa/mm) can be calculated as follow (4.1)

$$ks = \frac{69(kpa)}{average\ deflection(mm)} \quad (4.1)$$

- E_s: Young's modulus determined from the following equation:

$$E_s = ks * 0.492 \quad (4.2)$$

The soil parameters derived from 9 PLT tests for Al-Tahadi subgrade are listed in Table (4.2). The current load-deformations curve before correction showed that the values of minimum, maximum and average subgrade reaction modulus were 76.5 ,323.3 and 230.6 kPa/mm, respectively. The corrected load-deflection curve of the subgrade reaction modulus value varied from 135 to 202 kPa/mm, and the average is equivalent to 169.4 kPa/mm. The correction factor values were between 0.567 and 1.840 with an average of 1.341. The contact pressure ranged from 640 to 710 kPa, with an average of 681.7 kPa. The data shows that the settlement ranged from 3.7 to 5.2 mm, with an average of 4.3 mm and Es ranged from 66 kpa to 99 kpa. Figure (4.1) shows the average load-settlement curve of subgrade soils collected from Al-Tahadi

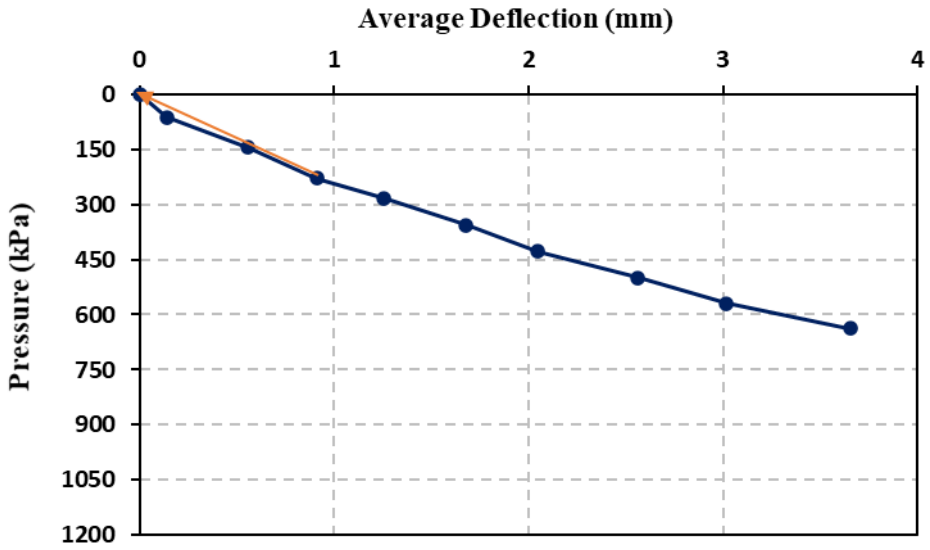

Figure (4.2) Average PLT load-deflection curve (Al-Tahadi).

Table (4.2). Results of PLT at Al-Tahadi

Subgrade Name	NOP	Point	p_{max} (kpa)	s_{max} (mm)	Un Corrected ks (kPa/mm)	Corrected ks (kPa/mm)	Correction Factor	E_s (MPa)
Al-Tahadi	10	A	650	5.2	76.5	135	0.567	66
		B	645	4.5	197.14	145	1.360	71
		C	700	4.8	276	150	1.840	74
	Average		665.0	4.8	183.2	143.3	1.3	70.5
	STD		30.41	0.35	100.48	7.64	0.64	3.76
	14	A	650	4.4	113.11	165	0.686	81
		B	670	4.2	300	176	1.705	87
		C	710	4.8	222.58	172	1.294	85
	Average		677	4	212	171	1.2	84
	STD		30.55	0.31	93.90	5.57	0.51	2.74
	18	A	700	3.3	345	200	1.725	98
		B	710	3.7	323.3	180	1.796	89
		C	700	3.7	222.1	202	1.100	99
	Average		703.3	3.6	296.8	194.0	1.5	95.4
	STD		5.77	0.22	65.60	12.17	0.38	5.99

Table (4.3) presents the soil parameters derived from 9 PLT tests for Al-Fares subgrade. The current load-settlement curve before correction showed the values of the minimum, maximum subgrade and average subgrade reaction modulus were 229, 372 and of 270 kPa/mm, respectively. The corrected load-deflection curve of the subgrade reaction modulus value varied from 172 to 210 kPa/mm, and the average is equivalent to 187.5 kPa/mm. The correction factor values were between 1.328 and 1.948 with an average of 1.498. The contact pressure ranged from 640 to 710 kPa, with an average of 664.11 kPa. The data shows that the settlement ranged from 3.7 to 5 mm and Es ranged from 85kpa to 95 kpa. Figure (4.2) shows the average load-settlement curve of subgrade soils collected from Al-Fares.

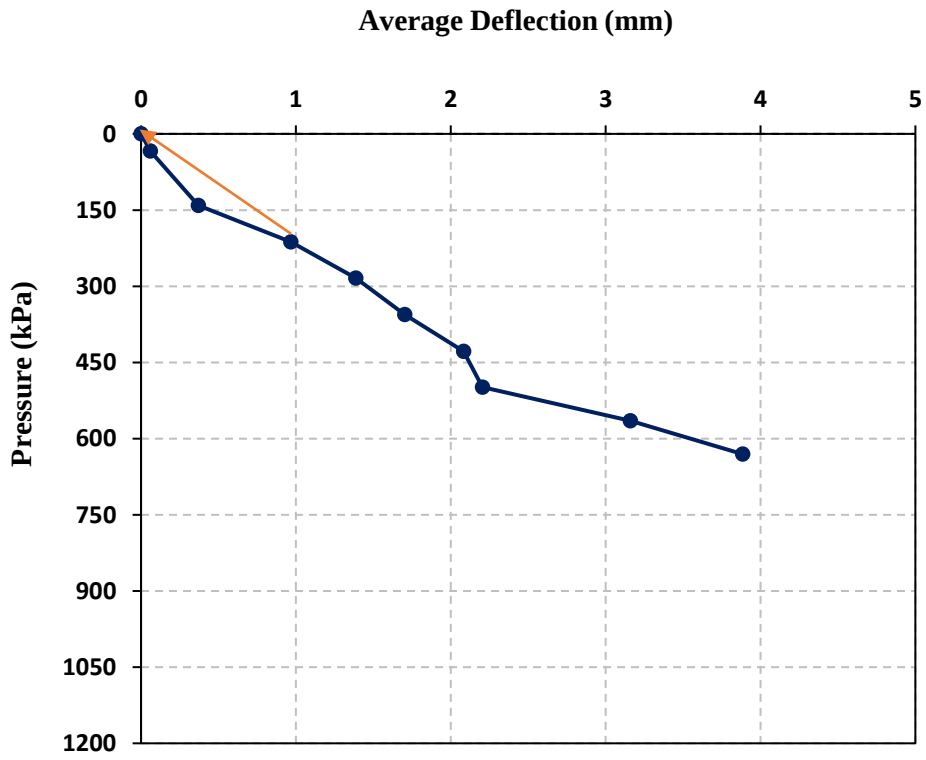

Figure (4.3) Average PLT load-deflection curve (Al-Fares).

Table (4.3) Results of PLT at Al-Fares

Subgrade Name	NOP	Point	p_{max} (kpa)	s_{max} (mm)	Un Corrected ks (kPa/mm)	Corrected ks (kPa/mm)	Correction Factor	E_s (MPa)
Al-Fares	10	A	640	4.2	232	172	1.349	85
		B	640	3.9	229	173	1.328	85
		C	642	3.7	261	178	1.466	88
	Average		641	4	241	174	1	86
	STD		1.15	0.25	17.67	3.33	0.07	2
	14	A	650	3.9	290	184	1.576	91
		B	700	4.8	287	185	1.551	91
		C	640	3.9	336	180	1.867	89
	Average		663	4	304	183	2	90
	STD		32.15	0.52	27.47	2.65	0.18	1.30
	18	A	710	4.4	327	197	1.660	97
		B	645	3.7	197	190	1.037	93
		C	710	5.0	372	191	1.948	94
	Average		688	4	299	193	2	95
	STD		37.53	0.65	90.88	3.79	0.47	1.86

Table (4.4) presents the parameters derived from 9 PLT tests for Al-Intifada subgrade soil. The current load-deformations curve before showed that the value of the minimum, maximum and average subgrade reaction modulus was 107.8, 328 and 280 kPa/mm, respectively. The corrected load-deflection curve of the subgrade reaction modulus value varied from 150 to 230 kPa/mm, and the average is equivalent to 189.67 kPa/mm. The correction factor values were between 0.719 and 1.989 with an average of 1.476. The contact pressure ranged from 590 to 715 kPa, with an average of 667.22 kPa. The data shows that the settlement ranged from 3.4 to 5.30 mm and Es ranged from 74 kpa to 113 kpa. Figure (4.3) shows the average load-settlement curve of subgrade soils collected from Al-Intifada.

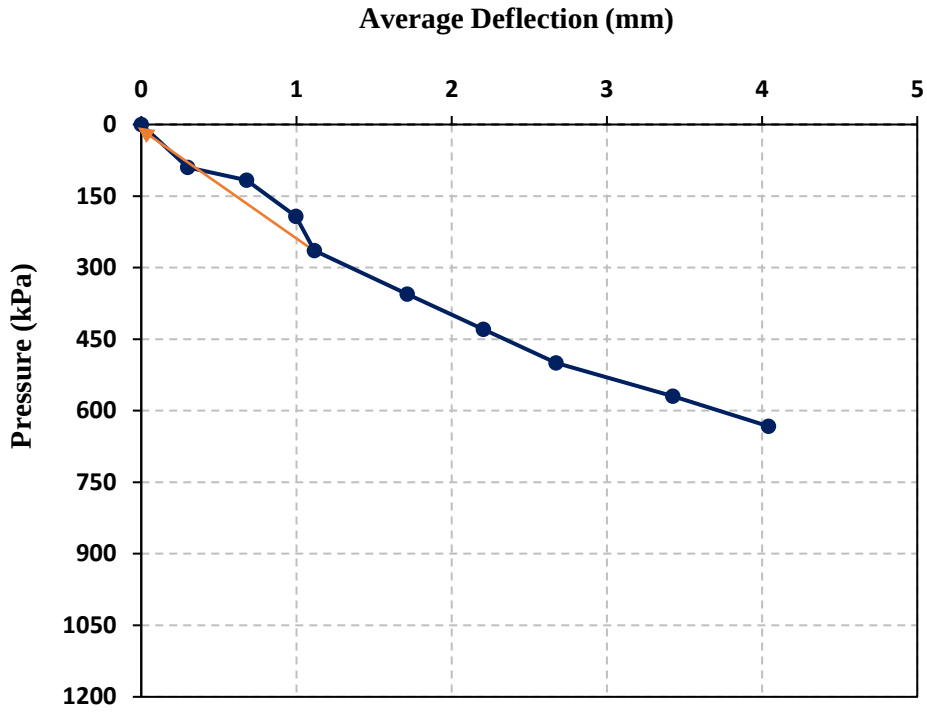

Figure (4.4) Average PLT load-deflection curve (Al-Intifada).

Table (4.4) Results of PLT at Al-Intifada

Subgrade Name	NOP	Point	p_{max} (kPa)	s_{max} (mm)	Un Corrected ks (kPa/mm)	Corrected ks (kPa/mm)	Correction Factor	E_s (MPa)
Al-Intifada	10	A	590	5.30	107.8	150	0.719	74
		B	640	3.90	325	172	1.890	85
		C	710	4.80	281	164	1.713	81
	Average		647	5	238	162	1	80
	STD		60.28	0.71	114.83	11.14	0.63	5.48
	14	A	640	3.70	360	181	1.989	89
		B	650	3.80	264.1	198	1.334	97
		C	710	4.75	300	200	1.500	98
	Average		666.7	4.1	308.0	193.0	1.6	95.0
	STD		37.86	0.58	48.45	10.44	0.34	5.14
	18	A	715	3.40	328	200	1.640	98
		B	710	3.70	287.5	230	1.250	113
		C	640	3.90	265	212	1.250	104
	Average		688.3	3.7	293.5	214.0	1.4	105.3
	STD		41.93	0.25	31.93	15.10	0.23	7.43

The result also shows that the ks value increases with the degree of compaction (i.e., with increase soil density). This behavior is attributed to the volume void reduction and arranging soil particles into a stable state with increase NOP. Figures (4.5), (4.6), (4.7) and (4.8) illustrate the effect of compaction effort (I.e., NOP) on pressure, settlement, ks and Es obtained from PLT test, respectively.

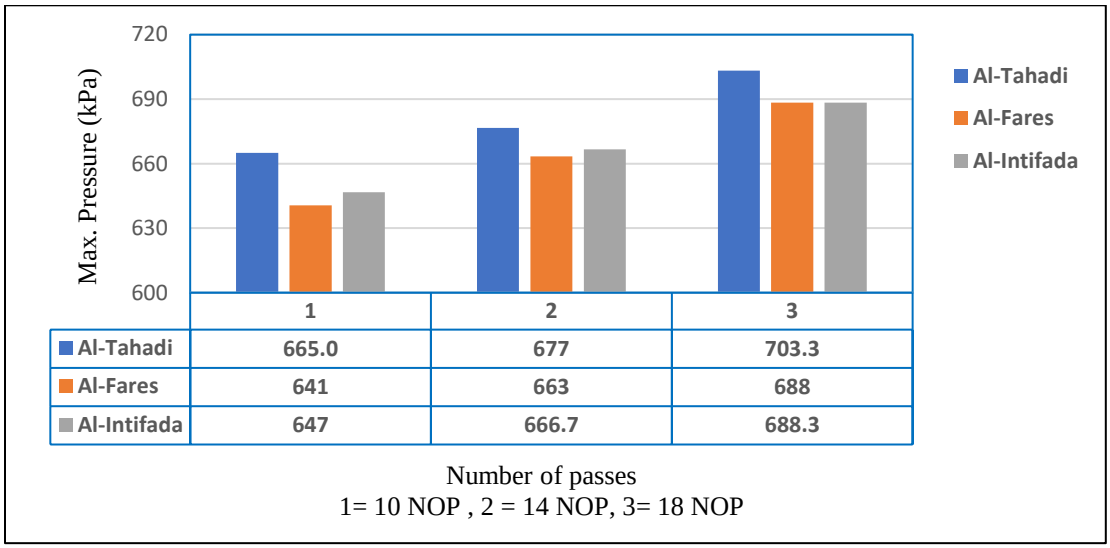

	1	2	3
Al-Tahadi	665.0	677	703.3
Al-Fares	641	663	688
Al-Intifada	647	666.7	688.3

Figure (4.5) Max. Pressure vs. NOP

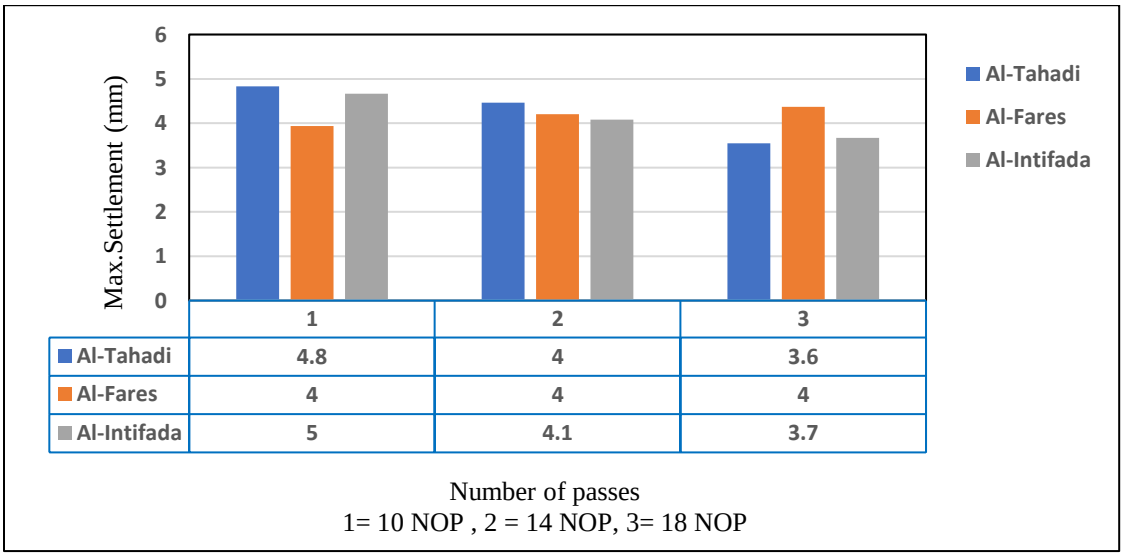

	1	2	3
Al-Tahadi	4.8	4	3.6
Al-Fares	4	4	4
Al-Intifada	5	4.1	3.7

Figure (4.6) Max. Settlement vs. NOP

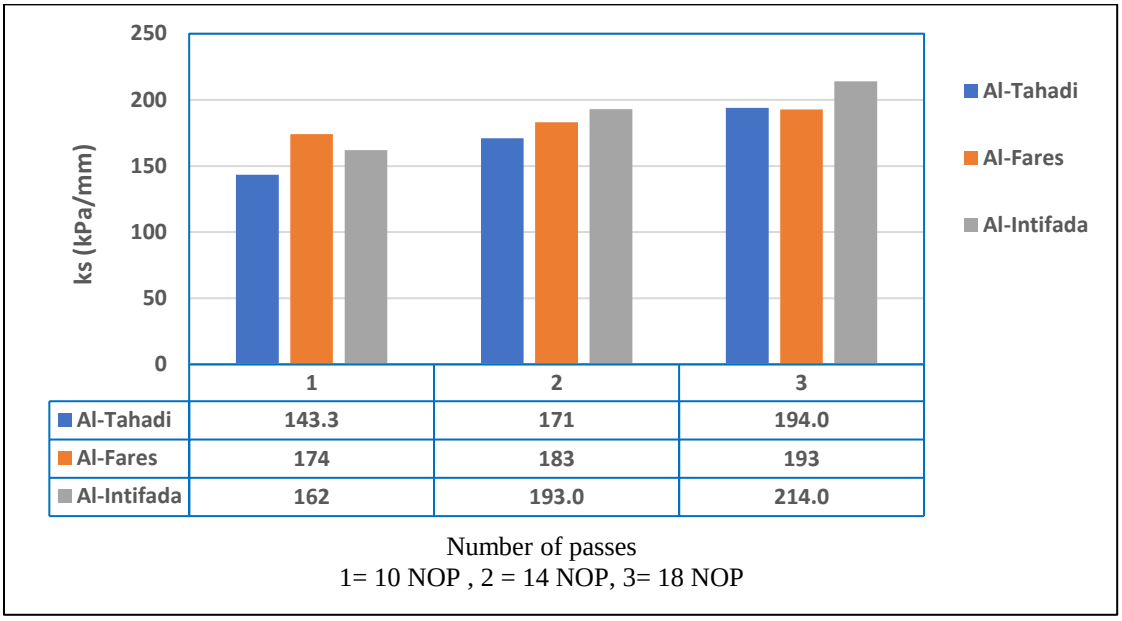

Figure (4.7) Subgrade Reaction Modulus vs. NOP

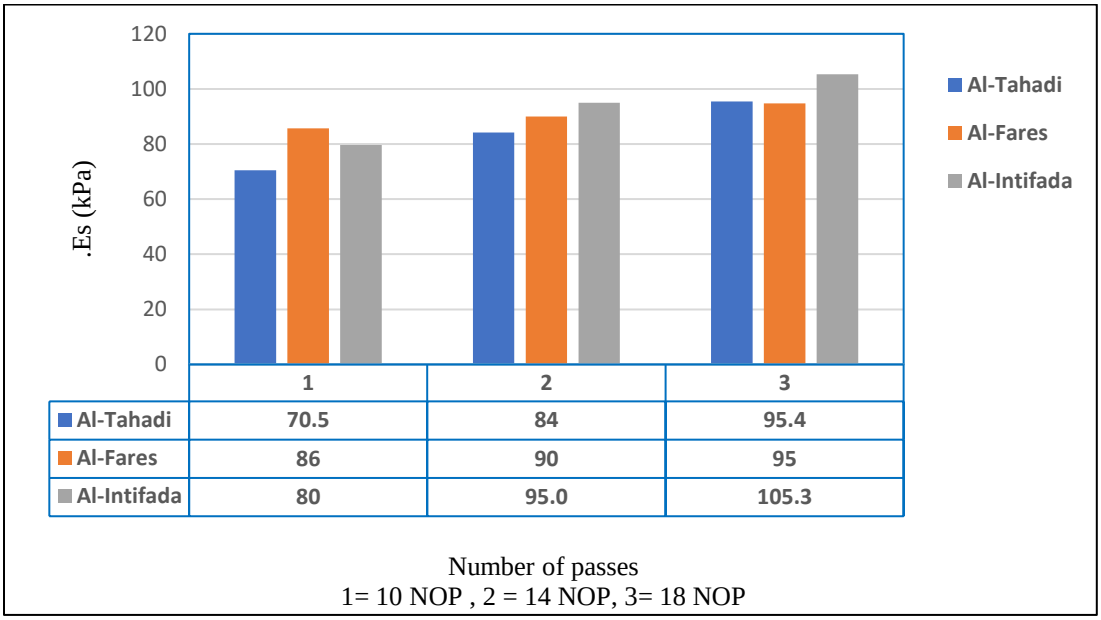

Figure (4.8) Elastic Modulus vs. NOP

The collected results for A-3 subgrades soils, ks value at three degrees of compaction increased because of increment that occurred in the amount of dry density. The A-3 (Al-Intifada) soil has a high subgrade reaction modulus of 230 kPa/mm, while the A-3 (Al-Tahadi) soil has a lower value of 135 kPa/mm, the

percentage of increase is 4 %. This indicates that increasing the compaction from 10 to 14 and then to 18 leads to an increase in the degree of compaction and higher ks values.

4.4 Results of DCP

The dynamic cone penetrometer test method includes measuring the penetration in accordance with (ASTM D 6951, 2009). In this study, the following DCP parameters were determined: dynamic cone penetrometer index (DCPI), California bearing ratio (CBR), bearing capacity (q). Table (4.5) presents the values of soil parameters calculated from DCP based on an empirical formula the as mentioned in equations below:

The California ratio for bearings (CBR) is based on an empirical formula that recommended and applied by engineering Corp of the US Army (Kelyn, 1975):

$$CBR = \frac{292}{(DCPI)^{1.12}} \quad (4.2)$$

Where:

DCPI: dynamic cone penetrometer index(blows/mm)

Several relationships were established throughout time for predicting bearing strength characteristics for different soil types. The correlations are applied in the following equation to determine the capacity (PCA, 1955):

$$q = 144 \text{ x } (3.794 \times CBR^{0.664}) \quad (4.3)$$

Where:

CBR: California bearing capacity

The DCPI value of point A was calculated from taking the average of two tests around PLT point test as shown in the Figure (3.6).

Table (4.5) Soil Parameters from DCP test

Site	Testing name	CBR (%)	DCPI	Bearing capacity (kPa)
Al-Tahadi	A	8	26	105.5
	B	9	24	108.3
	C	9	23	112
	Average	8.667	24.333	108.579
	Std	0.577	1.528	3.293
	A	10	23	118.5
	B	10.5	21	120.7
	C	11	19.5	129.3
	Average	10.5	21.17	122.83
	Std	0.5	1.76	5.75
	A	12.5	18	137.8
	B	12	18.5	136.1
	C	12.5	17.5	139.1
Al-Fares	Average	12.33	18	137.64
	Std	0.29	0.5	1.51
	A	10	20.5	122.5
	B	10	21	120.2
	C	10.5	20	121.9
	Average	10.17	20.5	121.55
	Std	0.29	0.5	1.19
	A	12.5	14.5	143.4
	B	12	17.5	135
	C	12	18	135
	Average	12.17	16.67	137.8
	Std	0.29	1.89	4.83
	A	14	16	149.43
	B	13	17	141.97
	C	13.5	16	148.42
	Average	13.5	16.33	146.61
	Std	0.5	0.58	4.05
Al-Intifada	A	10	20	122
	B	10.5	20	122.1
	C	10	20	121.8
	Average	10.17	20	121.96
	Std	0.29	0	0.15
	A	12	19	134.4
	B	11.5	19	129.1
	C	12	19	132.6
	Average	11.833	19	132.029
	Std	0.289	0	2.701
	A	13.5	17	143.4
	B	14	16.5	146.6
	C	13.5	17.5	139.4
	Average	13.67	17	143.13
	Std	0.29	0.5	3.61

The results presented in Table (4.5) indicate that DCPI value varied from 14.5 mm/blow to 26 mm/blow, CBR ranged from 8 % to 13.5, bearing capacity ranged from 105.45 kPa to 149.42 kPa. The degree of compaction can be increased by increasing NOP. It was observed that as soil compaction increases, DCP parameters (CBR and q) increase and DCPI decrease with increase NOP as shown in Figures (4.9) through (4.11).

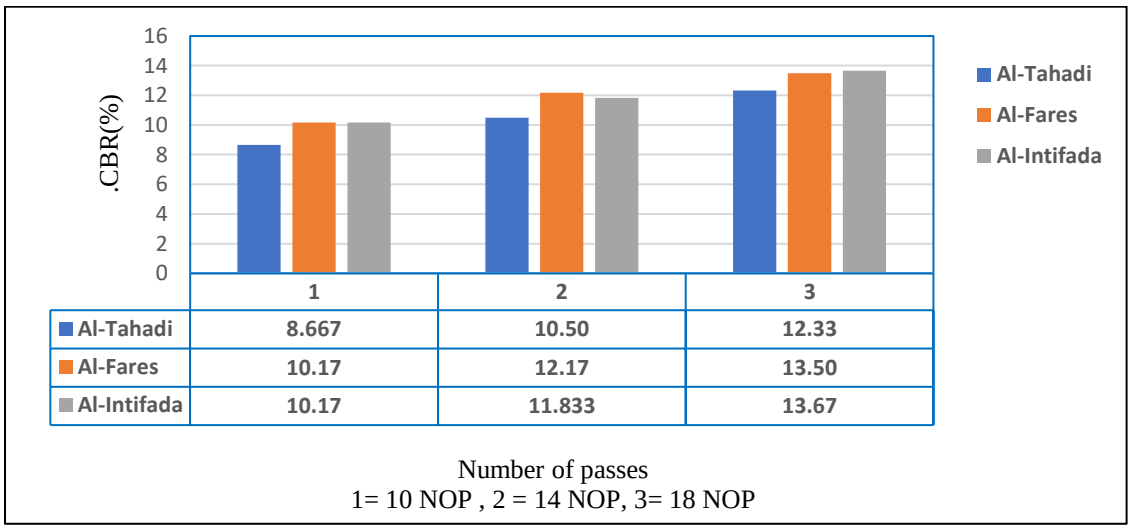

Figure (4.9) CBR vs. NOP

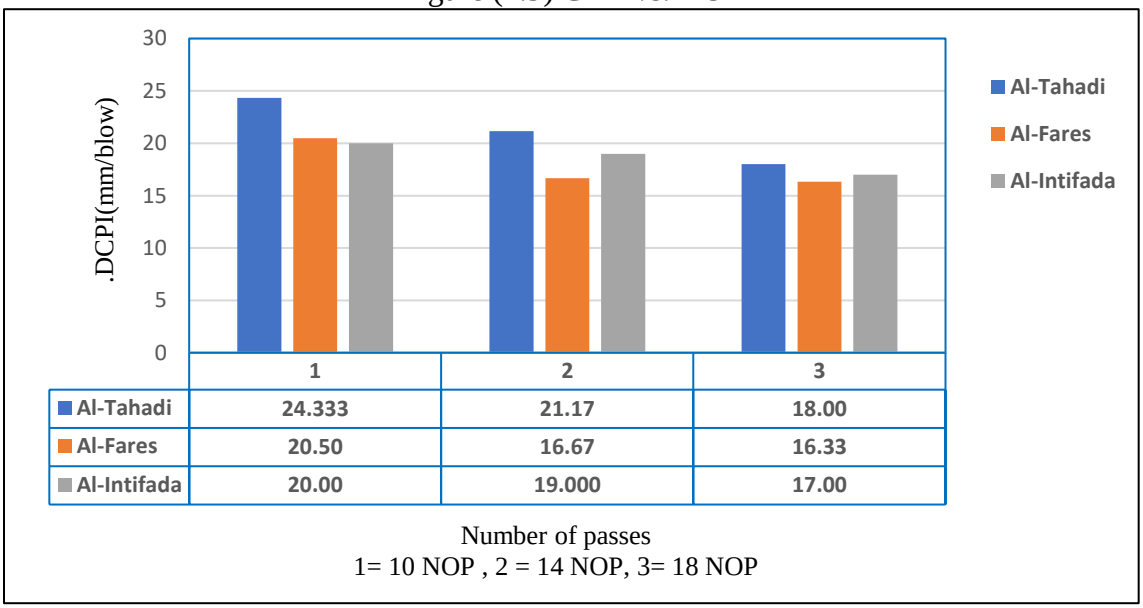

Figure (4.10) DCPI vs. NOP

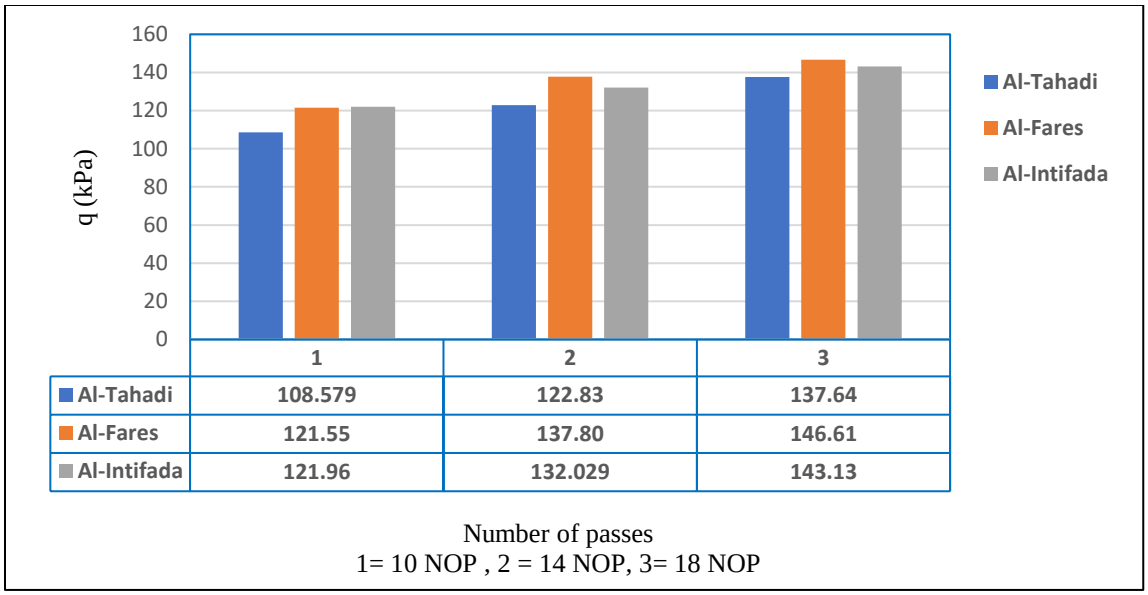

Figure (4.11) Bearing Capacity vs. NOP

The results of the PLT and DCP tests shows that there is a significant relationship between the ks value for three subgrade and DCP parameters such as CBR, DCPI, and degree of compaction at three stages. It can be noted from Figures (4.12) and (4.13) that ks have higher value with increase CBR, bearing capacity (kPa). Figure (4.14) shows the opposite happens with dynamic cone penetrometer index (mm/blow), whereby a decrease in the value of DCPI leads to an increase in ks value.

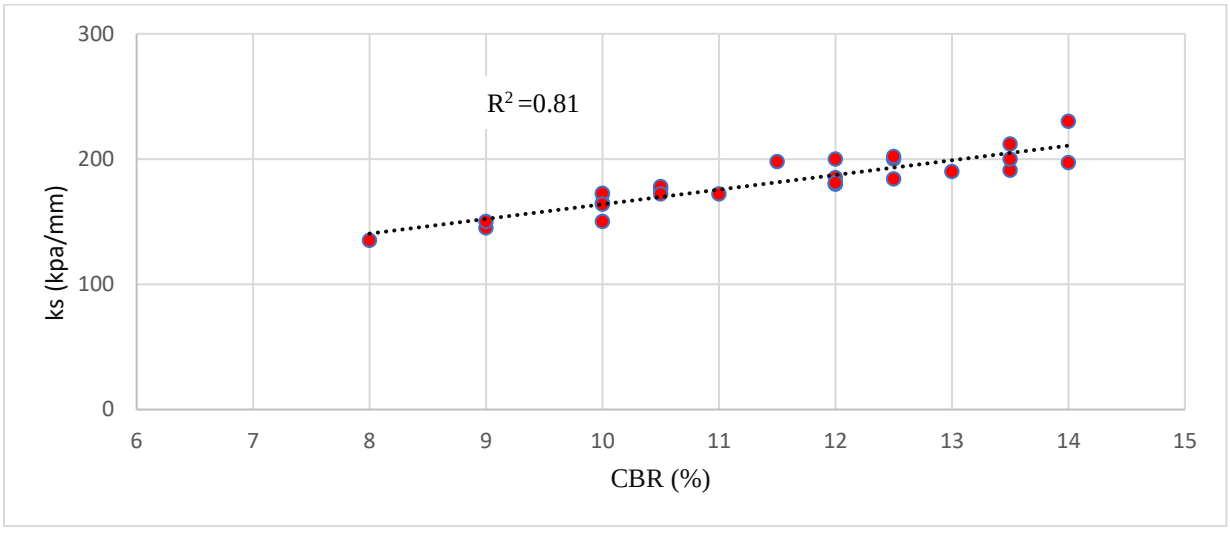

Figure (4.12) Subgrade reaction. Vs. CBR for all data.

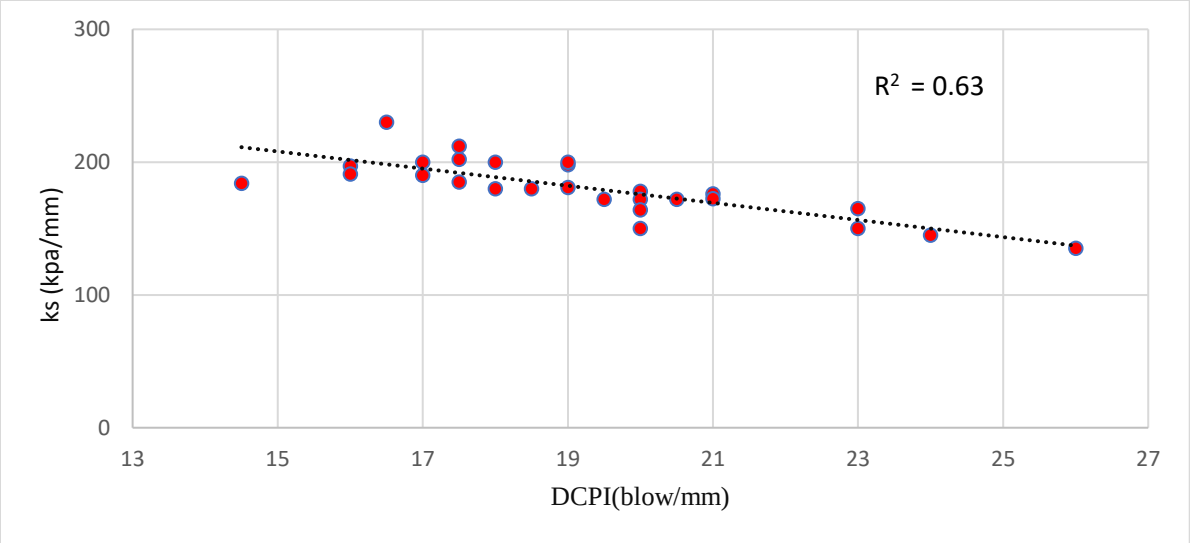

Figure (4.13) Subgrade reaction. Vs. DCPI for all data

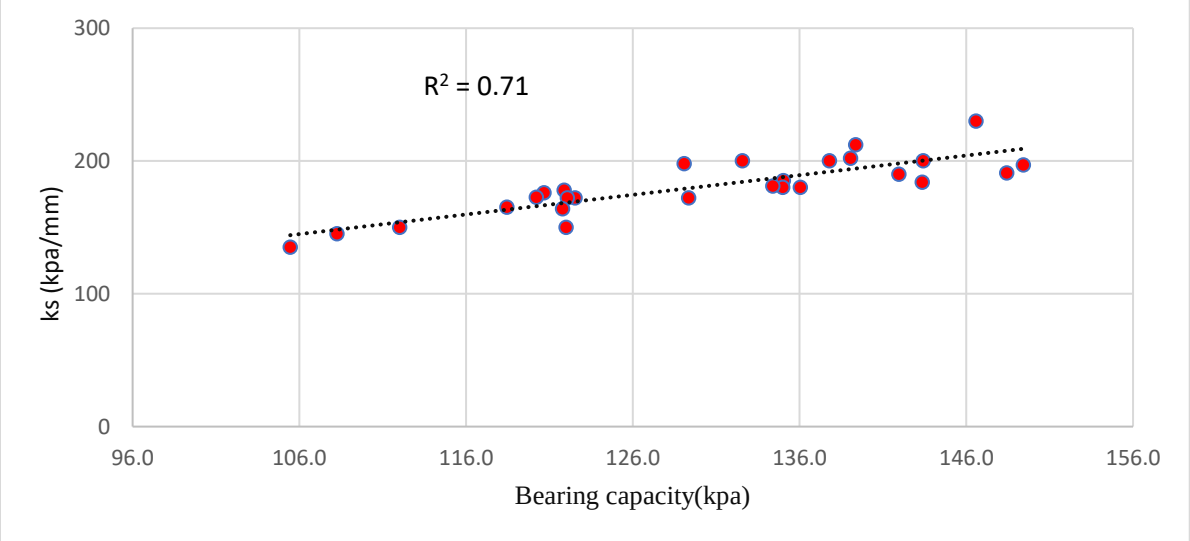

Figure (4.14) Subgrade reaction. Vs. Bearing capacity for all data

4.4 Summary

There is a significant relationship between the ks value for three subgrade and DCP parameters such as CBR, DCPI, and degree of compaction at three levels. It can be noted that ks has higher value with increase CBR and bearing capacity (kPa), and degree of compaction. The opposite is true for the dynamic cone penetrometer index (mm/blow), where a reduction in DCPI leads to an increase in ks.

Through a comprehensive look at all data, it can be noticed that there is a difference in the results between three locations of soils in the values of the PLT and DCP coefficients for the same NOP. This difference is due to the dry density value because it is directly influenced by the amount of water content, and size of soil particles (i.e., a soil with high SF tends to have high density and high strength characteristics).

Chapter Five

Statistical Modeling and Analysis

5.1 Introduction

The plate load test (PLT) and dynamic cone penetrometer (DCP) were used in the experimental study program to investigate if any correlations existed between subgrade reaction modulus and soil characteristics such as these obtained from DCP. The experimental measurements generated from (PLT and DCP) testing devices were compared and statically evaluated utilizing the regression analysis

In this study, the Statistical Package for The Social Sciences (SPSS) software (Version- 26) was used for the process of entering data, analysis, and the generation of tables and figures. The software is capable of managing huge quantities of data and perform numerous analytical techniques. The regression analysis was done to determine the most reliable statistical models for predicting subgrade reaction (ks) using basic soil properties and the DCP device. Statistical analysis is utilized to generate a mathematical model that describes the relationship between dependent and independent variables.

The dependent variable in this thesis was chosen to be ks, whereas the other factors such as: (dynamic cone penetration index (DCPI), California bearing capacity (CBR), bearing capacity (q), degree of compaction (Dc), elastic modulus (Es), curvature coefficient (Cc) and uniformity coefficient (Cu) were determined from other physical properties tests, where used as independent variables for building three statistical models. These statistical models can be described as three groups, namely:1st group: models based on DCP measurements ,2nd group: models based on basic soil properties,3rd group: models based on DCP and basic Soil properties. Additionally, a statistical model was developed to predict Es based on DCP and basic physical properties.

5.2 Basic Statistical Description

5.2.1 Outliers Test

A data point that differs significantly from other observations is referred to as an outlier in statistics. An outlier can be caused by measurement variability or by experimental error, with both being eliminated from the data set. In statistical analysis, an outlier can be quite significant.

A box plot which is a graphical representation of numerical data groups based on their quartiles was used to visually estimate for the reliability of data. The terms box-and-whisker diagram refer to box plots with lines extending from the boxes (whiskers) indicating variability beyond the top and lower quartiles. As shown in Figure (5.1), the results of outlier's test found no outliers in all data.

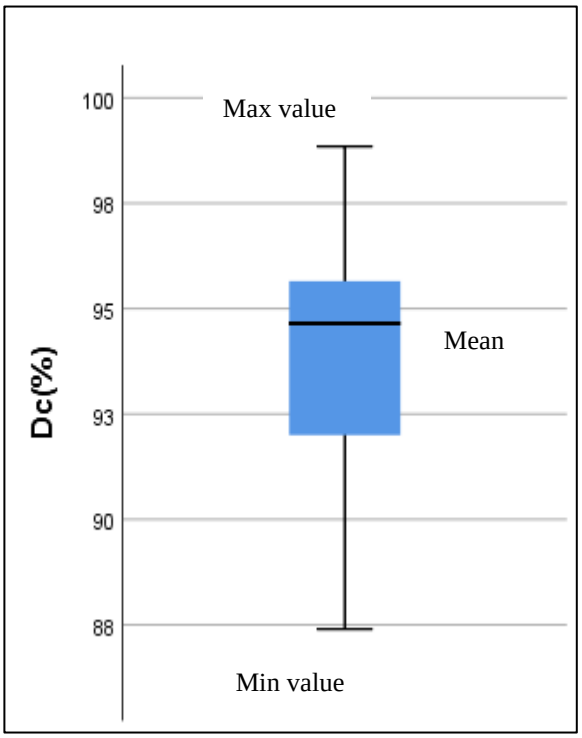

(a) Box plot for degree pf compaction

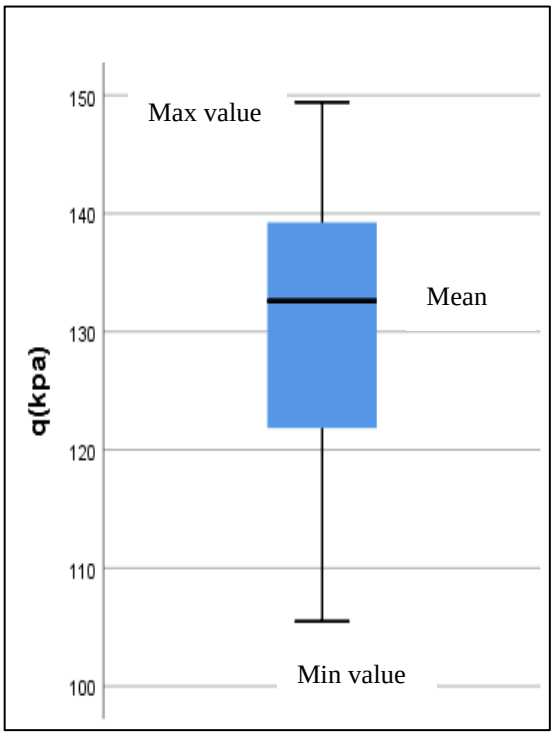

(b) Box plot for bearing capacity

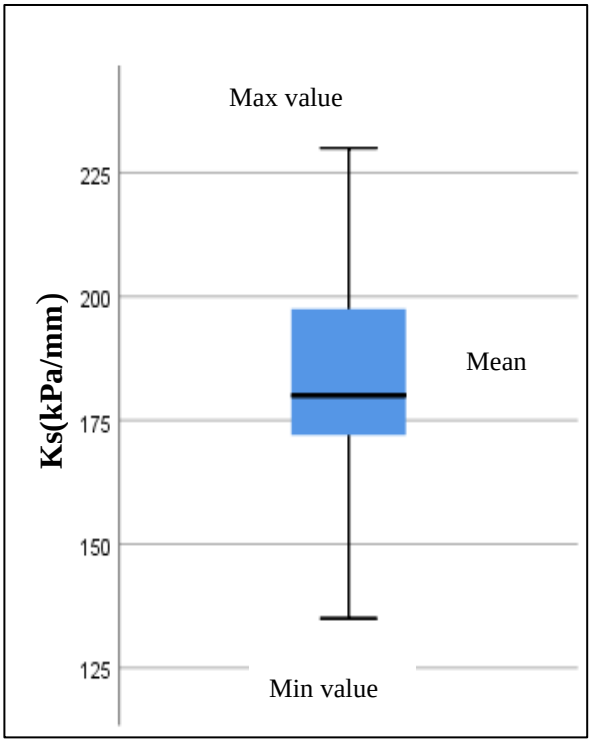

(c) Box plot for subgrade reaction modulus

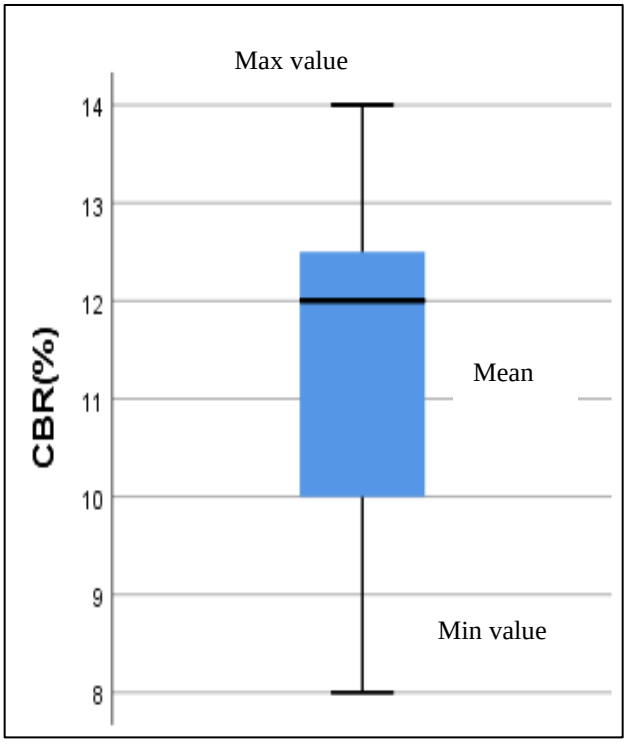

(d) Box plot for California bearing capacity

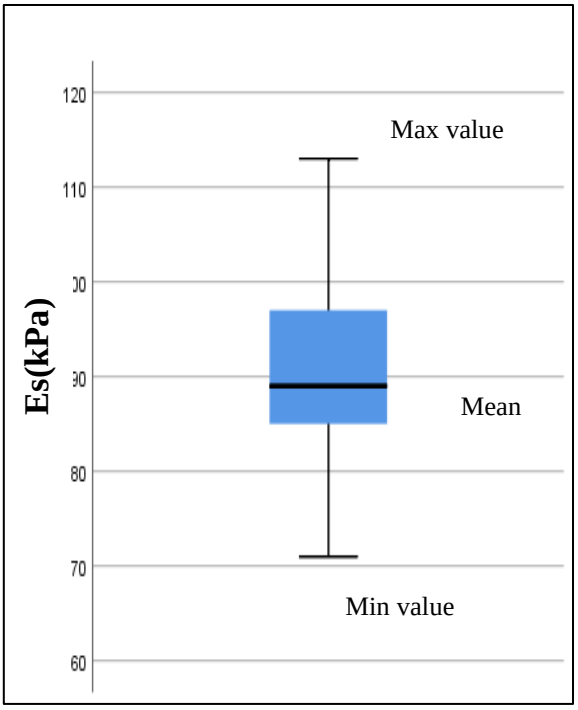

(e) Box plot for elastic modulus

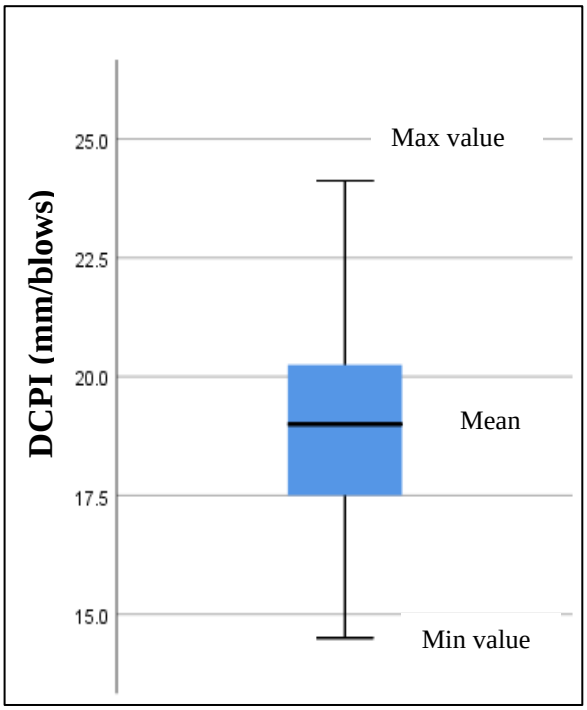

(f) Box plot for DCPI index

Figures (5.1) Results of Outliers Test

5.2.2 Normality Test

Normality tests are used in statistics to examine if a data set is well-modeled by a normal distribution and to compute the confidence that a random variable underlying the data set is normally distributed.

The normal probability plot, a quantile-quantile plot (QQ plot) of the standardized data with the standard normal distribution was utilized for assessing normality. The correlation between the sample data and normal quantiles in this case shows how well the data is described by a normal distribution. The normal Q-Q plot provides a graphical way to determine the level of normality. As shown in Figure (5.2), all experimental data lie somewhere near the black line, indicating that the data are normally distributed.

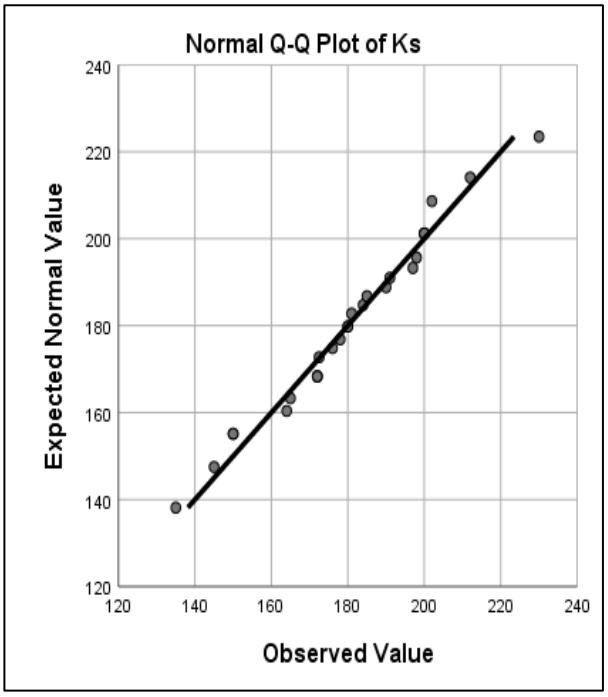

(a) Q-Q plot for ks

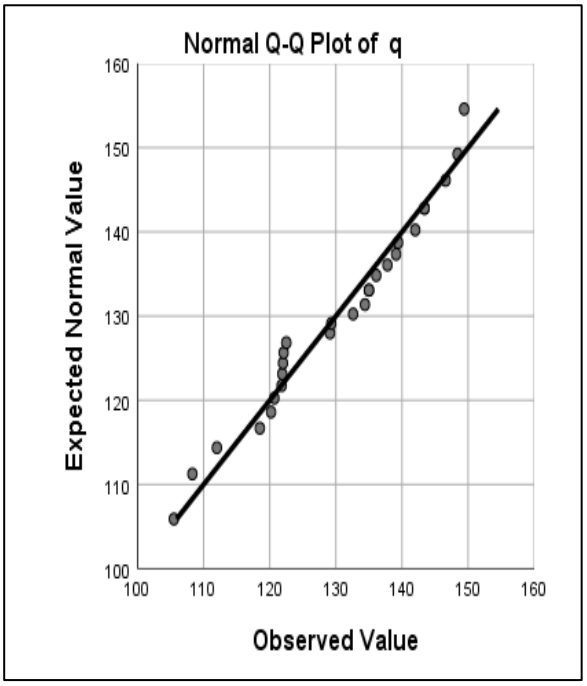

(b) Q-Q plot for q

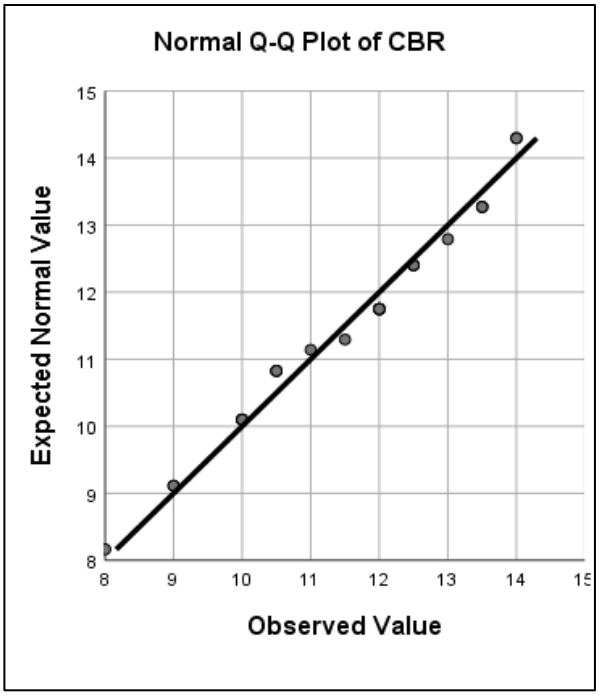

(c) Q-Q plot for CBR

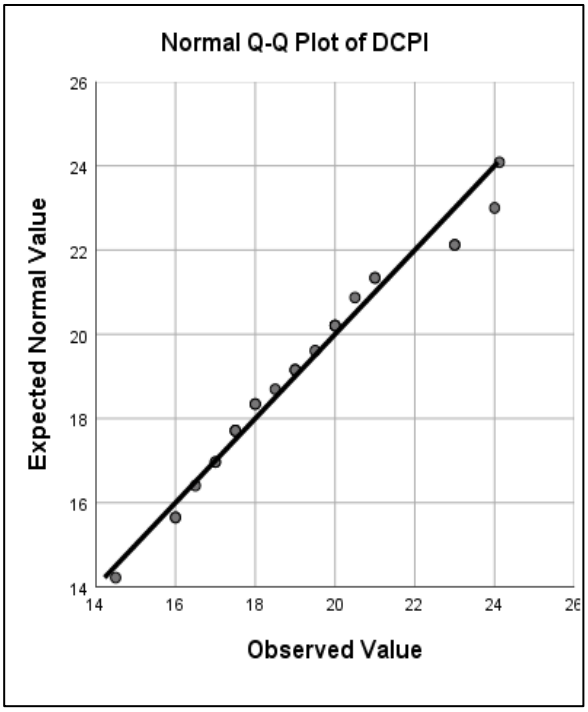

(d) Q-Q plot for DCPI

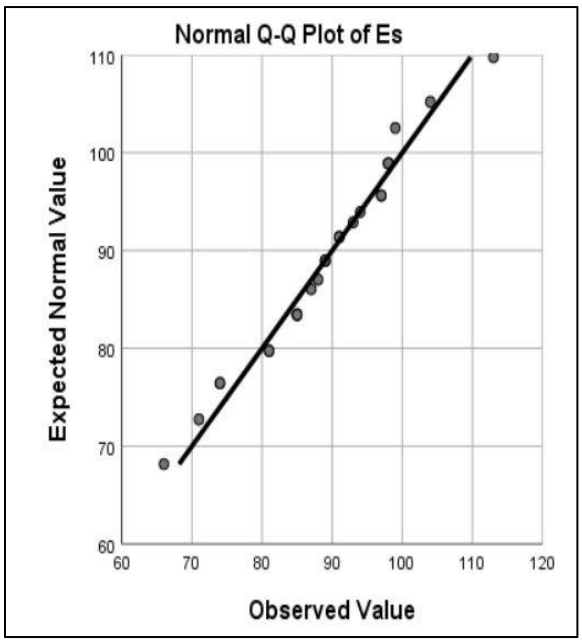

(e) Q-Q plot for Es

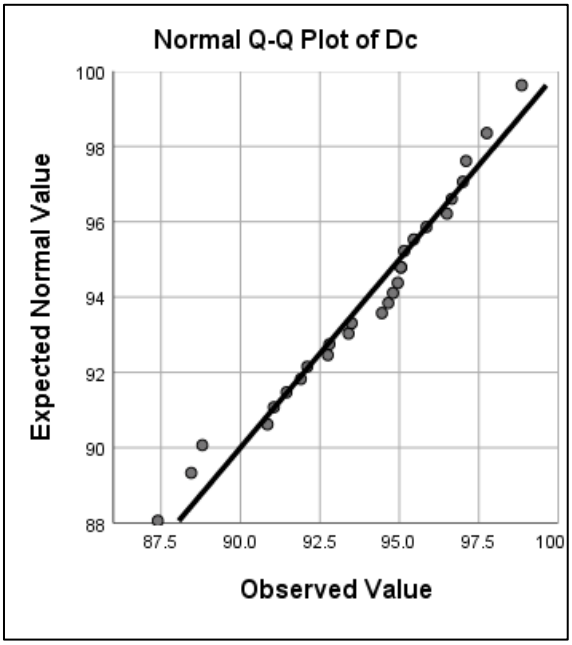

(f) Q-Q plot for Dc

Figures (5.2) Data results of normality test

5.3 Variables and their Correlation Coefficients

SPSS is used to determine the relationship between the variables. As the first step in developing a model, Pearson matrix correlations for (A-3) subgrade soils are employed. Correlation is a statistical method for determining how closely two variables are related.

The formula gives a value ranging from -1 to 1, with 1 signifying a strong positive correlation, -1 significant negative correlation, A zero result implies that there is no link at all.

The results using SPSS Pearson's applied math analysis to correlate between the variables are presented in Table 5.1. This table can be show:

1. The dependent parameter (ks) has a positive high degree of correlation with several independent variables from the DCP test, such as CBR and bearing capacity, and a negative high correlation with DCPI. It is possible to develop a theoretical correlation model between these parameters and subgrade reaction modulus.

2. The DCP measurements (i.e., CBR, bearing capacity, and DCPI) found a high correlation. It was shown that there is a high negative connection between DCPI and (CBR, bearing capacity). In addition, the connection between (CBR) and (bearing capacity) is a high correlation.

3. The subgrade reaction modulus (ks) indicates a significant positive connection with a degree of compaction.

Table (5-1) Pearson matrix correlations for (A-3) subgrade soils

		ks	CBR	DCPI	q	Dc	Es
ks	Pearson Correlation	1	.900**	-.787**	.845**	.918**	1.000**
	Sig. (2-tailed)		0.000	0.000	0.000	0.000	0.000
	N	27	27	27	27	27	27
CBR	Pearson Correlation	.900**	1	-.919**	.981**	.979**	.901**
	Sig. (2-tailed)	0.000		0.000	0.000	0.000	0.000
	N	27	27	27	27	27	27
DCPI	Pearson Correlation	-.787**	-.919**	1	-.961**	-.907**	-.794**
	Sig. (2-tailed)	0.000	0.000		0.000	0.000	0.000
	N	27	27	27	27	27	27
q	Pearson Correlation	.845**	.981**	-.961**	1	.959**	.849**
	Sig. (2-tailed)	0.000	0.000	0.000		0.000	0.000
	N	27	27	27	27	27	27
Dc	Pearson Correlation	.918**	.979**	-.907**	.959**	1	.922**
	Sig. (2-tailed)	0.000	0.000	0.000	0.000		0.000
	N	27	27	27	27	27	27
Es	Pearson Correlation	1.000**	.901**	-.794**	.849**	.922**	1
	Sig. (2-tailed)	0.000	0.000	0.000	0.000	0.000	
	N	27	27	27	27	27	27

**. Correlation is significant at the 0.01 level (2-tailed).

5.4 Regression Analysis

There are various types of regression analysis, such as linear, multiple linear, and nonlinear. Simple linear and multiple linear models are the most popular. Nonlinear regression analysis is typically employed for more complex data sets with a nonlinear connection between the dependent and independent variables. (Blunch, 2012)

Linear regression is a statistical method for modeling the connection between a scalar response and one or more explanatory variables (also known as dependent and independent variables). Simple linear regression is used when there is only one explanatory variable; multiple linear regression is used when there are more than one.

- Simple linear: The simple linear equation between a dependent coefficient and one independent coefficient are represented by the equation below:(Jawad, 2019)

$$y = a + xb + c \tag{5.1}$$

Where:

y: dependent parameter

x: independent parameter

a: Constant represents y intercept

b: slope of the regression line

c: estimating value error for y

- Multiple linear regression: the following equation use to predict the value of a dependent variable based on at least two coefficient other variables, as shown in eq (5.2)

$$y = a + a_1 \text{ x } X_1 + a_2 \text{ x } X_2 \ldots \text{etc} \quad (5.2)$$

Where:

y: dependent parameters

X1, and X2: independent parameters

a: Constant represent y intercept

a1, a2... an: slope of the regression

Nonlinear regression is a type of statistics analysis, which observational data modeled by a function that is a nonlinear combination model parameters and is dependent on at least one independent variable. The relations between the dependent and independent parameters are represented as non-linear (commonly as a curve). The model's purpose is to reduce the sum of the squares as much as possible. (Archontoulis and Miguez,2013).

The determination of the influence that independent variables have on the dependent variable in a regression analysis, for which analysts utilize the ANOVA. The analysis of variance (ANOVA) method is a parameterized statistical method for analyzing samples. It is employed in the comparison of means and their respective variances.

5.4.1 Models based on physical soil properties

A model for estimating subgrade reaction modulus for subgrade (A-3) soils was constructed using plate load test to calculate ks value and physical soil parameters including: Dc, Cc, Cu. The modeling results are shown in Tables (5.2) and (5.3), which include the model expression and ANOVA test, respectively.

The analysis was carried out by examining into the correlation of each physical variable's - ks value independently. Multi - linear correlations was developed using the principles of a selected regression model, which has a higher R^2 value than other models (linear, inverse, logarithmic, quadratic, cubic, power, … etc.) as shown in Table (5.2). The models' expressions for these relationships were shown in Figure (5.3). Table (5.2) depicts the created model and its limitation with a confidence range of 95%. Table (5.3) shows the ANOVA results, which indicate that the MSE is low and the residual sum of squares (SSE) is lower than the regression sum of squares (SSR), indicating that the model is still significant. Furthermore, the high R square (0.846) value implies a good prediction. Figure (5.3) explains the adequacy of the model and the acceptability of scattered between the predicted and measured ks. Also, it can be recognized that all values within the significant 95 % level boundaries. Figure (5.4) shows the scatter of residual points around the mean zero. In this Figure the residuals are plotted against the independent variable (ks).

Table (5-2) Multi – linear for ks - physical properties (A-3) soils

ks = -425.253 + 6.875 Dc +23.105 Cc + 19.465 Cu				
parameter	Estimate	Std. Error	95% Confidence Interval	
			lower Bound	Upper Bound
b	-425.253	55.665	-540.405	-310.101
b1	6.875	0.632	5.567	8.182
b2	23.105	19.113	-16.432	62.643
b3	-19.465	11.249	-42.737	3.806
R Square	0.846	R Adjusted Square		0.864

Table (5-3) ANOVA test result for ks - physical properties

source	Sum of Squares	df	Mean Square
Regression	10248	3	3416
Residual	1618	23	700350
Total	11866.130	26	
Dependent Variable: ks			
Predictors: (Constant), Dc, Cc, Cu			

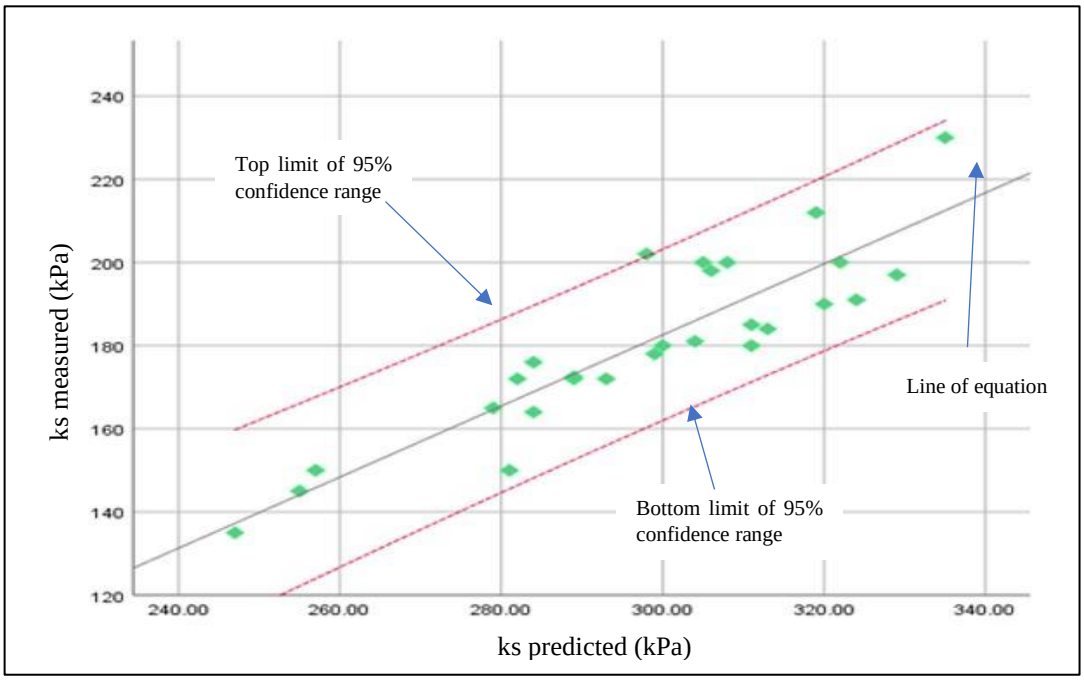

Figure (5.3) ks measure vs ks predicted from ks – physical properties equation for (A-3) soil.

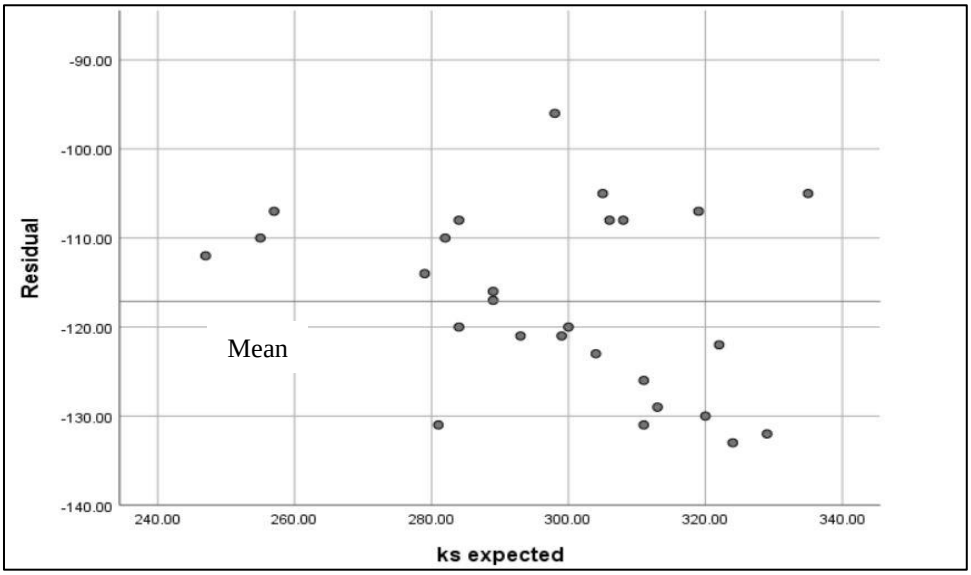

Figure (5.4) Residuals vs. ks – from physical properties for (A-3) subgrade soils.

5.4.2 Models based on DCP measurements

Three models for estimating subgrade reaction modulus for subgrade (A-3) soils were developed using three DCP parameters (CBR, DCPI, q). The modeling results are shown in Tables (5.4), (5.5) and (5.6) which include the model expression and ANOVA, respectively.

The analysis was carried out by examining into the correlation of each DCP variable's - ks value independently as shown in Figures (5.5) throughout (5.7). Linear correlations were developed using the principles of a selected regression model, which had a higher R^2 value than other models (linear, inverse, logarithmic, quadratic, cubic, power, … etc.) as shown in Table (5.4). The models' expressions for these relationships were shown in Figure (5.5) throughout (5.7). Table (5.5) depicts the created model and its limitation with a confidence range of 95%. Table (5.6) shows the ANOVA results, which show that the MSE is low and the residual sum of squares (SSE) is lower than the regression sum of squares (SSR), indicating that the model is still significant. Furthermore, the high R square (0.854) value implies a good prediction. Figure (5.8) explains the adequacy of the model and the

acceptability of scattered between the predicted and measured Ks. From the figure, it can be recognized that all values within the significant level 95 % boundaries. Figure (5.9) shows the scatter of residual points around the mean zero. In this Figure the residuals are plotted against the independent variable (ks) to check the normality assumption with 95 % level of confidence.

Table (5-4) Linear regression for ks – DCP parameter (A-3) soil

Ind. coefficient	D. coefficient	Equations of models	R square	Std. Error	Predicted parameters
ks	CBR	ks= b + b(CBR)	0.81	9.485	b = 46.816 b1 = 11.707
	DCPI	ks= b + b1 (DCPI)	0.619	13.449	b = 311.130 b1 = - 6.805
	q	ks= b + b1 (q)	0.714	11.648	b = - 12.074 b1 = 1.481

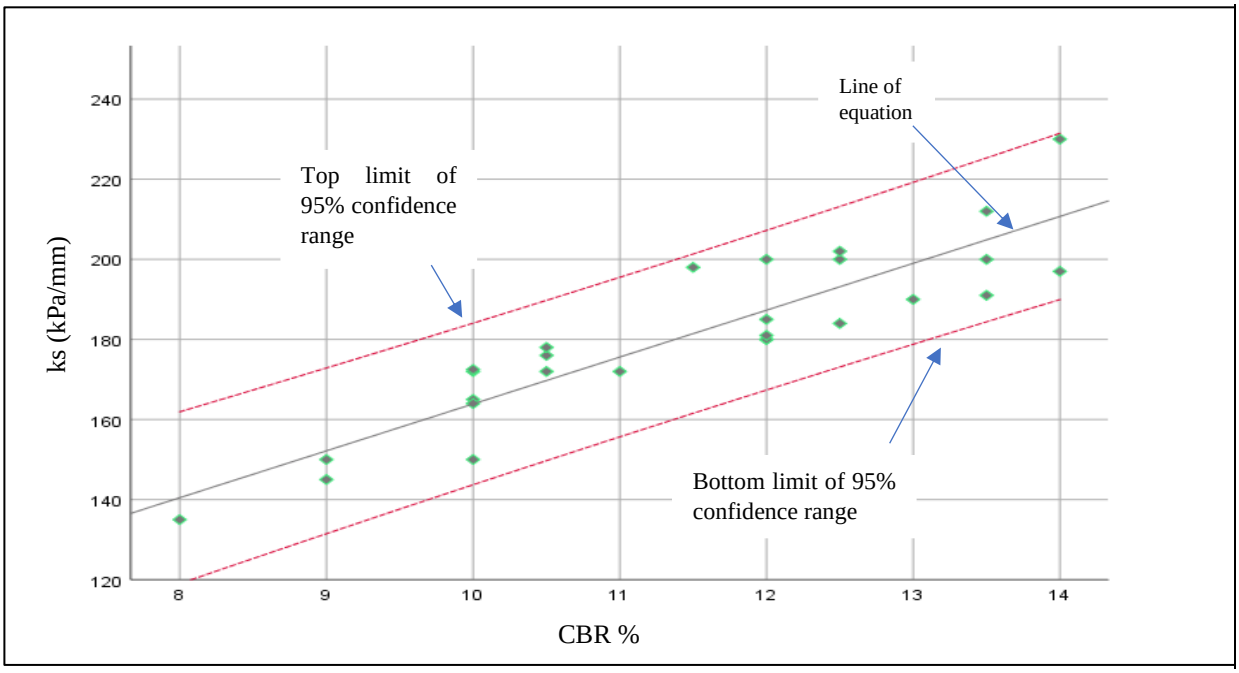

Figure (5.5) ks vs California bearing ratio expression for (A-3) soil.

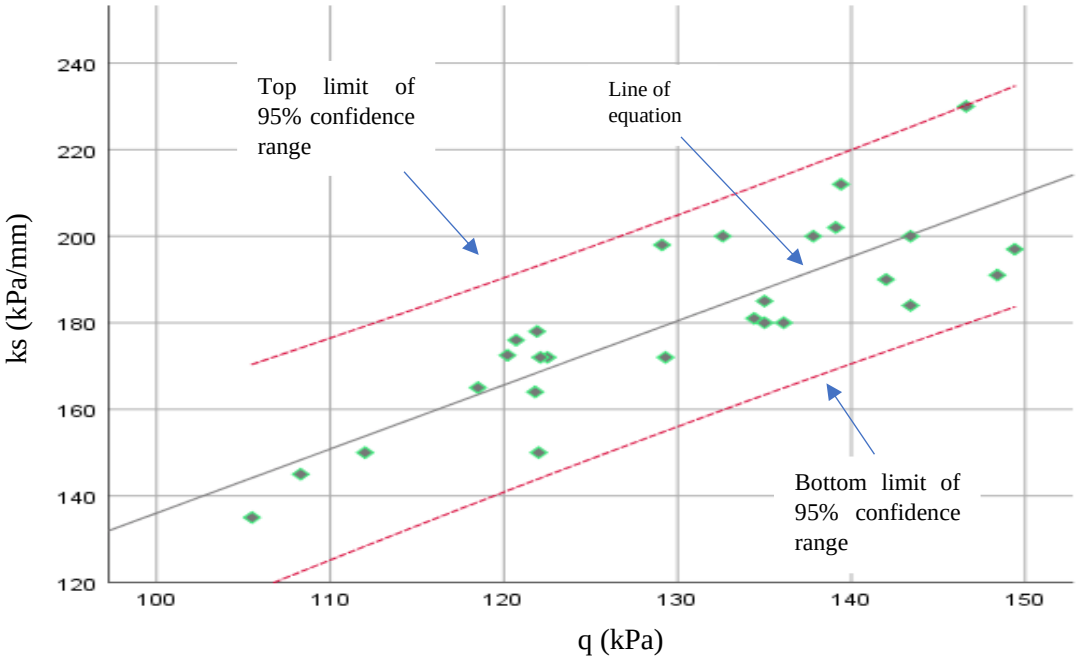

Figure (5.6) ks vs bearing capacity expression for (A-3) soil

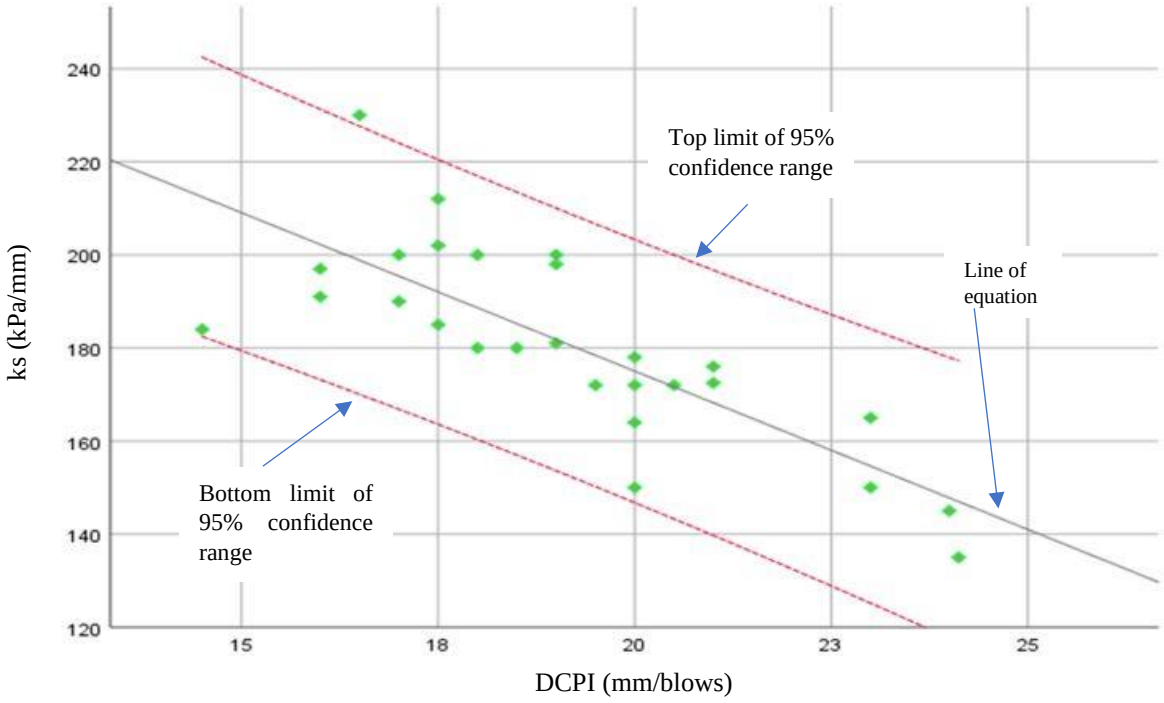

Figure (5.7) ks vs DCPI expression for (A-3) soil

Table (5-5) Multi - linear regression for ks – DCP parameter **(**A-3) soils

ks = 259.478 + 26.943 CBR - 2.608 DCPI -2.588 q				
parameter	Estimate	St. Error	95% Confidence Interval	
			lower Bound	Upper Bound
b	259.478	141.687	-33.624	552.580
b1	26.943	5.903	14.732	39.153
b2	-2.608	2.75	-8.297	3.081
b3	-2.588	1.13	-4.925	-0.251
R Square	0.854	R Adjusted Square	0.835	

Table (5-6) ANOVA test result for ks – DCP parameters

Model	Sum of Squares	df	Mean Square	F
Regression	10137.232	3	3379.077	44.953
Residual	1728.897	23	75.169	
Total	11866.130	26		
Dependent Variable: ks				
Predictors: (Constant), q, DCPI, CBR				

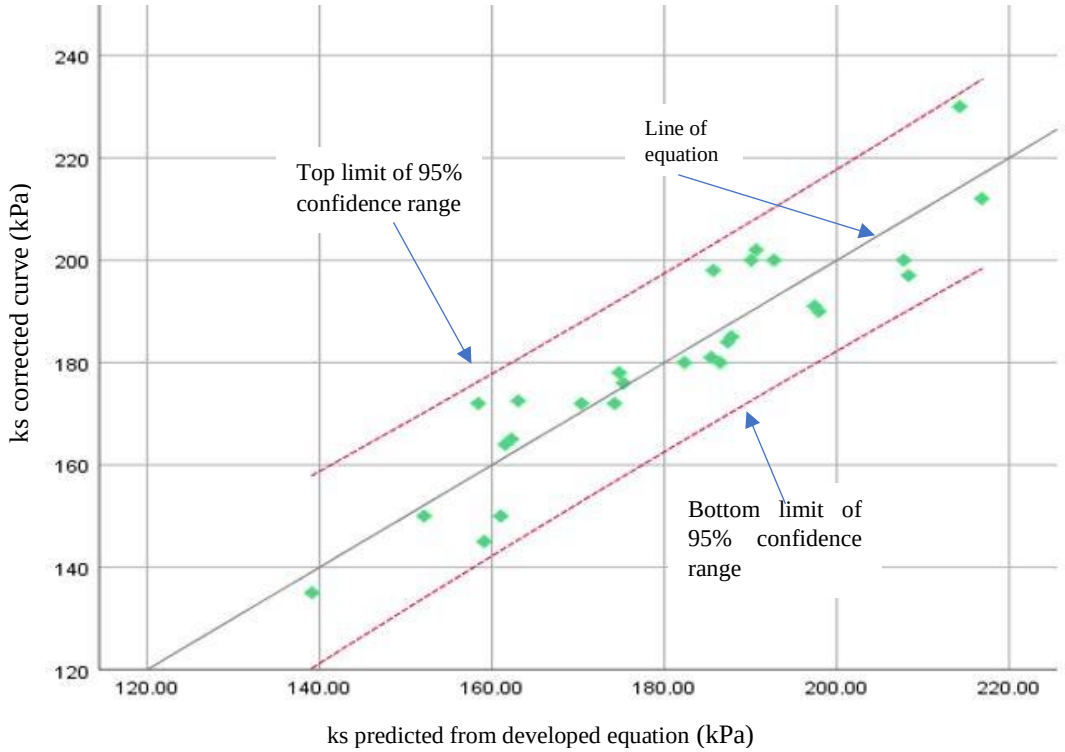

Figure (5.8) ks measure vs ks predicted from DCP- ks equation for (A-3) soil.

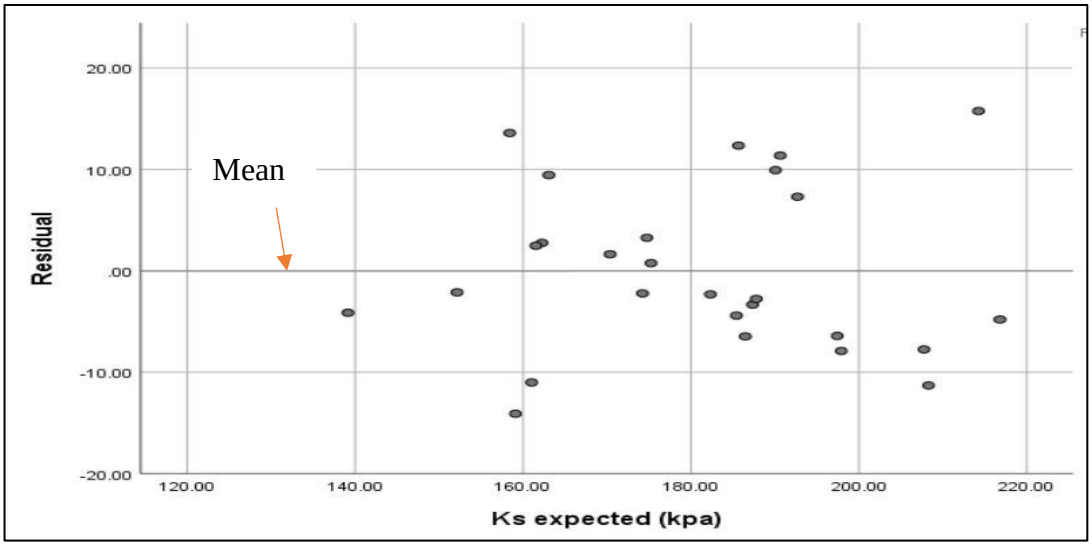

Figure (5.9) Residuals vs. ks from DCP measurements for (A-3) subgrade soils.

5.4.3 Model based on DCP – Basic physical properties

A model for estimating subgrade reaction modulus for subgrade (A-3) soils was developed based on physical parameters (Dc, Cc, Cu) and DCP parameters (CBR, DCPI, q). The modeling results are shown in Tables (5.7) and (5.8), which include the model expression, parameter estimate, ANOVA, respectively.

The analysis was carried out by examining into the correlation of each physical variable's - ks value independently. Multi - linear correlations was developed using the principles of a selected regression model, which has a higher R^2 value than other models (linear, inverse, logarithmic, quadratic, cubic, power, … etc.). Table (5.7) depicts the created model and its limitation with a confidence range of 95%. Table (5.8) shows the ANOVA results, which indicate that the MSE is low and the residual sum of squares (SSE) is lower than the regression sum of squares (SSR), indicating that the model is still significant. Furthermore, the high R square (0.886) value implies a good prediction. Figure (5.10) explains the adequacy of the model and the acceptability of scattered between the predicted and measured Ks. From the figure, it can be recognized that all values within the significant level 95 % boundaries, one point out of the confidence level. Figure (5.11) shows the scatter of residual points

around the mean zero. In this Figure the residuals are plotted against the independent variable (ks).

Table (5-7) Multi - linear regression for ks – DCP and physical properties (A-3) soils

ks = -228.773+13.066 CBR - 2.084 DCPI -2.057 q + 6.340 DC + 7.985 Cc - 11.245 Cu				
parameter	Estimate	Std. Error	95% Confidence Interval	
			lower Bound	Upper Bound
b	-228.773	277.710	-808.066	350.520
b1	13.066	8.302	-4.251	30.383
b2	-2.084	3.045	-8.436	4.268
b3	-2.057	1.204	-4.568	0.454
b4	6.340	2.829	0.438	12.242
b5	7.985	20.801	-35.406	51.376
b6	-11.245	12.739	-37.817	15.328
R Square	0.886	R Adjusted Square		0.852

Table (5-8) ANOVA test result for ks – DCP and physical parameters

Model	Sum of Squares	df	Mean Square
Regression	10512.330	6	1752.055
Residual	1353.799	20	67.690
Total	11866.130	26	
Dependent Variable: ks			
Predictors: (Constant), Cu, CBR, Cc, DCPI, Dc, q			

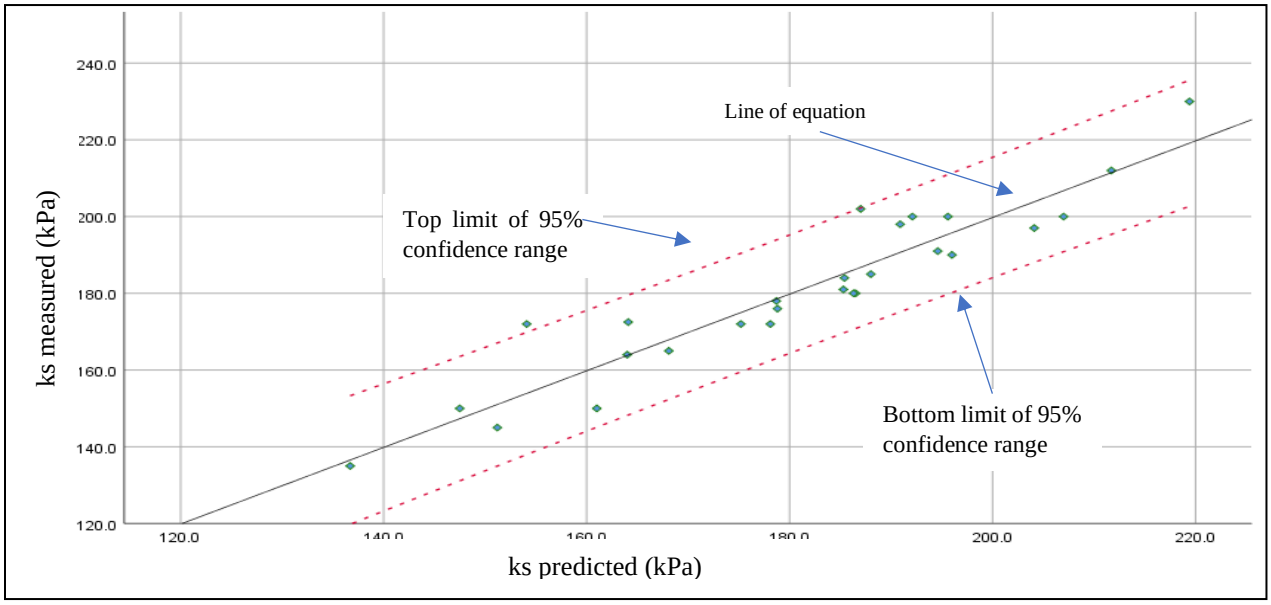

Figure (5.10) ks measure vs ks predicted based on ks-DCP and Basic Soil Properties equation for (A-3) soil.

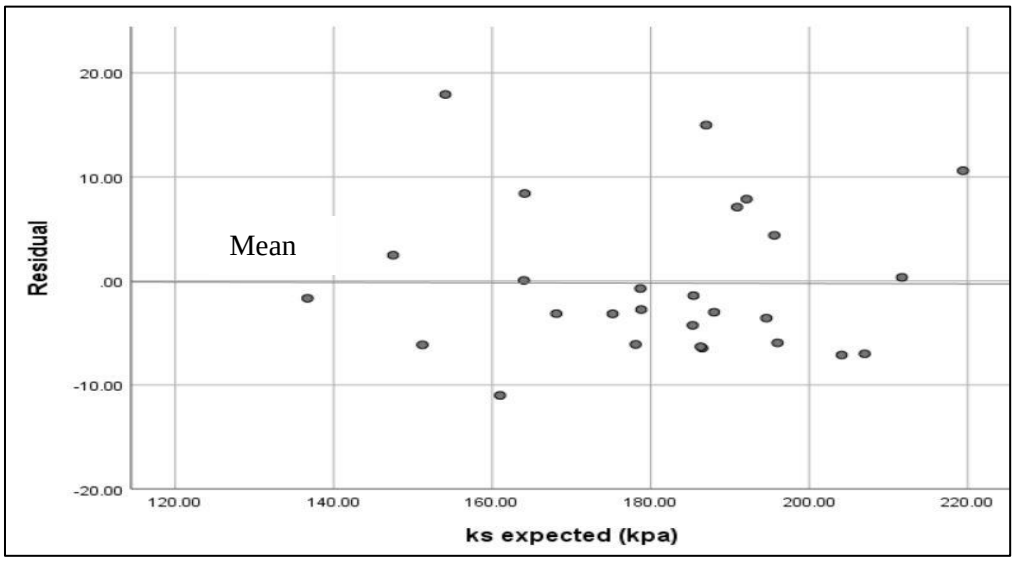

Figure (5.11) Residuals vs. ks from DCP and physical properties model for (A-3) subgrade soils.

5.4.4 Model predict Es based on DCP – Basic physical properties

A model for estimating elastic modulus for subgrade (A-3) soils was developed based on physical parameters (Dc, Cc, Cu) and DCP parameters (CBR, DCPI, q). Tables (5.9) and (5.10) illustrate the modeling results, model expression and ANOVA, respectively.

The analysis was carried out by examining into the correlation of each physical variable's - Es value independently. Multi - linear correlations was developed using the principles of a selected regression model, which has a higher R^2 value than other models (linear, inverse, logarithmic, quadratic, cubic, power, … etc.) as shown in Table (5.9). Table (5.10) depicts the created model and its limitation with a confidence range of 95%. Table (5.10) shows the ANOVA results, which indicate that the MSE is low and the residual sum of squares (SSE) is lower than the regression sum of squares (SSR), indicating that the model is still significant. Furthermore, the high R square (0.887) value implies a good prediction. Figure (5.10) explains the adequacy of the model and the acceptability of scattered between the predicted and measured Es. From the figure, it can be recognized that all values

within the significant level 95 % boundaries, one point out of the confidence level. Figure (5.11) shows the scatter of residual points around the mean zero. In this Figure the residuals are plotted against the independent variable (ks).

Table (5-9) Multi - linear regression for Es – DCP and physical properties (A-3) soils

Es = -119.962+5.813 CBR - 1.158 DCPI -0.995 q + 3.273 DC + 3.495 Cc - 5.272 Cu				
parameter	Estimate	Std. Error	95% Confidence Interval	
			lower Bound	Upper Bound
b	-119.962	134.604	-400.740	160.816
b1	5.813	4.024	-2.580	14.207
b2	-1.158	1.476	-4.237	1.921
b3	-0.995	0.583	-2.213	0.222
b4	3.273	1.371	0.412	6.133
b5	3.495	10.082	-17.536	24.526
b6	-5.272	6.174	-18.151	7.607
R Square	0.887	R Adjusted Square		0.85

Table (5-10) ANOVA test results for Es – DCP and physical parameters

Model	Sum of Squares	df	Mean Square
Regression	2502.921	6	417.153
Residual	318.042	20	15.902
Total	2820.963	26	
Dependent Variable: Es			
Predictors: (Constant), Cu, CBR, Cc, DCPI, Dc, q			

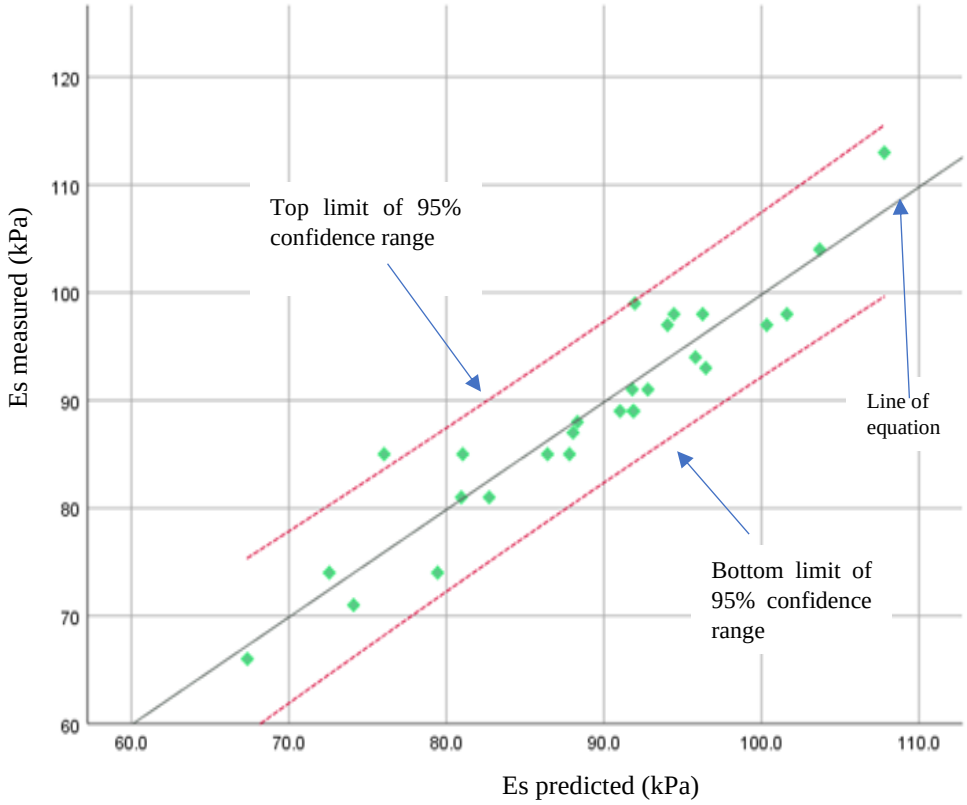

Figure (5.12) Es measure vs Es predicted based on Es-DCP and Basic Soil Properties equation for (A-3) soil.

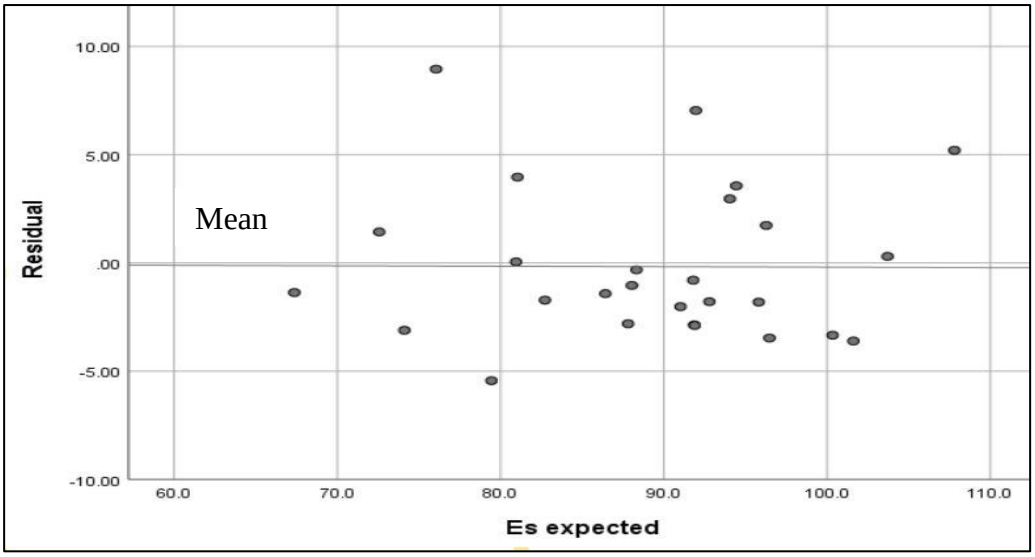

Figure (5.13) Residuals vs. Es from DCP and Basic Soil Properties for (A-3) subgrade soils.

5.5 Comparison between developed and published model

The comparison study using the FFA equation confirmed the validity of our developed empirical formula. Federal Aviation Administration (2009) shows the result of statistical analysis in the equation below:

$$Ks = (1500CBR/26)^{0.7788} \text{---------- (2.6)}$$

Table (5.11) shows that the values predicted from the developed model equation by published model.

Table (5-11) Linear regression for ks – CBR (A-3) soils

Ind. variable	D. variable	Models' expression	R square	Std. Error	Estimated parameters
ks	CBR	ks= b + b(CBR)	0.81	9.485	b = 46.816 b1 = 11.707

The difference has a maximum value of 15% and a minimum value of 13%, this indicates that there is a good convergence between the model that was developed and the FAA model, which also verifies the accuracy of the predicted data from experimental work.

Table (5-12) Comparison between developed and published model

NO	CBR (%)	ks from developed model(kPa/mm)	ks Federal Aviation Administration (2009) (kPa/mm)	Different between ks developed .vs ks Federal
1	8	140.47	118.82	0.15
2	9	152.18	130.23	0.14
3	9	152.18	130.23	0.14
4	10	163.89	141.37	0.14
5	10.5	169.74	146.85	0.13
6	11	175.59	152.26	0.13
7	12.5	193.15	168.20	0.13
8	12	187.30	162.94	0.13
9	12.5	193.15	168.20	0.13
10	10	163.89	141.37	0.14
11	10	163.89	141.37	0.14
12	10.5	169.74	146.85	0.13
13	12.5	193.15	168.20	0.13

Table (5-11) comparison between developed and published model(continue)

14	12	187.30	162.94	0.13
15	12	187.30	162.94	0.13
16	14	210.71	183.72	0.13
17	13	199.01	173.42	0.13
18	13.5	204.86	178.59	0.13
19	10	163.89	141.37	0.14
20	10.5	169.74	146.85	0.13
21	10	163.89	141.37	0.14
22	12	187.30	162.94	0.13
23	11.5	181.45	157.63	0.13
24	12	187.30	162.94	0.13
25	13.5	204.86	178.59	0.13
26	14	210.71	183.72	0.13
27	13.5	204.86	178.59	0.13

5.6 Summary

Statistical analysis modeling is an essential tool for evaluating the subgrade reaction modulus because it helps to understand the significance of various characteristics including DCP parameters and physical parameters. This chapter showed the potential of three sets of statistical models for (A-3) sand soil to start up an effective model for predicting subgrade reaction modulus. These statistical models are classified into three groups:1st group: Models depended on DCP Measurements ,2nd group: Models depended on Basic Soil Properties,3rd group: Models depended on DCP and subgrade basic Properties Additionally, a statistical model was developed to predict Es based on DCP and basic physical properties. The FAA model verifies the accuracy of the predicted data from experimental work. The difference has a maximum value of 15% and a minimum value of 13%.

Chapter six

Conclusions and Recommendations

6.1 Conclusions

1. (A-3) subgrade soil which is categorized as a poorly graded sand soil with a gypsum content, is the most common subgrade soil type in Karbala city.

2. It was observed that as a soil compaction increase, strength and stiffness characteristics determined from the PLT test and DCP test increase as well.

3. Based on physical soil properties including (Dc, Cc and Cu), it was found that a multi-linear statistical model with R^2= 84 % provides a highly accurate subgrade reaction modulus prediction.

4. The soil bearing resistance (i.e., CBR) obtained from DCP test was found to be the most significant statistical independent parameter to estimate subgrade reaction modulus using linear statistical model with R^2= 81%.

5. Based on DCP measurements (CBR, DCPI, q) and physical properties measurements, it was found that multi linear statistical model provides the best subgrade reaction modulus prediction with R^2=88%.

6. The findings indicated that DCP devices could be used as a non-destructive device to estimate the subgrade reaction modulus in rigid pavement design accurately and quickly.

7. The results of experimental work showed that the highest value of degree of compaction is (98.85%) for (18 NOP) and the lowest value is (87.43%) in for (10 NOP)، the values of ks ranged from 135 to 230 kPa/mm, DCPI value varied from 14.5 to 26 mm/blow, CBR ranged from 8 to 13.5%, q ranged from 105.45 to 149.42

kPa. These results were statistically analyzed and related with each other to find the best fit regression model to predict ks.

8. The comparison study using the FFA equation confirmed the validity of our developed empirical formula. There is good convergence between the developed model and the FAA model, with a maximum difference of 15% and a minimum difference of 13%.

6.2 Recommendations and Further Works

1. Additional field experiments (PLT and DCP) are suggested to verify the theoretical models developed in this study, such as using finite element method to measure the subgrade reaction modulus.

2. To develop other statistical models, various types of subgrade soils, such as clay soils, should be selected.

3. Because of its simplicity, ability to carry it and shorten inspection times, the dynamic cone penetrometer is a successful device for construction examination of any pavement project.

4. It is recommended to evaluate properties of subgrade soils stabilized using chemical stabilization method to improve the strength.

References

AASHTO *M145*, (2012),"Standard Specification for Classification of Soils and Soil-Aggregate Mixtures for Highway Construction Purposes," American Association of State and Highway Transportation Officials, Washington, DC.

AASHTO T222, (2007), "Nonrepetitive static plate load test of soil and flexible pavement components for use in evaluation and design of airport and highway pavements. "American Association of State Highway and Transportation Officials, Washington, .

Abu-Farsakh, M., Nazzal, M., Alshibli, K., and Seyman, E. (2005). Part 2: Soil Parameters for Pavement Design and Subgrade Resilient Modulus: Application of Dynamic Cone Penetrometer in Pavement Construction Control. *Transportation Research Record: Journal of the Transportation Research Board*, *1913*, 52–61. https://doi.org/10.3141/1913-06

Al-Refeai, T., and Al-Suhaibani, A. (1997). Prediction of CBR Using Dynamic Cone Penetrometer. *Journal of King Saud University - Engineering Sciences*, *9*(2), 191–203. https://doi.org/10.1016/S1018-3639(18)30676-7

Arau´jo, D. A. M., Costa, C. M. L., and Costa, Y. D. J. (2017). Dimension effect on plate load test results. *World Congress on Civil, Structural, and Environmental Engineering*, *c*, 1–6. https://doi.org/10.11159/icgre17.191

Aron, C., Jonas, E., Caselunghe, A., and Eriksson, J. (2012). Structural Element Approaches for Soil-Structure Interaction. *Master of Science Thesis in the Master's Programme Structural Engineering and Building Performance Design*, 64.

ASTM D1556. (2000). Standard Test Method for Density and Unit Weight of Soil in Place by the Sand-Cone Method. *ASTM International, West Conshohocken, PA, American Society for Testing and Materials*, *04*, 1–7.

ASTM D6951. (2003). Standard Test Method for Use of the Dynamic Cone Penetrometer in Shallow Pavement Applications. ASTM International, West Conshohocken, PA., June, 1–7. https://doi.org/10.1520/D6951

Archontoulis S. V. and Fernando E. Miguez., (2013).,"Nonlinear Regression Models and Applications in Agricultural Research." Agronomy Journal: Agron. J. 105:1–13 (2013).

ASTM D 1196, 2004. “Standard Test Method for Nonrepetitive Static Plate Load Tests of Soils and Flexible Pavement Components, for Use in Evaluation and Design of Airport and Highway Pavements," American Society for Testing and Materials (ASTM), West Conshohocken, PA.

ASTM D1883, 2014. “Standard Test Method for California Bearing Ratio (CBR) of Laboratory-Compacted Soils," American Society for Testing and Materials (ASTM), West Conshohocken, PA.

ASTM D6951,2009. “Standard Test Method for Use of the Dynamic Cone Penetrometer in Shallow Pavement Applications," American Society for Testing and Materials (ASTM), West Conshohocken, PA.

Atarigiya, B. (2019). Plate Load Test : Getting it Right Sustainable Development Plate Load Test : Getting it Right. *GHIE 50th Anniversary*, *March 2018*, 0–7.

Ayers, T. (2015). Rapid Shear Strength Evaluation of In Situ Granular Materials. *Transportation Research Record*. , 2(1), , 2(1), 34–40. https://doi.org/10.5923/j.jce.20120201.05

Barker, W. R. and Alexander, D. R., (2012)."Determining the Effective Modulus of Subgrade Reaction for Design of Rigid Airfield Pavements Having Base Layers.", Report No. 12-2 (ERDC/GSL TR), US Army Corps of Engineers, Engineer Research and Development Center, Geotechnical and Structures Laboratory.

Chukka, D., and Chakravarthi, V. K. (2012). Evaluation of Properties of Soil Subgrade Using Dynamic Cone Penetration Index – A Case Study. *International Journal of Engineering Research and Development*, *4*(4 ISSN: 2278-067X,p-2278-800X), 7–15.

CRD-C 655-95. (1995). "Standard test method for determining the modulus of soil reaction." Handbook for Concrete and Cement. U.S. Army Corps of Engineers.

Diner, I. (2011). Models to predict the deformation modulus and the coefficient of subgrade reaction for earth filling structures. Advances in Engineering Software, *42*(4), 160–171. https://doi.org/10.1016/j.advengsoft.2011.02.001

Eka Putri, E., V Kameswara Rao, N. S., and Mannan, M. A. (2012). Evaluation of Modulus of Elasticity and Modulus of Subgrade Reaction of Soils Using CBR Test. Journal of Civil Engineering Research, 2(1), 34–40. https://doi.org/10.5923/j.jce.20120201.05

Ghorbani, B., Arulrajah, A., Narsilio, G., Horpibulsuk, S., and Bo, M. W. (2020). Development of genetic-based models for predicting the resilient modulus of cohesive pavement subgrade soils. *Soils and Foundations*, *60*(2), 398–412. https://doi.org/10.1016/j.sandf.2020.02.010

Gupta, A., and Krawinkler, H. (1999). *S Eismic D Emands for P Erformance E Valuation of*. *132*, 141–148.

Hamid, A. M. (2015). The Dynamic Cone Penetration Test: A Review of its Correlations and Applications. International Conference on Advances in Civil and Environmental Engineering, August, 1–16. https://doi.org/10.13140/RG.2.2.13275.46882

Islam, K. M., Gassman, S., and Rahman, M. M. (2020). Field and Laboratory Characterization of Subgrade Resilient Modulus for Pavement Mechanistic-Empirical Pavement Design Guide Application. *Transportation Research Record*, *2674*(8), 921–930. https://doi.org/10.1177/0361198120926171

Khasawneh, M. A. (2019). Investigation of factors affecting the behaviour of subgrade soils resilient modulus using robust statistical methods. International Journal of Pavement Engineering, 20(10), 1193–1206. https://doi.org/10.1080/10298436.2017.1394101

Kim, D., and Park, S. (2011). Relationship between the subgrade reaction modulus and the strain modulus obtained using a plate loading test. *9th World Congress on Railway Research*, 11.

Kim, J. (2018). response of beams resting on linear and non- linear elastic foundations and subjected to harmonic high-speed moving loading askar ibrayev , beng in civil engineering submitted in fulfillment of the requirements for the degree of masters of science in civi. january.

Kleyn, E. G. (1975). The use of the dynamic cone penetrometer (DCP). Transvaal Provincial Administration.

Kofi Ampadu, S. I., and Yao Fiadjoe, G. J. (2015). The influence of water content on the Dynamic Cone Penetration Index of a lateritic soil stabilized with various percentages of a quarry by-product. Transportation Geotechnics, 5, 68–85. https://doi.org/10.1016/j.trgeo.2015.09.007

Konard and Lachance, 2000. (2008). Application of the Dynamic Cone Penetrometer (DCP) for determination of the engineering parameters of sandy soils. *Engineering Geology*, *101*(3–4), 195–203. https://doi.org/10.1016/j.enggeo.2008.05.006

Khazanovich, L., Tayabji, S. D., and Darter, M. I. (2001). "Back calculation of layer parameters for LTPP test sections, Volume I: Slab on elastic solid and slab on dense-liquid foundation analysis of rigid pavements. " Technical Rep. No. FHWA-RD-00-086, Federal Highway Administration, McLean, Va.

Lee, J., and Jeong, S. (2016). Experimental study of estimating the subgrade reaction modulus on jointed rock foundations. *Rock Mechanics and Rock Engineering*, *49*(6), 2055–2064. https://doi.org/10.1007/s00603-015-0905-9

shaban, A., and Engineering, G. (2018). Innovations in Geotechnical Engineering GSP 299 358. *Innovations in Geotechnical Engineering*, 358–370.

Ping, W. V., and Sheng, B. (2011). Developing correlation relationship between modulus of subgrade reaction and resilient modulus for Florida subgrade soils. *Transportation Research Record*, *2232*, 95–107. https://doi.org/10.3141/2232-10

Setiadji B. H., and Fwa T. F., ASCE. M. (2009). "Examining k - E Relationship of Pavement Subgrade Based on Load-Deflection Consideration." Journal of Transportation Engineering, Vol. 135, No. 3, March 1, 2009. ©ASCE, ISSN.

Scala, A.J. (1956). Simple Methods of Flexible Pavement Design using Cone Penetrometers, Proceedings of the 2nd Australian and New Zealand Conference on Soil Mechanics and Foundation Engineering, Christchurch.

Sowers, G.F.; and Hedges, C.S. (1966). Dynamic Cone for Shallow in- Situ Penetration Testing. Vane Shear and Cone Penetration Resistance Testing of In-Situ Soils, 29-37.

Rahim, A. M., and George, K. P. (2002). Automated dynamic cone penetrometer for subgrade resilient modulus characterization. *Transportation Research Record*, *1806*, 70–77. https://doi.org/10.3141/1806-08

Rajpurohit, V. K., Gore, N. G., and Sayagavi, V. G. (2014). Analysis of Structure Supported on Elastic Foundation. *International Journal of Engineering and Advanced Technology (IJEAT)*, *1*, 2249–8958.

Thach Nguyen, B., and Mohajerani, A. (2015). Determination of CBR for fine-grained soils using a dynamic lightweight cone penetrometer. *International Journal of Pavement Engineering*, *16*(2), 180–189. https://doi.org/10.1080/10298436.2014.937807

Truebe, M. A., Evans, G. L., and Bolander, P. (1995). Lowell test road: helping improve road surfacing design. *Proc. 6th Int. Conf. on Low-Volume Roads, Minneapolis, Minnesota*, *2*(1).

Tuleubekov, K., and Brill, D. R. (2014). Correlation between subgrade reaction modulus and CBR for airport pavement subgrades. *T and DI Congress 2014:* Planes, Trains, and Automobiles - Proceedings of the 2nd Transportation and Development Institute Congress, 813–822. https://doi.org/10.1061/9780784413586.079

U.S. Army Waterways Experiment Station. (1945). " Rigid plate bearing test investigation. ", Vicksburg, MS: U.S. Army Waterways Experiment Station.

Unified Facilities Criteria (UFC). (2001). "Pavement design for airfields". UFC 3-260-02. Washington, DC: Departments of the Army, Air Force, and Navy.

Van Vuuren, D.J. (1969). Rapid Determination of CBR with the Portable Dynamic Cone Penetrometer. The Rhodesian Engineer, 7(5),

Ziaie, R., and Alibolandi, M. (2012). Determination of subgrade reaction modulus of two layered soil Soil Reinforcement View project. June 2012. https://www.researchgate.net/publication/284730664

Appendix A

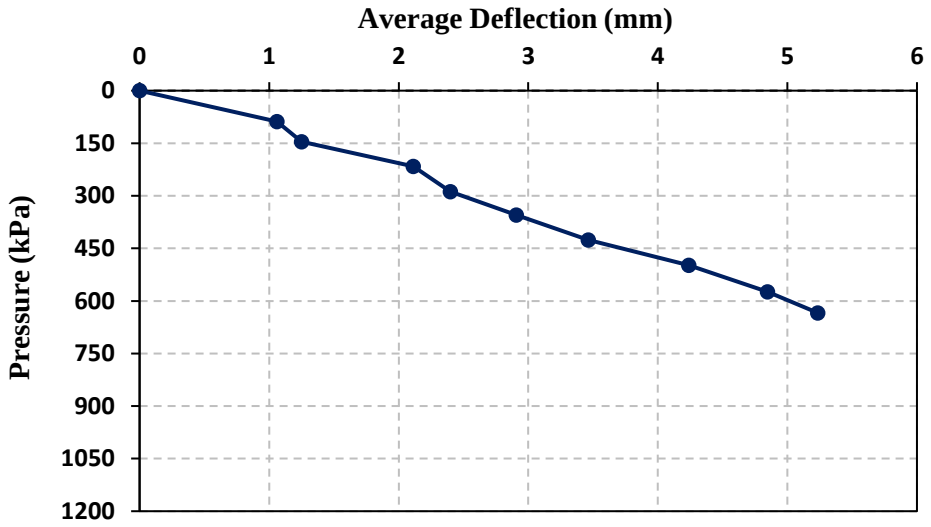

Figure (A-1) load-settlement curve of PLT tests(10 Nop) for (A-3) soil at Al-Tahadi

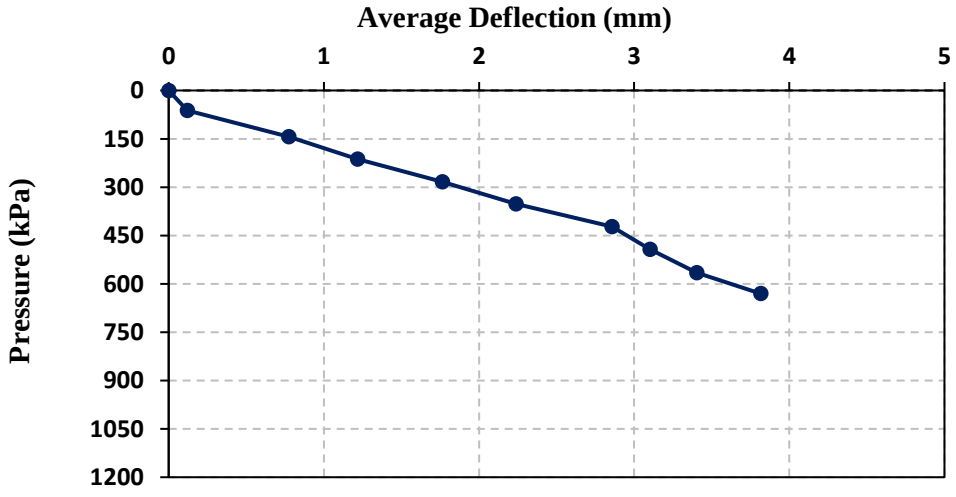

Figure (A-2) load-settlement curve of PLT tests(10 Nop) for (A-3) soil at Al-Tahadi

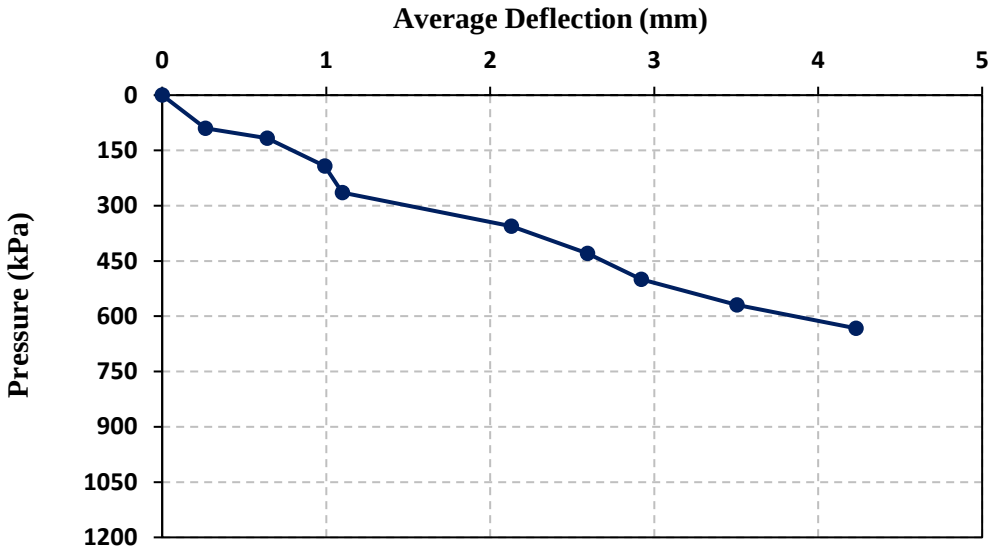

Figure (A-3) load-settlement curve of PLT tests(10 Nop) for (A-3) soil at Al-Tahadi

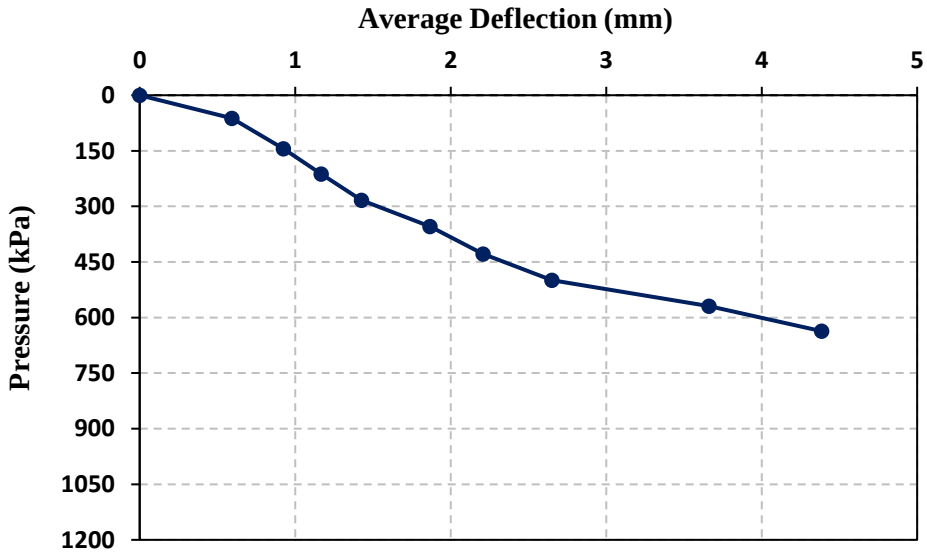

Figure (A-4) load-settlement curve of PLT tests(14 Nop) for (A-3) soil at Al-Tahadi

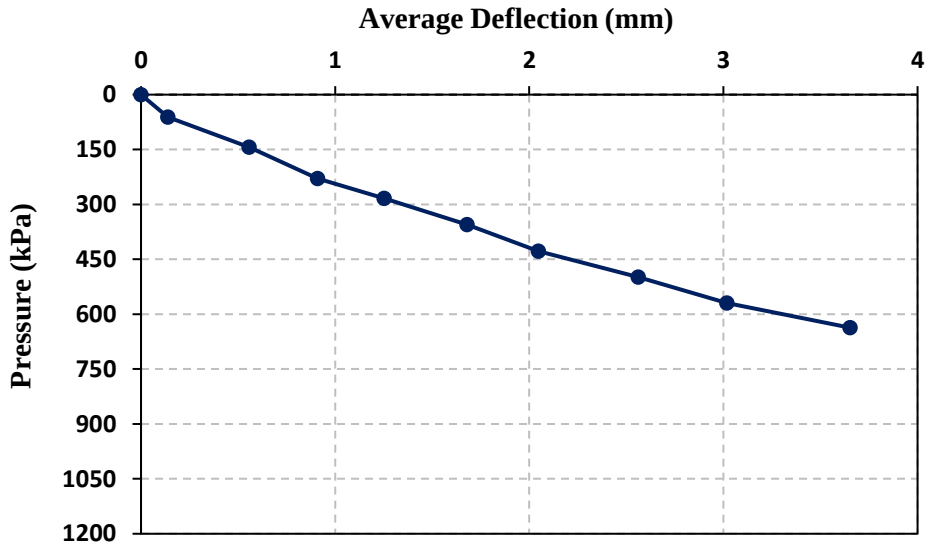

Figure (A-5) load-settlement curve of PLT tests(14 Nop) for (A-3) soil at Al-Tahadi

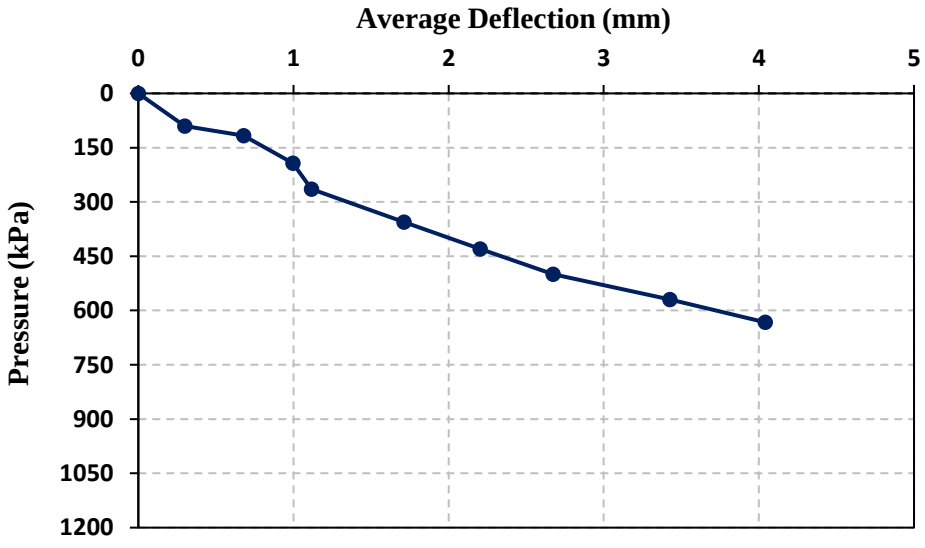

Figure (A-6) load-settlement curve of PLT tests(14 Nop) for (A-3) soil at Al-Tahadi

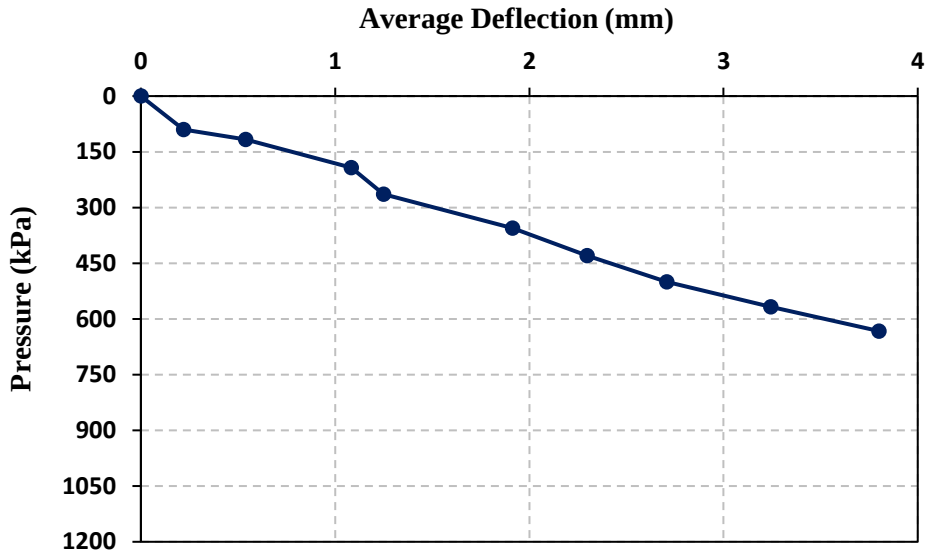

Figure (A-7) load-settlement curve of PLT tests(18 Nop) for (A-3) soil at Al-Tahadi

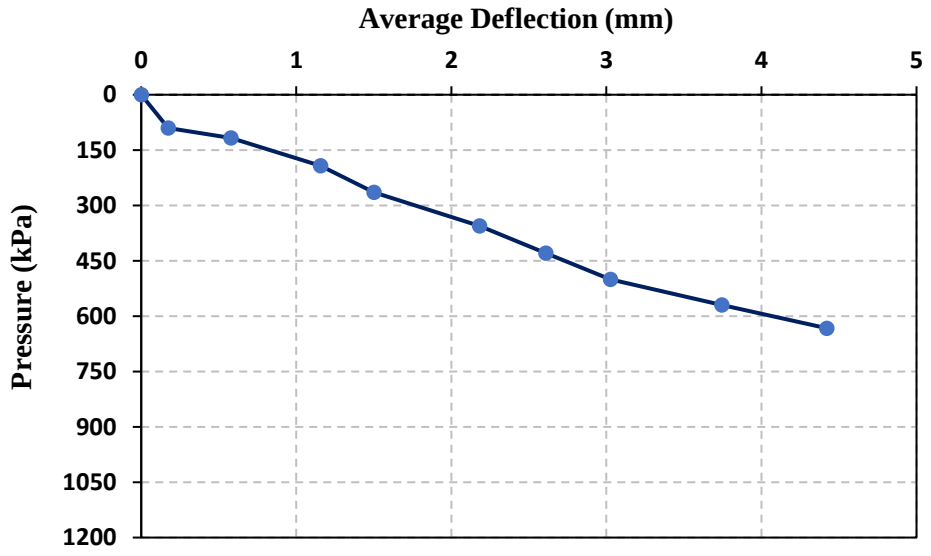

Figure (A-8) load-settlement curve of PLT tests(18 Nop) for (A-3) soil at Al-Tahadi

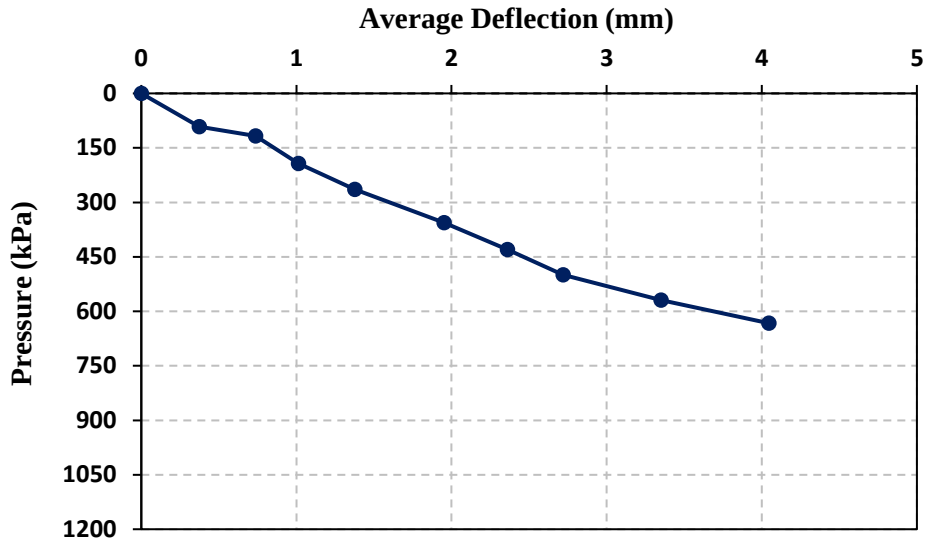

Figure (A-9) load-settlement curve of PLT tests(18 Nop) for (A-3) soil at Al-Tahadi

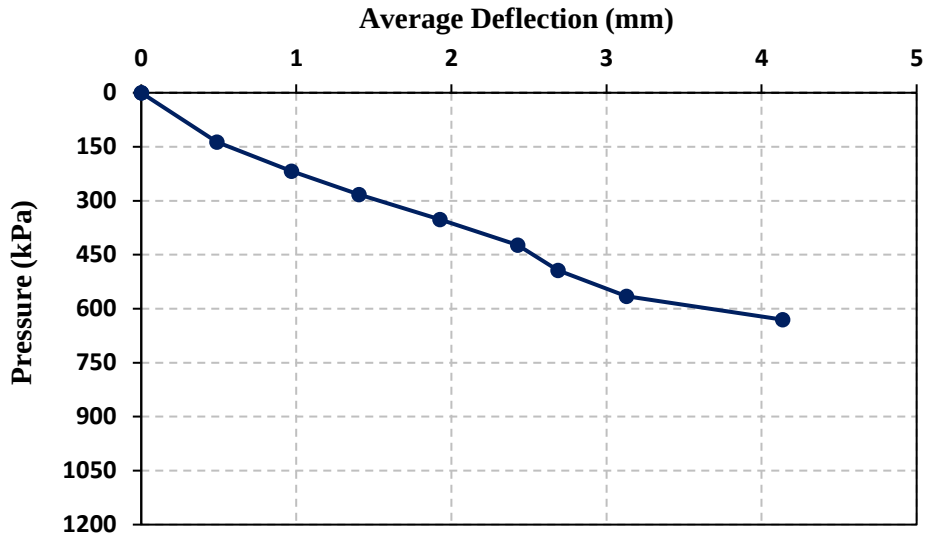

Figure (A-10) load-settlement curve of PLT tests(10 Nop) for (A-3) soil at Al-Fares

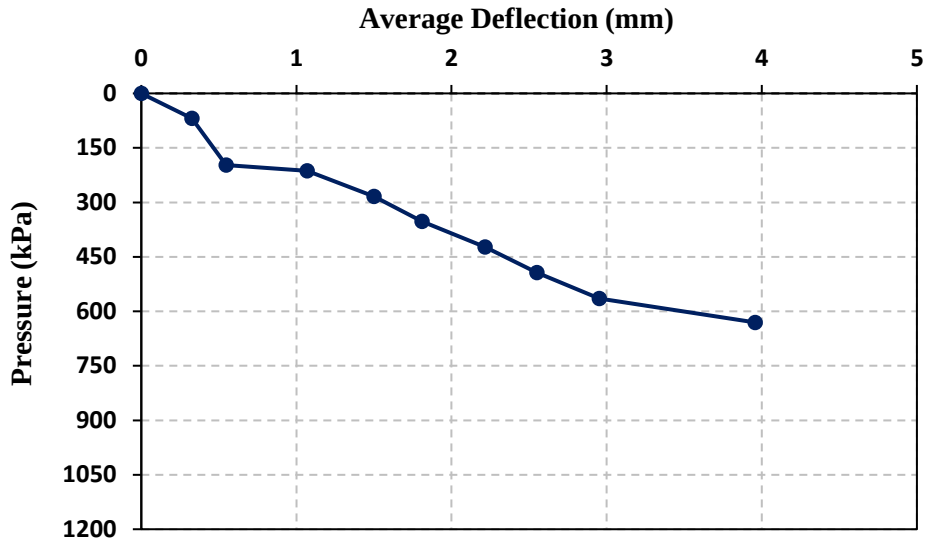

Figure (A-11) load-settlement curve of PLT tests(10 Nop) for (A-3) soil at Al-Fares

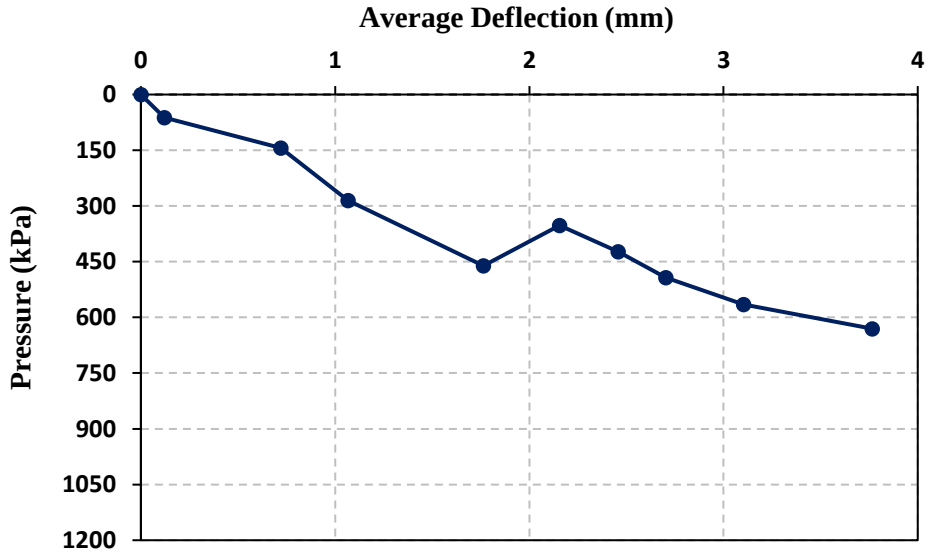

Figure (A-12) load-settlement curve of PLT tests(10 Nop) for (A-3) soil at Al-Fares

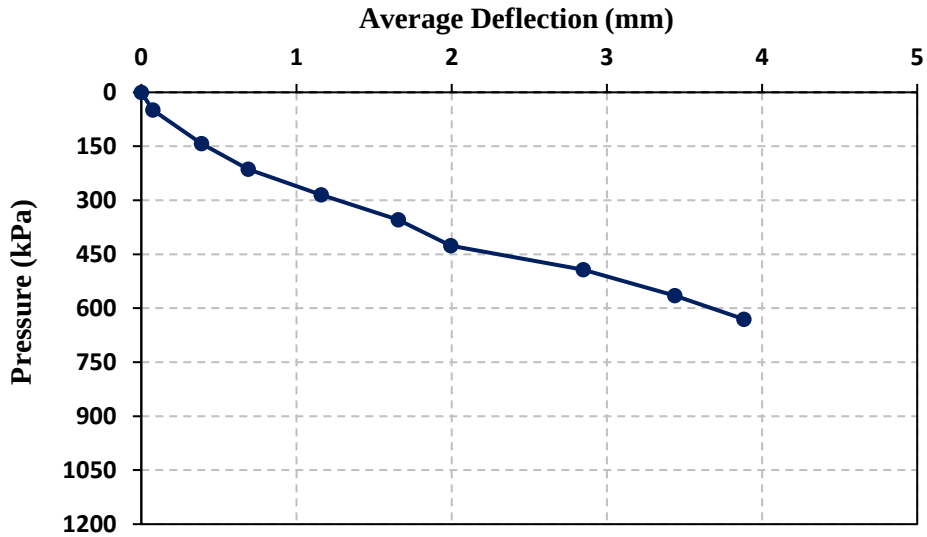

Figure (A-13) load-settlement curve of PLT tests(14 Nop) for (A-3) soil at Al-Fares

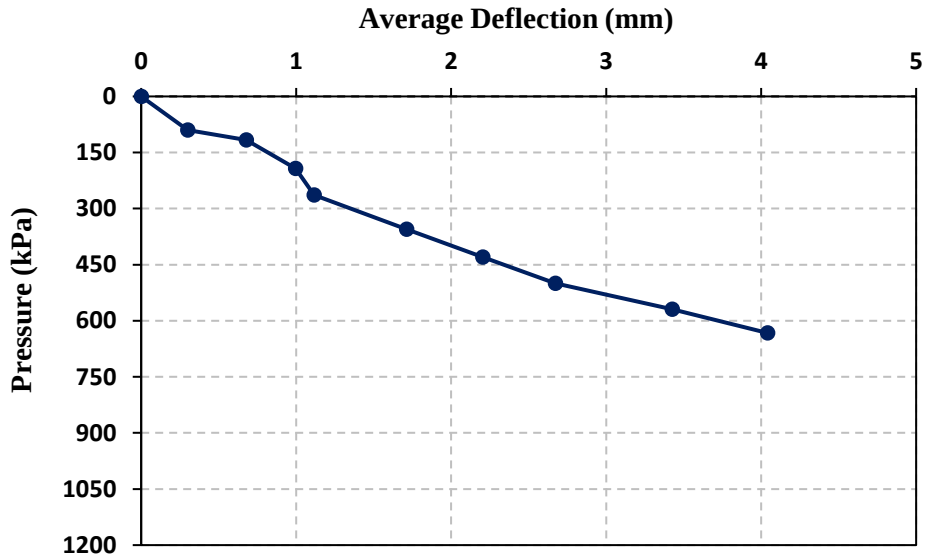

Figure (A-14) load-settlement curve of PLT tests(14 Nop) for (A-3) soil at Al-Fares

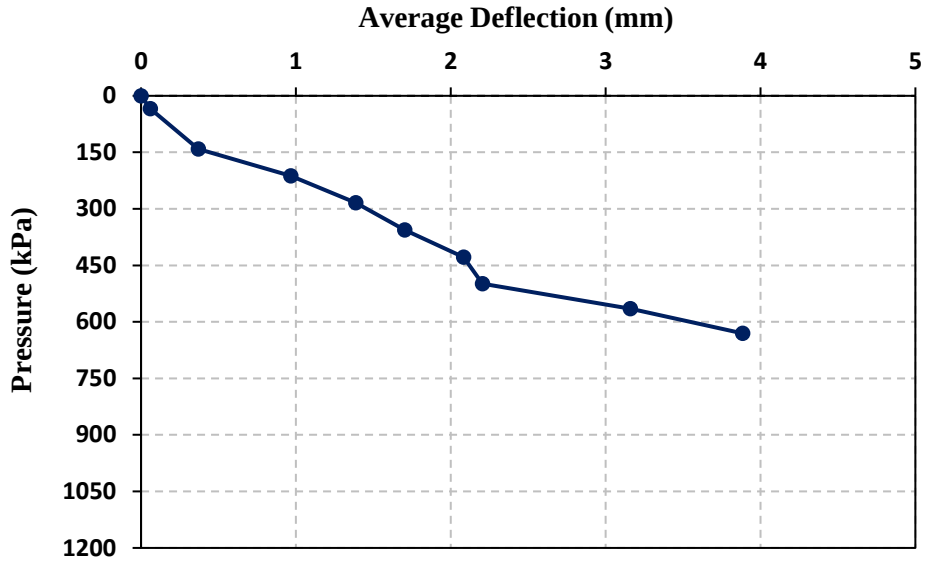

Figure (A-15) load-settlement curve of PLT tests(14 Nop) for (A-3) soil at Al-Fares

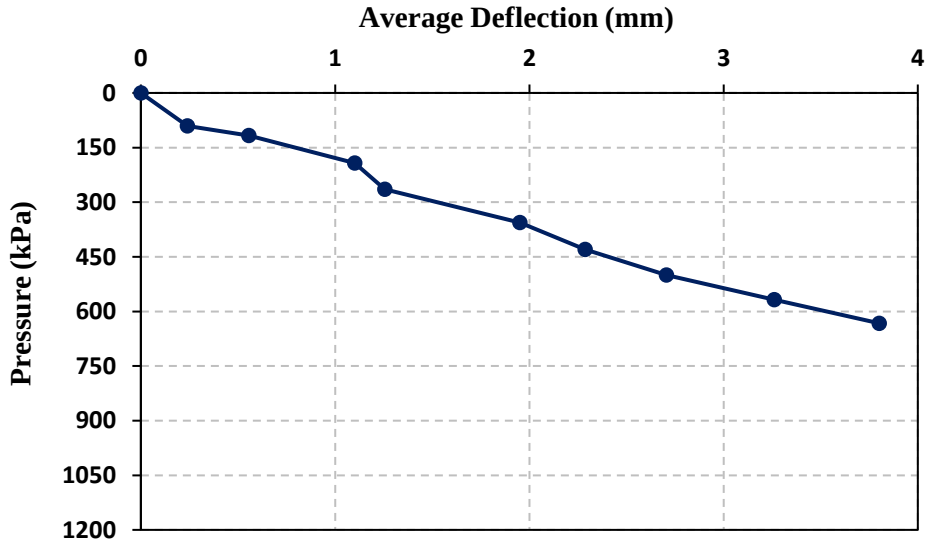

Figure (A-16) load-settlement curve of PLT tests(18 Nop) for (A-3) soil at Al-Fares

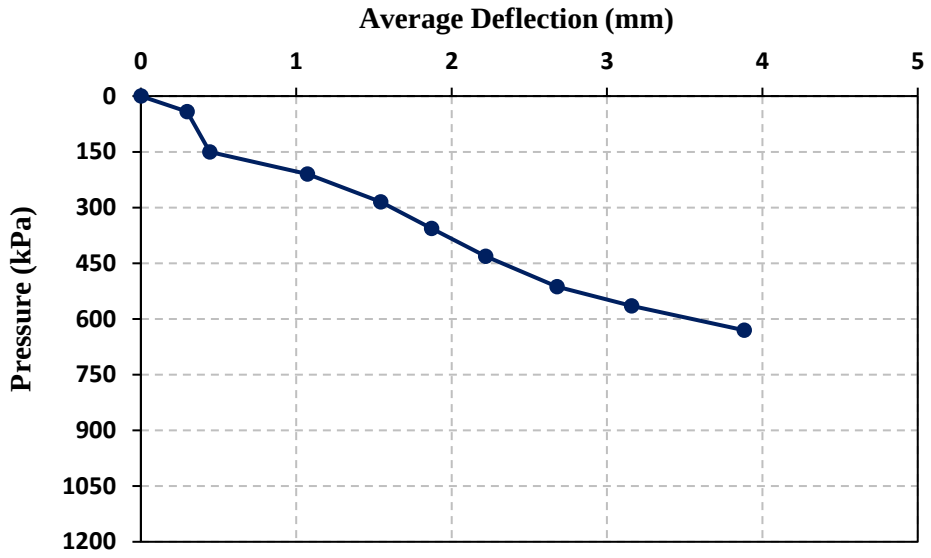

Figure (A-17) load-settlement curve of PLT tests(18 Nop) for (A-3) soil at Al-Fares

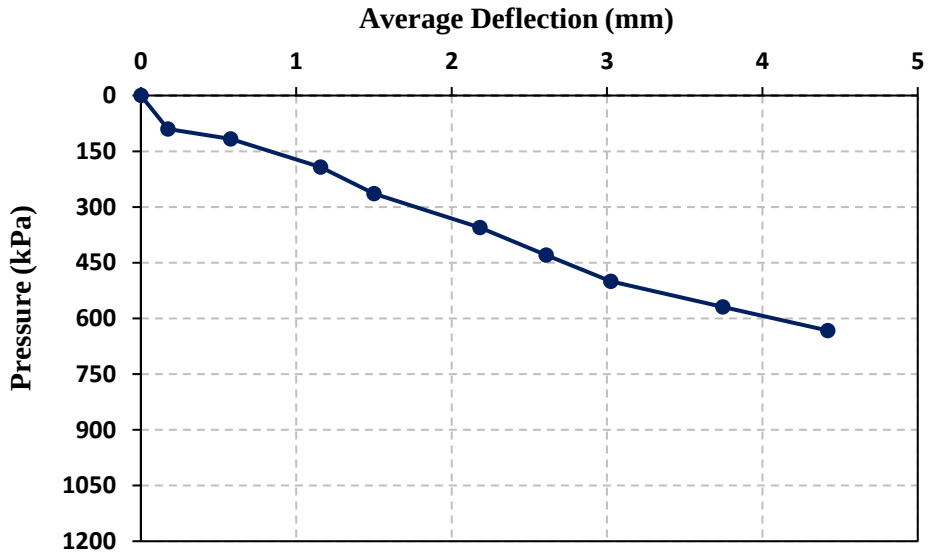

Figure (A-18) load-settlement curve of PLT tests(18 Nop) for (A-3) soil at Al-Fares

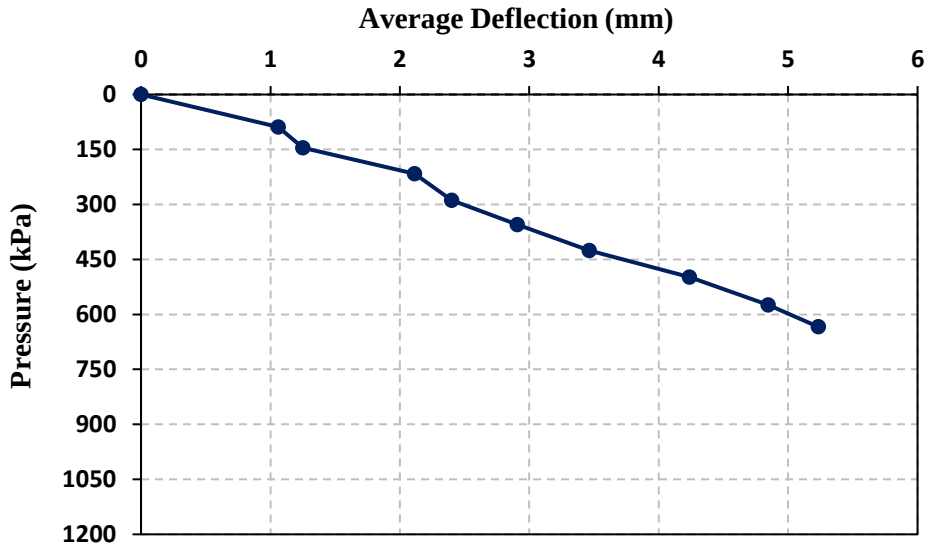

Figure (A-19) load-settlement curve of PLT tests(10 Nop) for (A-3) soil at Al-Intifada

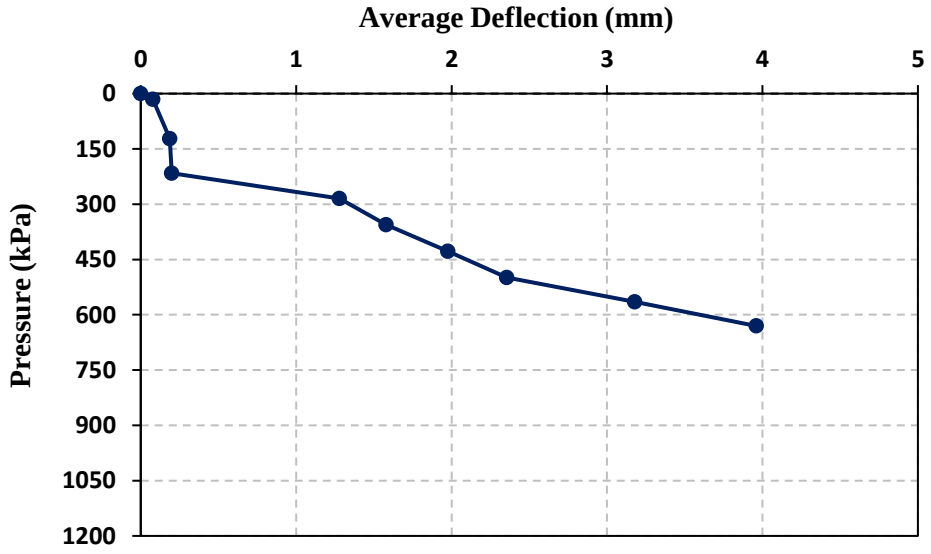

Figure (A-20) load-settlement curve of PLT tests(10 Nop) for (A-3) soil at Al-Intifada

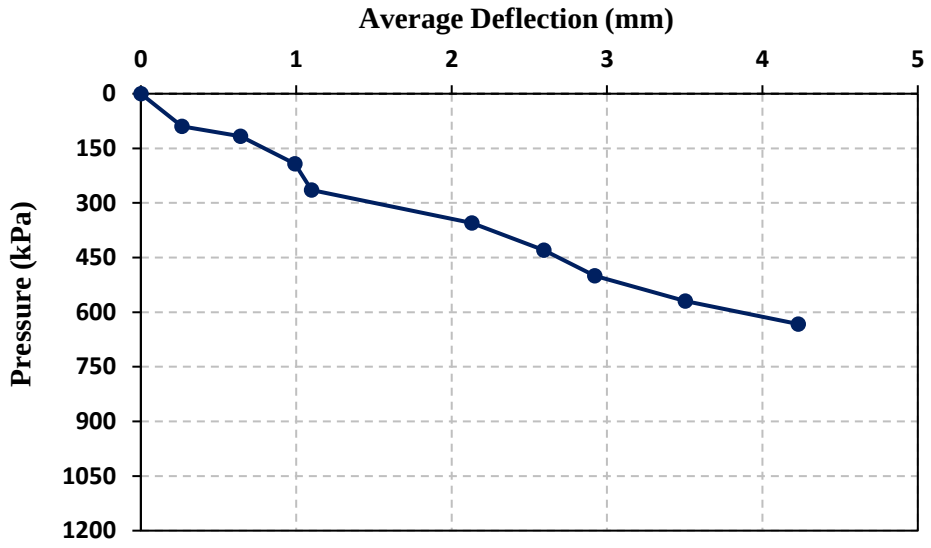

Figure (A-21) load-settlement curve of PLT tests(10 Nop) for (A-3) soil at Al-Intifada

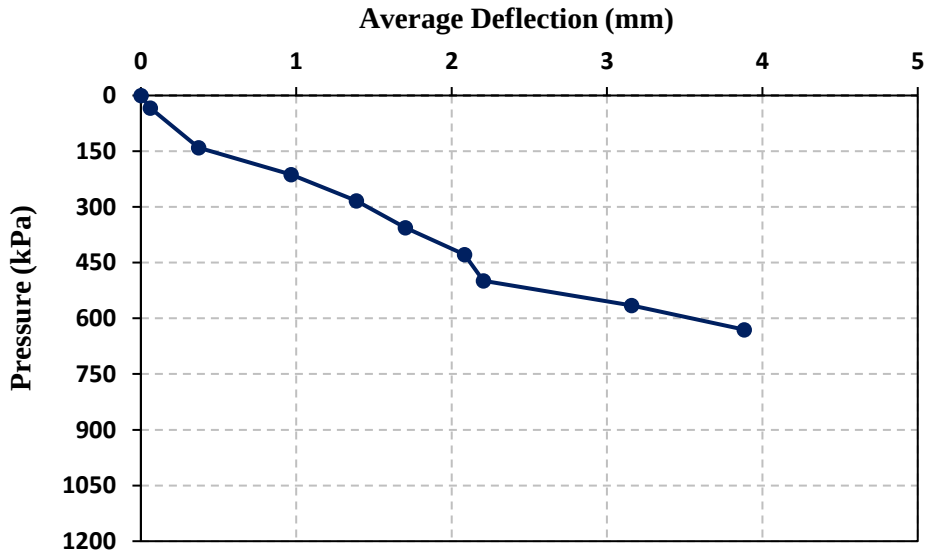

Figure (A-22) load-settlement curve of PLT tests(14 Nop) for (A-3) soil at Al-Intifada

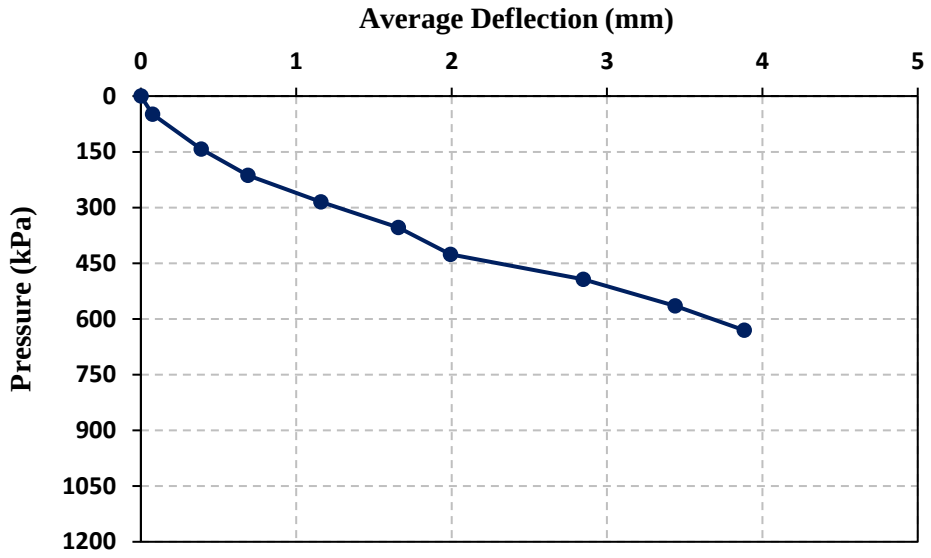

Figure (A-23) load-settlement curve of PLT tests(14 Nop) for (A-3) soil at Al-Intifada

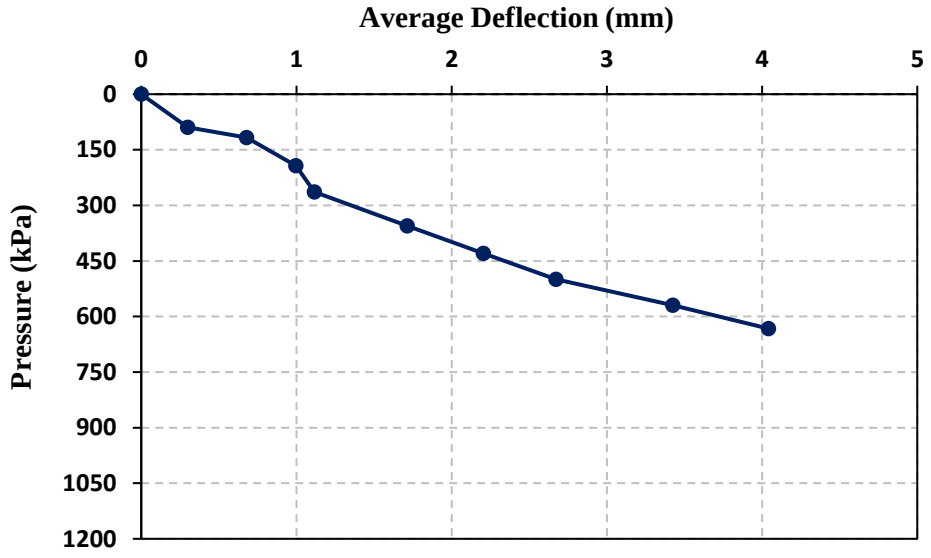

Figure (A-24) load-settlement curve of PLT tests(14 Nop) for (A-3) soil at Al-Intifada

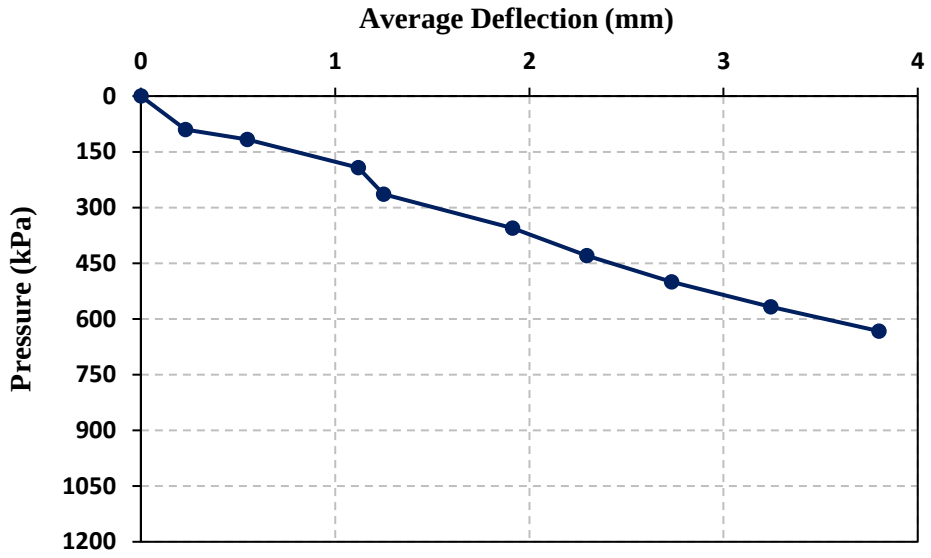

Figure (A-25) load-settlement curve of PLT tests(18 Nop) for (A-3) soil at Al-Intifada

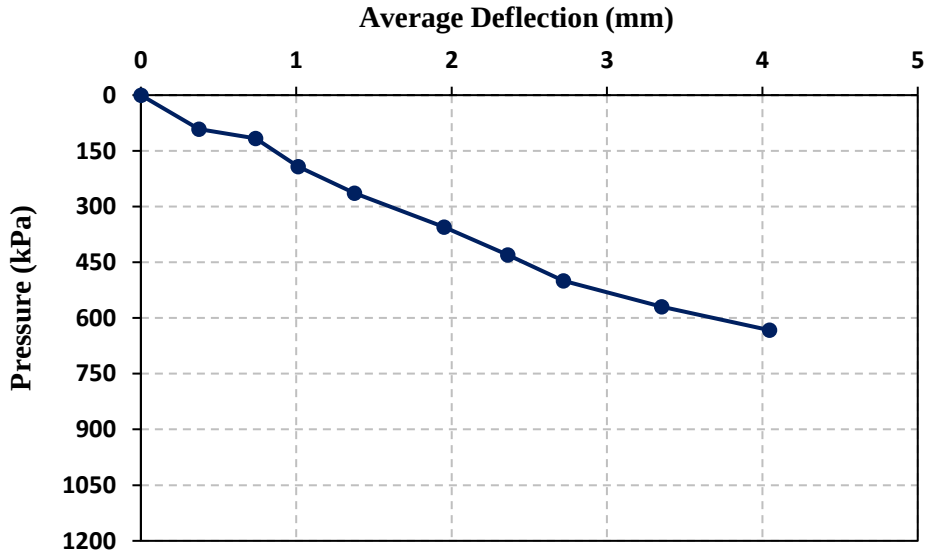

Figure (A-26) load-settlement curve of PLT tests(18 Nop) for (A-3) soil at Al-Intifada

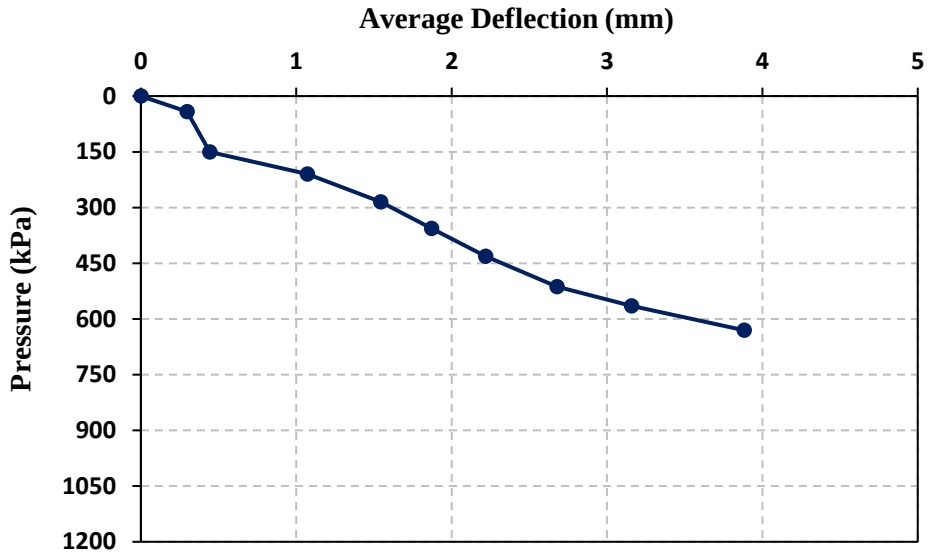

Figure (A-27) load-settlement curve of PLT tests(18 Nop) for (A-3) soil at Al-Intifada

Table (A-1) CBR calculation for Al-Tahadi

Al-Tahadi			
10 passes			
	point 1	point 2	average
A	9	7	8
B	9	9	9
C	9	9	9
14 passes			
	point 1	point 2	average
A	10	10	10
B	10	11	10.5
C	11	11	11
18passes			
	point 1	point 2	average
A	13	12	12.5
B	12	12	12
C	14	11	12.5

Table (A-2) CBR calculation for Al-Fares

Al-Fares			
10 passes			
	point 1	point 2	average
A	10	10	10
B	11	9	10
C	10	11	10.5
14 passes			
	point 1	point 2	average
A	12	13	12.5
B	12	12	12
C	12	12	12
18passes			
	point 1	point 2	average
A	14	14	14
B	13	13	13
C	13	14	13.5

Table (A-3) CBR calculation for Al-Intifada

Al-Intifada			
10 passes			
	point 1	point 2	average
A	10	10	10
B	11	10	10.5
C	10	10	10
14 passes			
	point 1	point 2	average
A	13	11	12
B	12	11	11.5
C	12	12	12
18passes			
	point 1	point 2	average
A	14	13	13.5
B	14	14	14
C	14	13	13.5

Table (A-4) DCPI calculation for Al-Tahadi

Al-Tahadi			
10 passes			
	point 1	point 2	average
A	23	29	26
B	24	24	24
C	22	24	23
14 passes			
	point 1	point 2	average
A	22	24	23
B	21	21	21
C	19	20	19.5
18passes			
	point 1	point 2	average
A	17	19	18
B	18	19	18.5
C	16	19	17.5

Table (A-5) DCPI calculation for Al-Fares

Al-Fares			
10 passes			
	point 1	point 2	average
A	21	20	20.5
B	20	22	21
C	20	20	20
14 passes			
	point 1	point 2	average
A	16	13	14.5
B	18	17	17.5
C	18	18	18
18passes			
	point 1	point 2	average
A	16	16	16
B	17	17	17
C	17	15	16

Table (A-6) DCPI calculation for Al-Intifada

Al-Intifada			
10 passes			
	point 1	point 2	average
A	20	20	20
B	20	20	20
C	20	20	20
14 passes			
	point 1	point 2	average
A	19	19	19.0
B	18	20	19.0
C	20	18	19.0
18passes			
	point 1	point 2	average
A	16	18	17
B	17	16	16.5
C	16	19	17.5

Appendix B

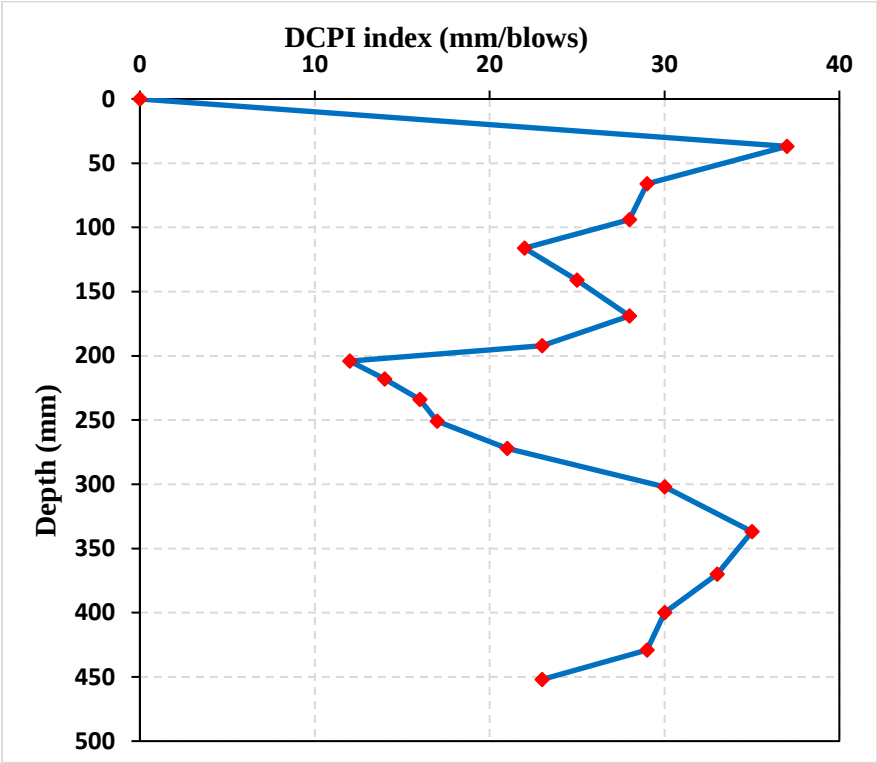

Figure (B-1) Average DCPI index curve of DCP tests(10 Nop) for (A-3) soil at Al-Tahadi

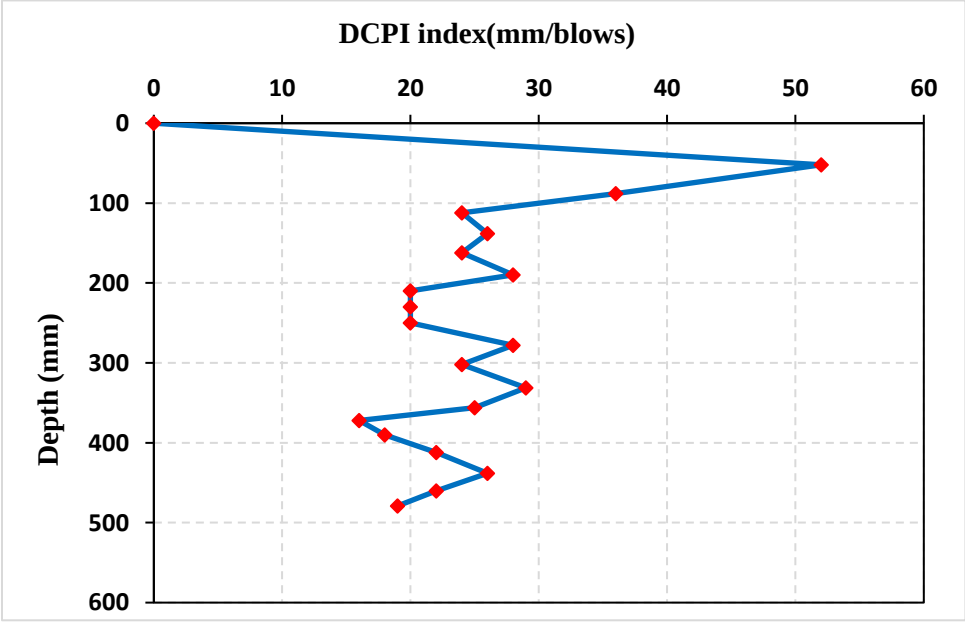

Figure (B-2) Average DCPI index curve of DCP tests(10 Nop) for (A-3) soil at Al-Tahadi

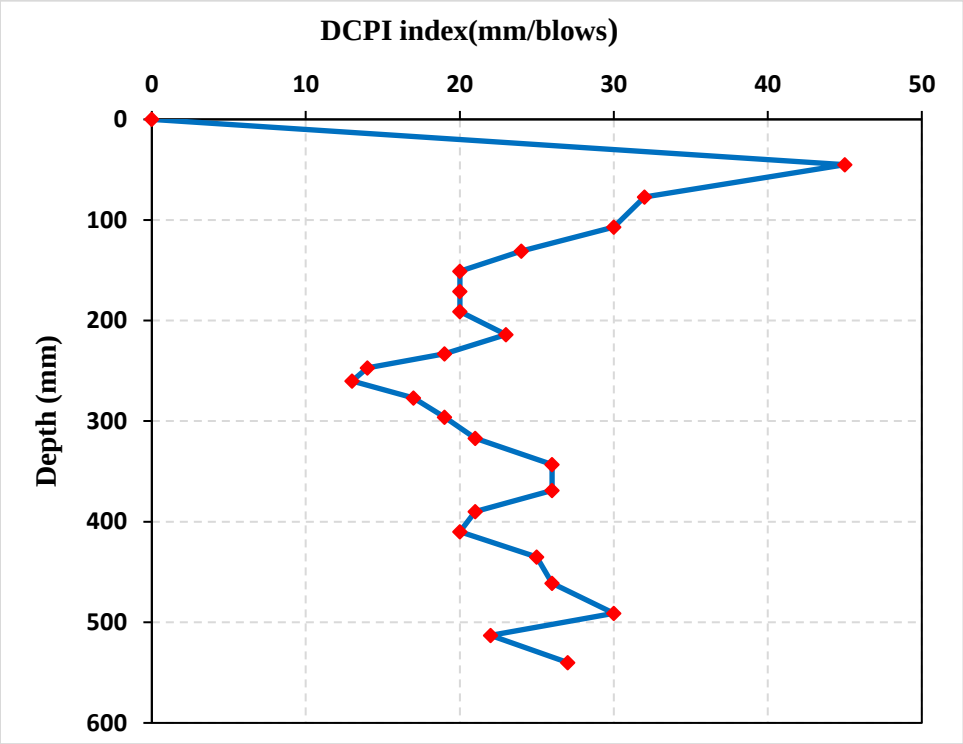

Figure (B-3) Average DCPI index curve of DCP tests(10 Nop) for (A-3) soil at Al-Tahadi

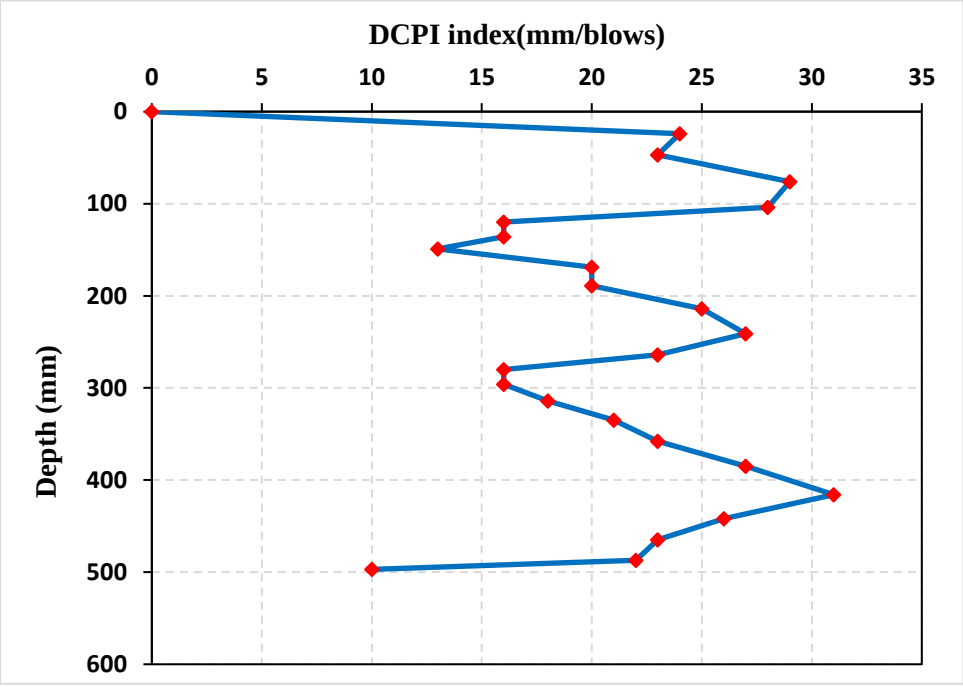

Figure (B-4) Average DCPI index curve of DCP tests(14 Nop) for (A-3) soil at Al-Tahadi

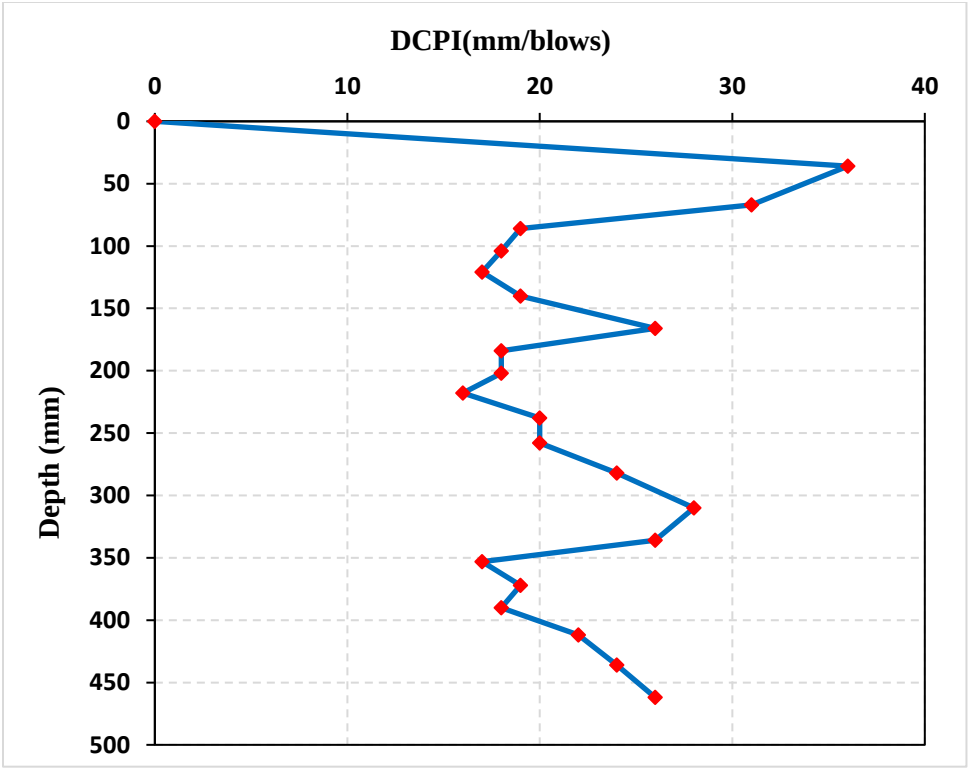

Figure (B-5) Average DCPI index curve of DCP tests(14 Nop) for (A-3) soil at Al-Tahadi

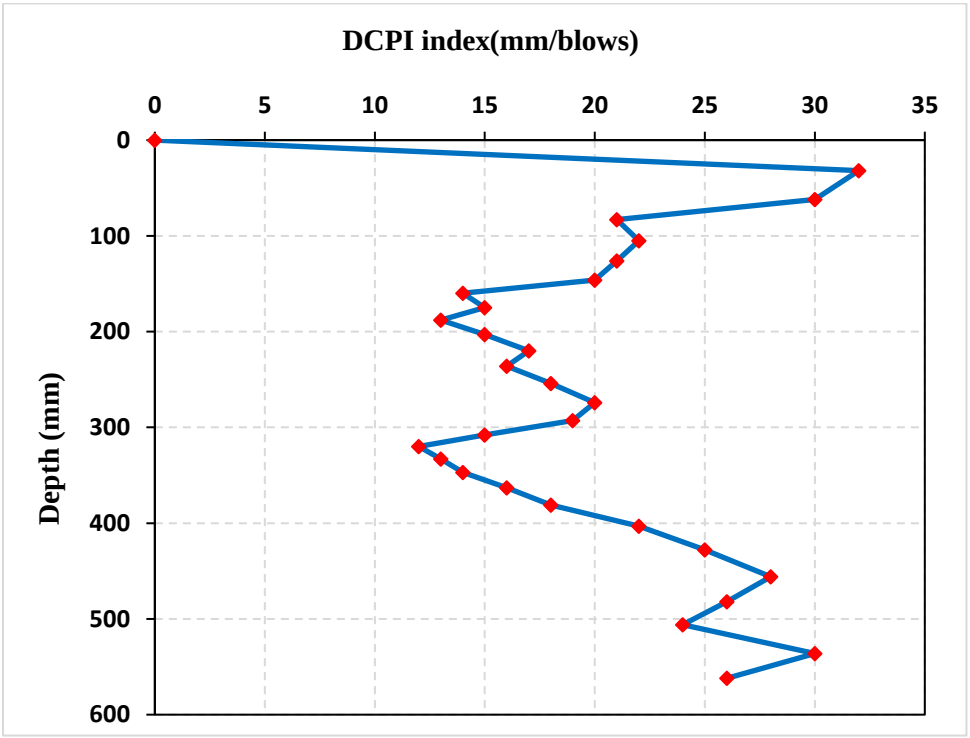

Figure (B-6) Average DCPI index curve of DCP tests(14 Nop) for (A-3) soil at Al-Tahadi

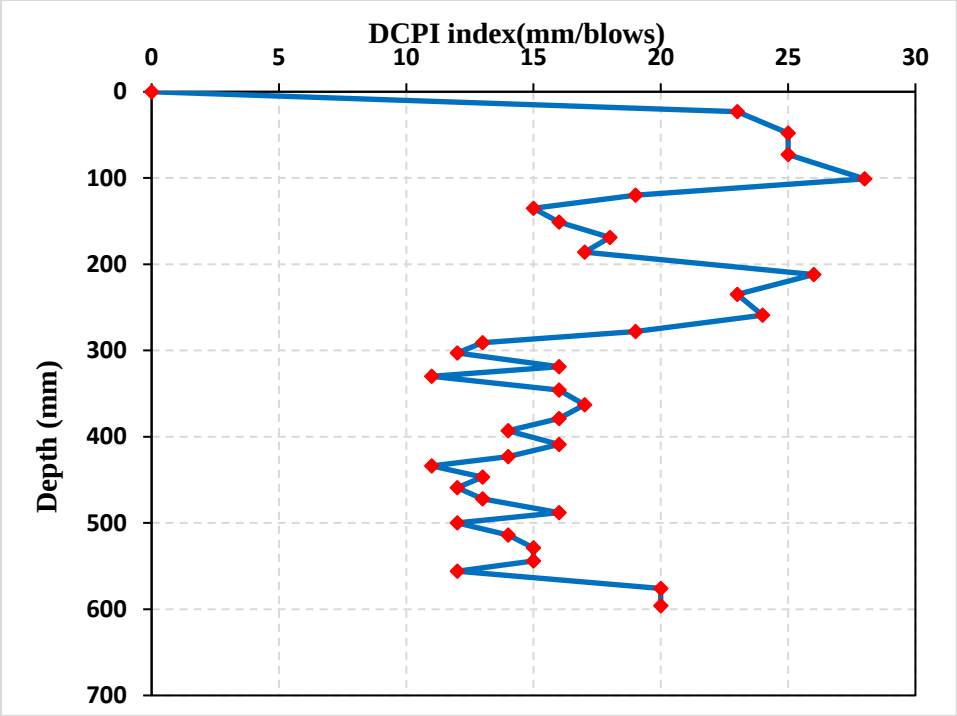

Figure (B-7) Average DCPI index curve of DCP tests(18 Nop) for (A-3) soil at Al-Tahadi

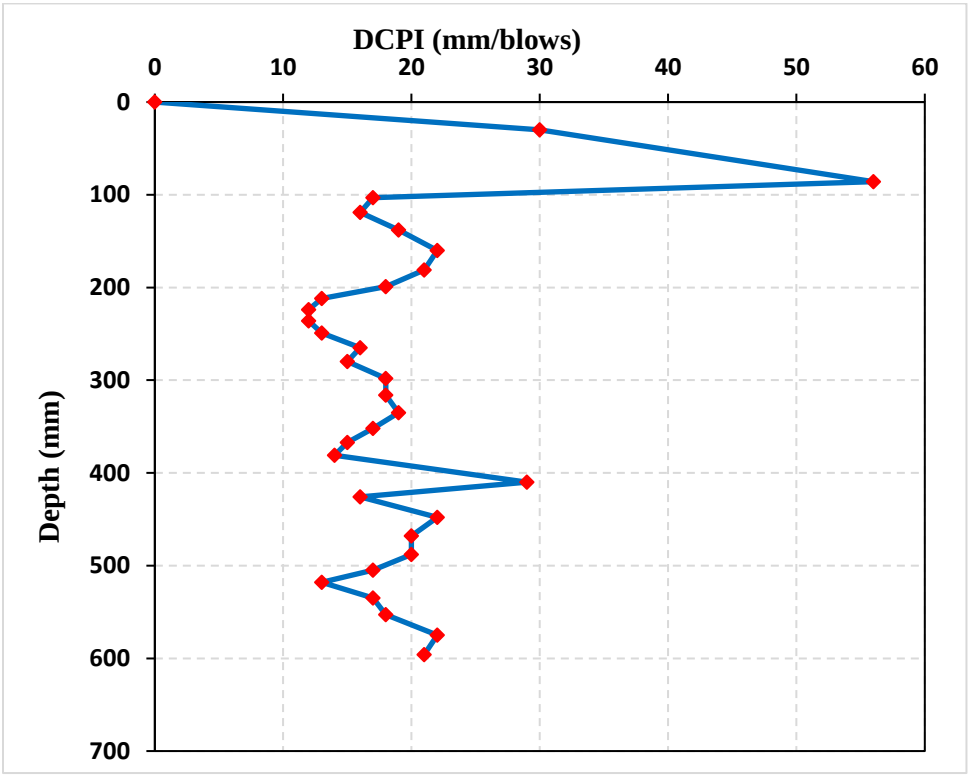

Figure (B-8) Average DCPI index curve of DCP tests(18 Nop) for (A-3) soil at Al-Tahadi

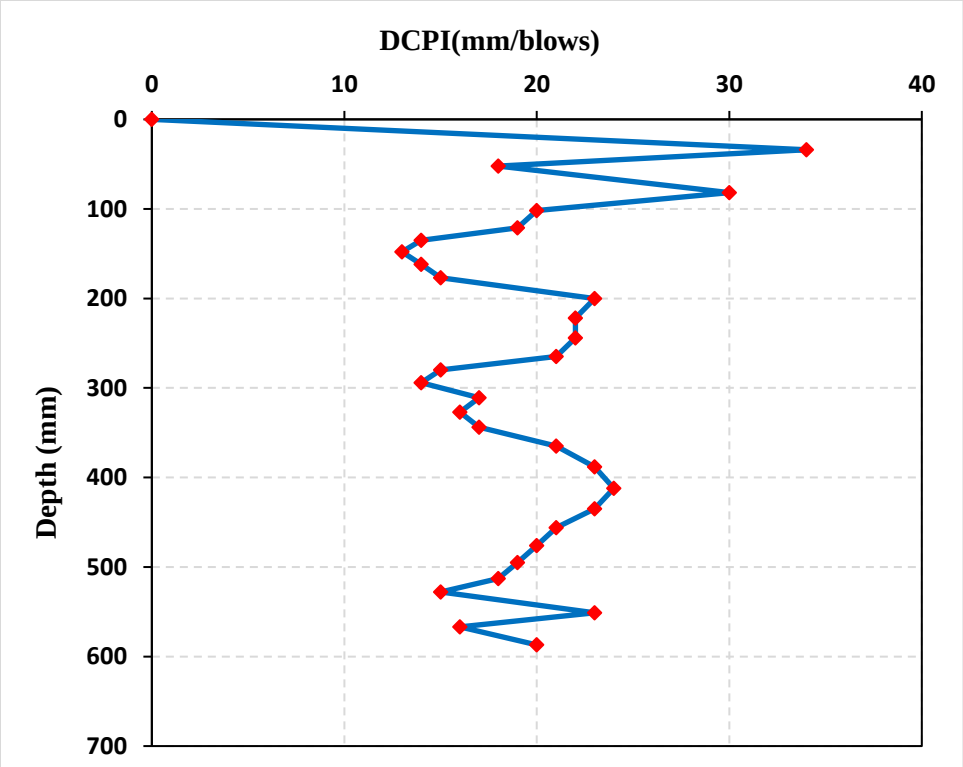

Figure (B-9) Average DCPI index curve of DCP tests(18 Nop) for (A-3) soil at Al-Tahadi

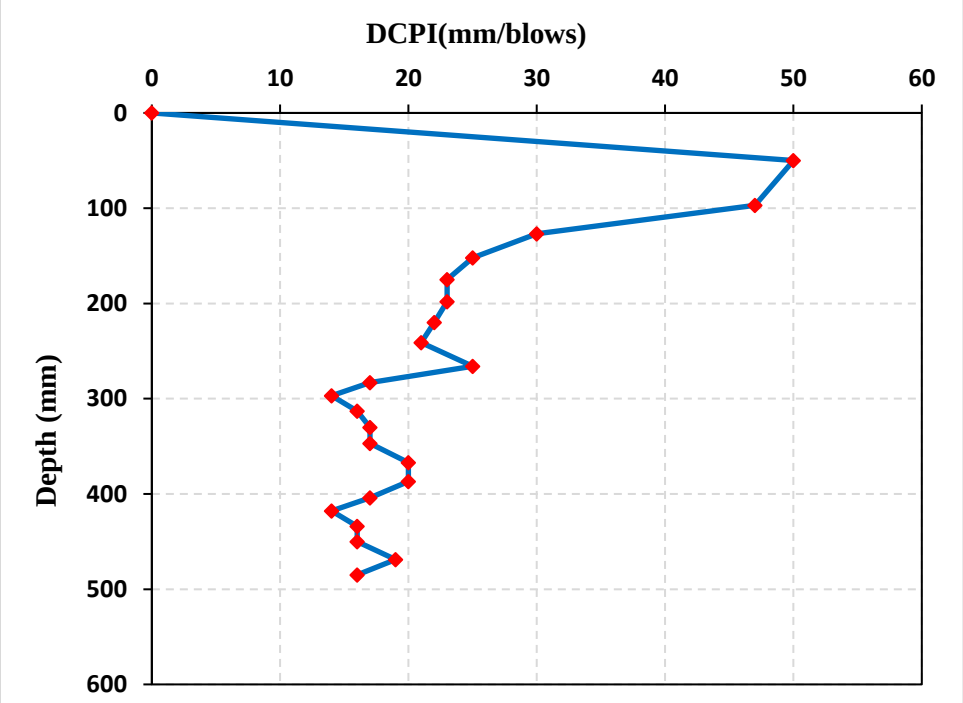

Figure (B-10) Average DCPI index curve of DCP tests(10 Nop) for (A-3) soil at Al-Fares

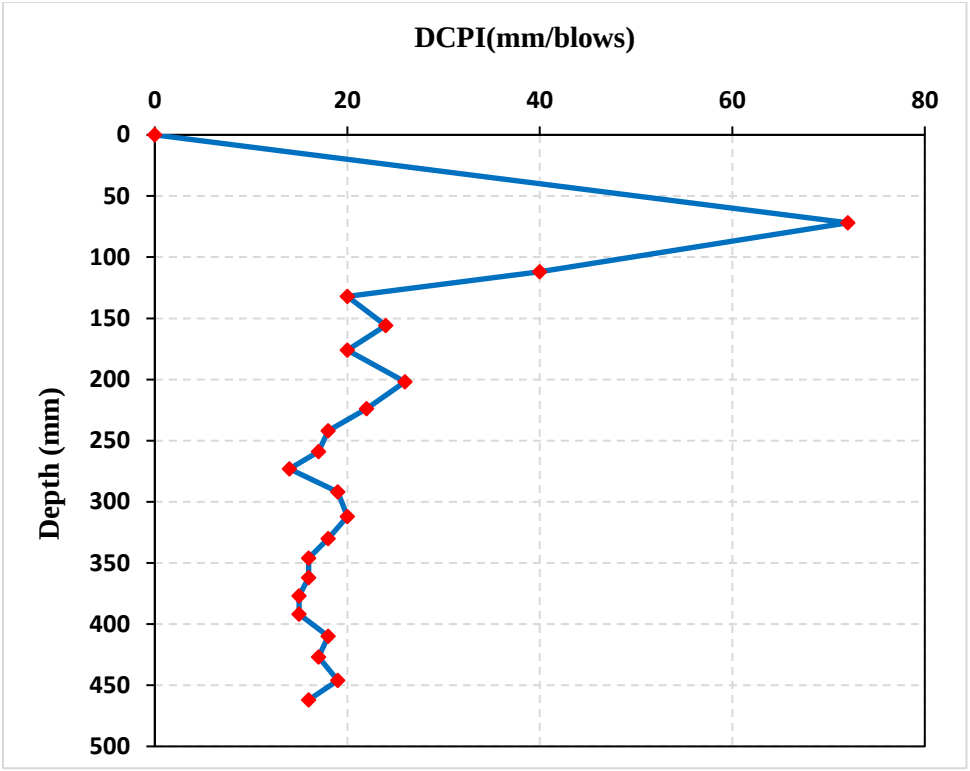

Figure (B-11) Average DCPI index curve of DCP tests(10 Nop) for (A-3) soil at Al-Fares

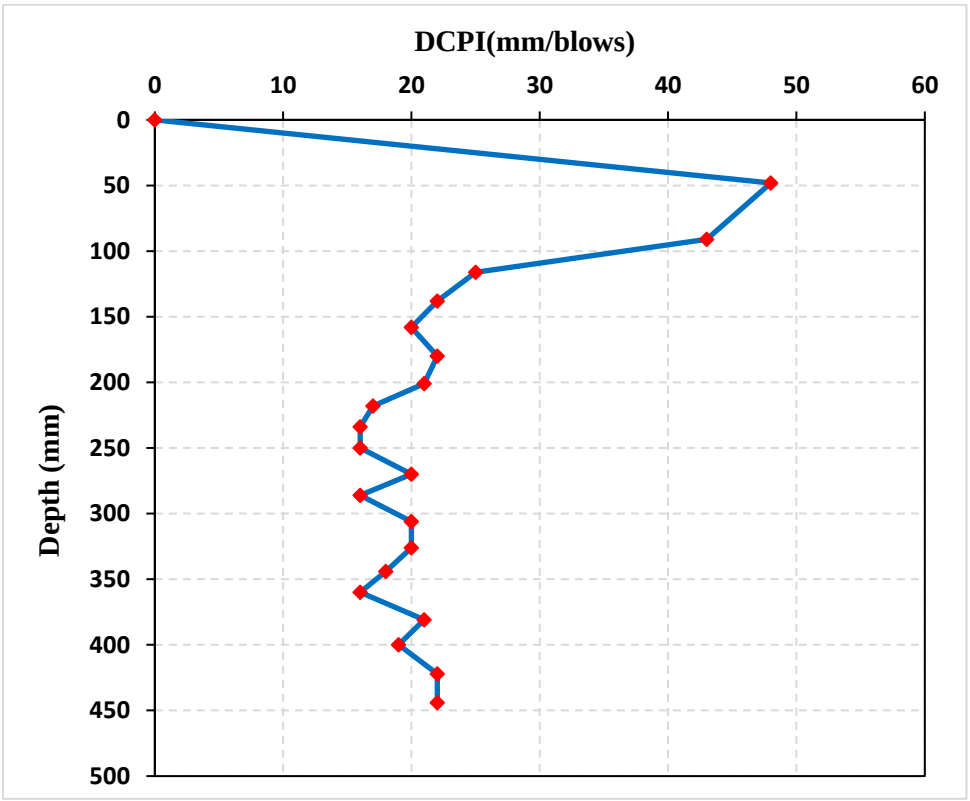

Figure (B-12) Average DCPI index curve of DCP tests(10 Nop) for (A-3) soil at Al-Fares

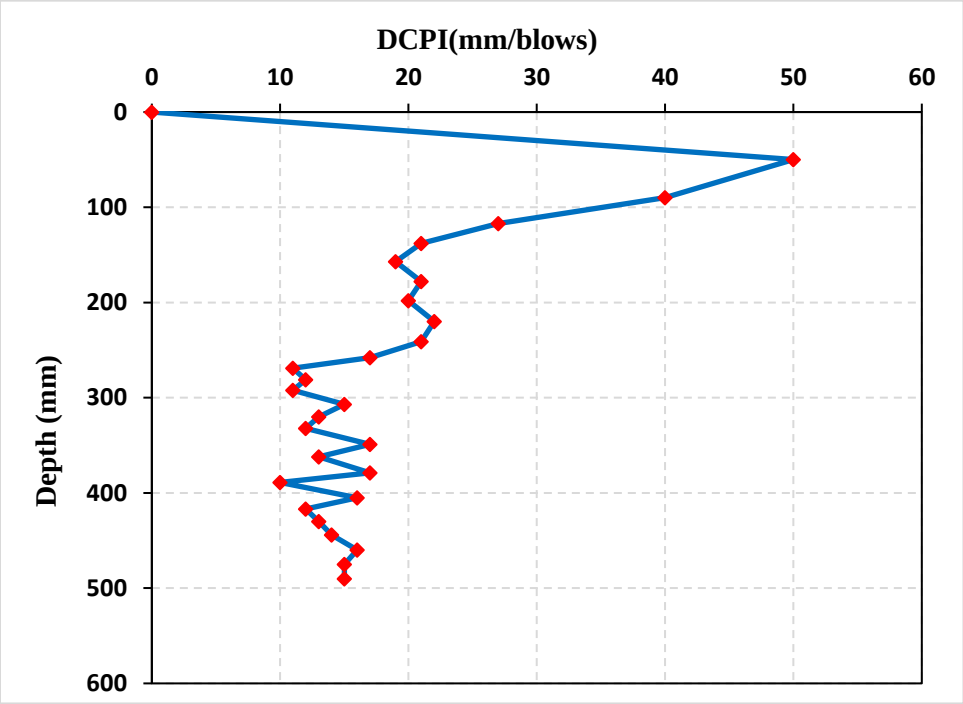

Figure (B-13) Average DCPI index curve of DCP tests(14 Nop) for (A-3) soil at Al-Fares

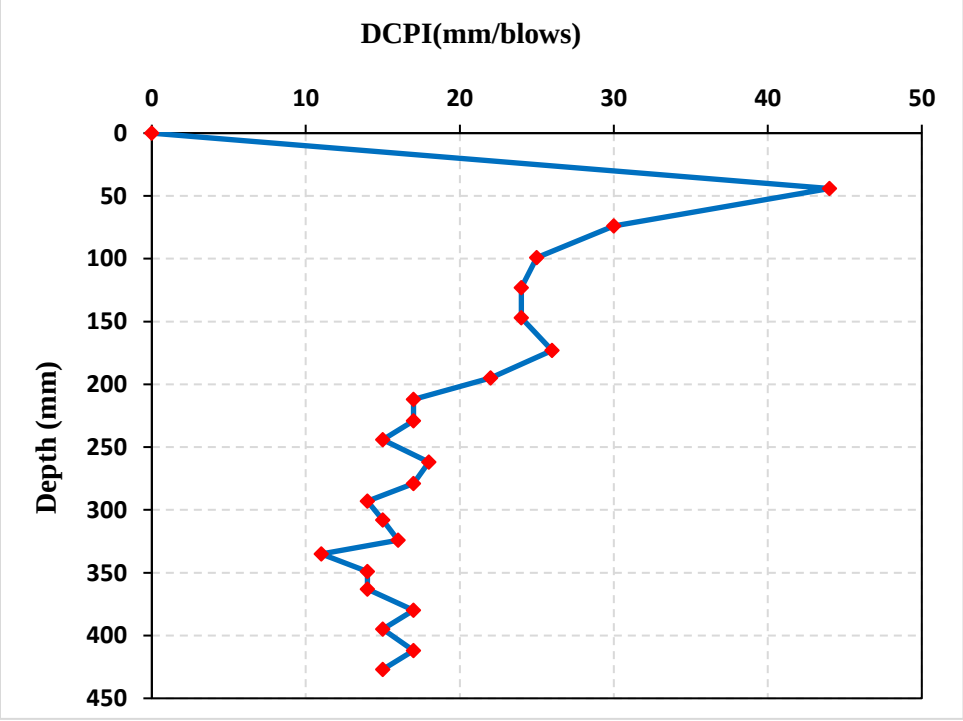

Figure (B-14) Average DCPI index curve of DCP tests(14 Nop) for (A-3) soil at Al-Fares

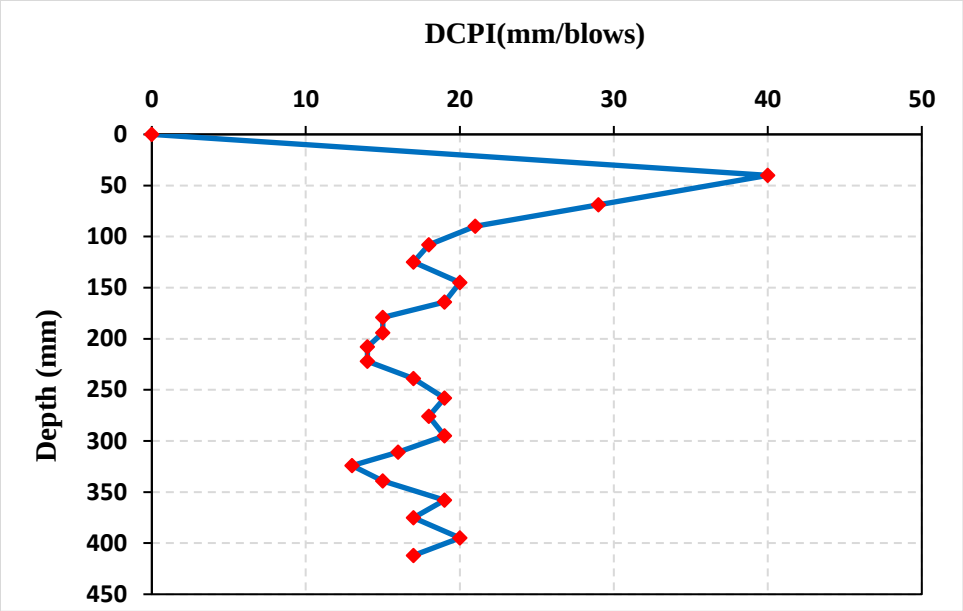

Figure (B-15) Average DCPI index curve of DCP tests(14 Nop) for (A-3) soil at Al-Fares

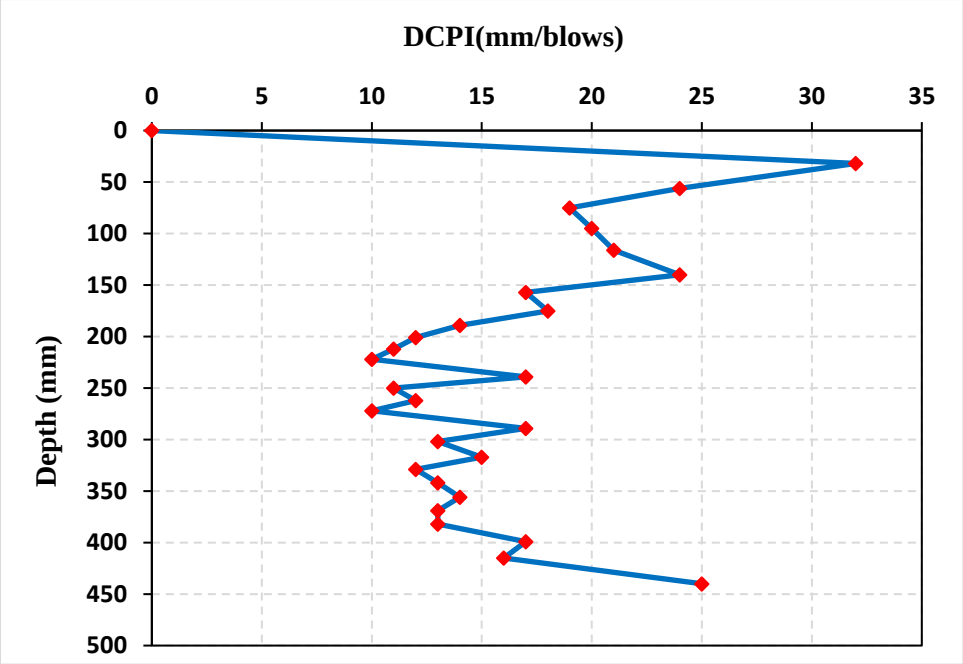

Figure (B-16) Average DCPI index curve of DCP tests(18 Nop) for (A-3) soil at Al-Fares

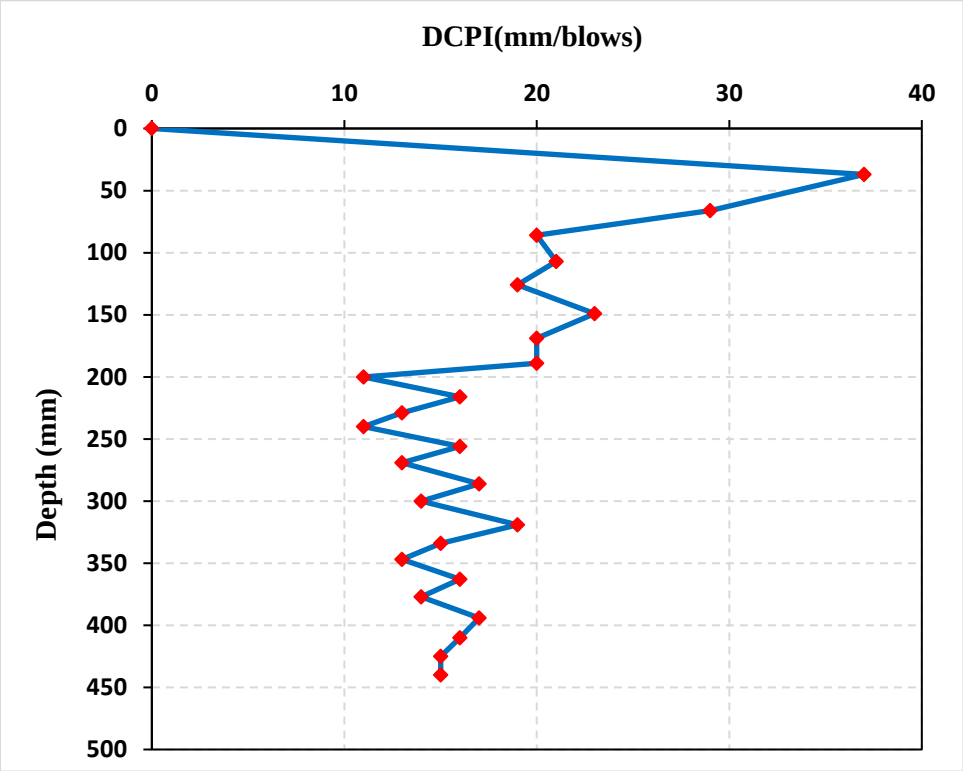

Figure (B-17) Average DCPI index curve of DCP tests(18 Nop) for (A-3) soil at Al-Fares

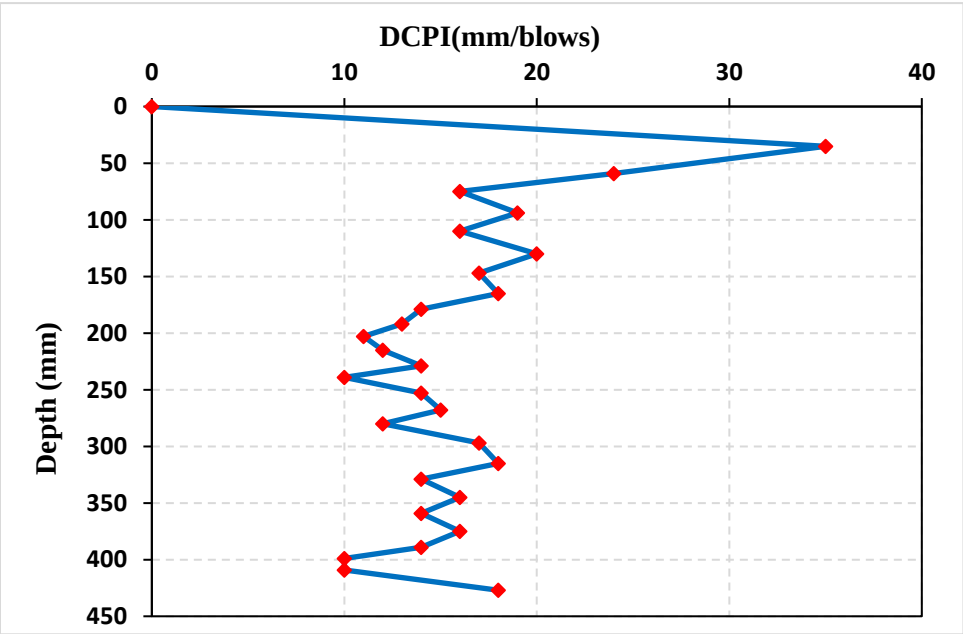

Figure (B-18) Average DCPI index curve of DCP tests(18 Nop) for (A-3) soil at Al-Fares

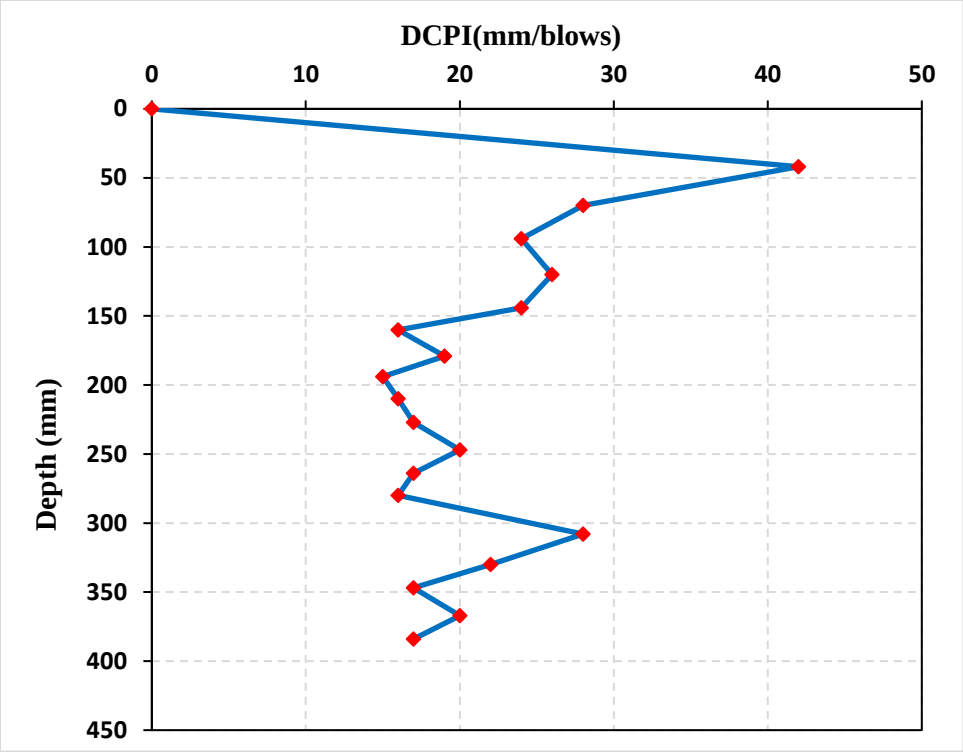

Figure (B-19) Average DCPI index curve of DCP tests(10 Nop) for (A-3) soil at Al-Intifada

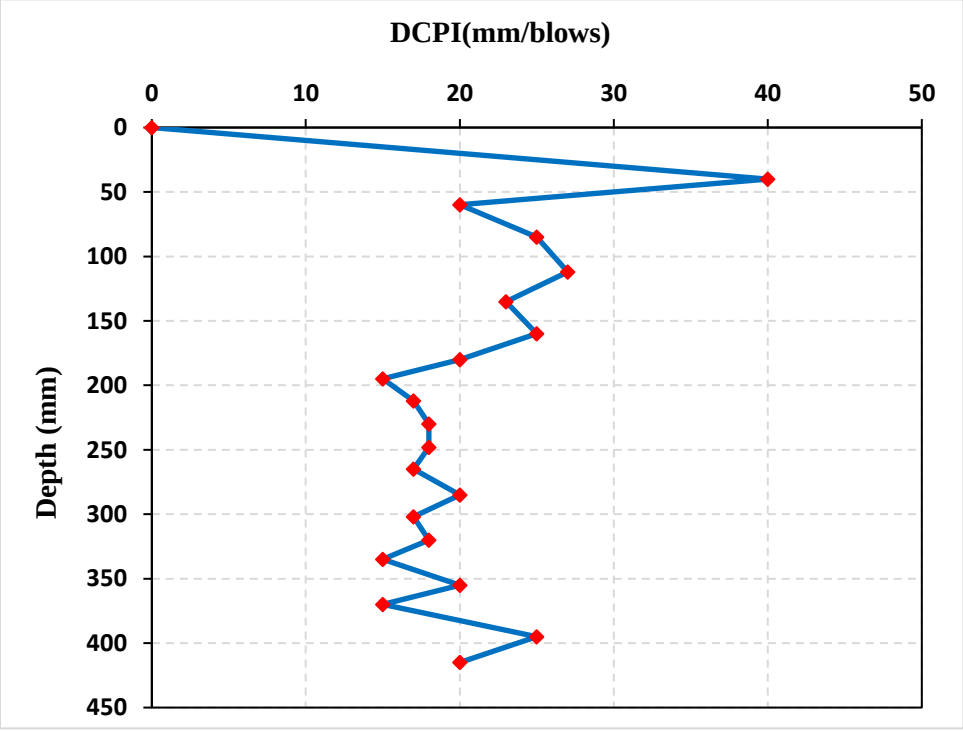

Figure (B-20) Average DCPI index curve of DCP tests(10 Nop) for (A-3) soil at Al-Intifada

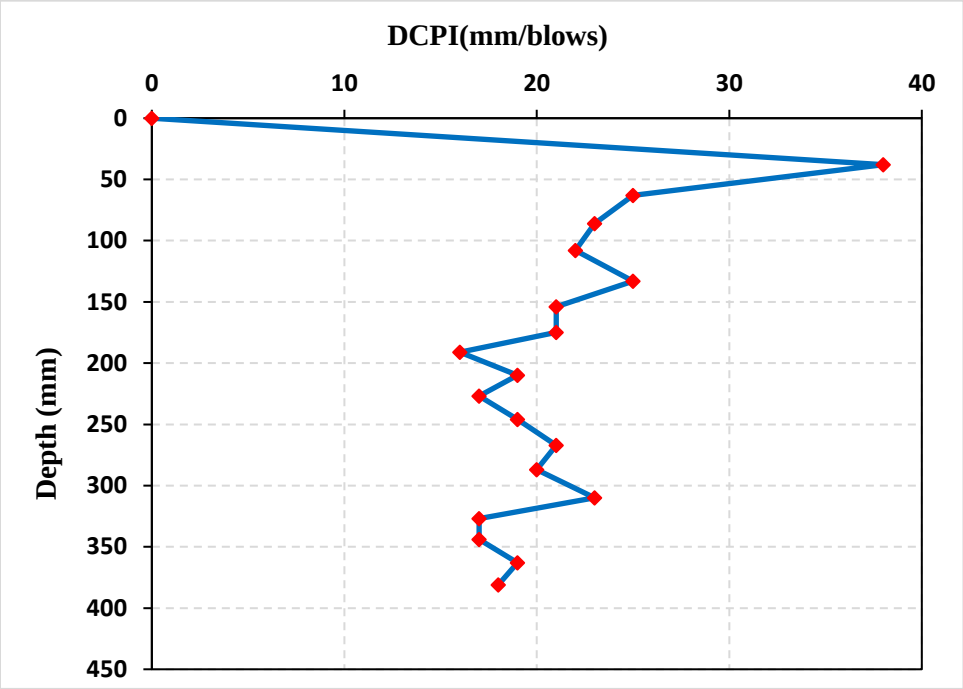

Figure (B-21) Average DCPI index curve of DCP tests(10 Nop) for (A-3) soil at Al-Intifada

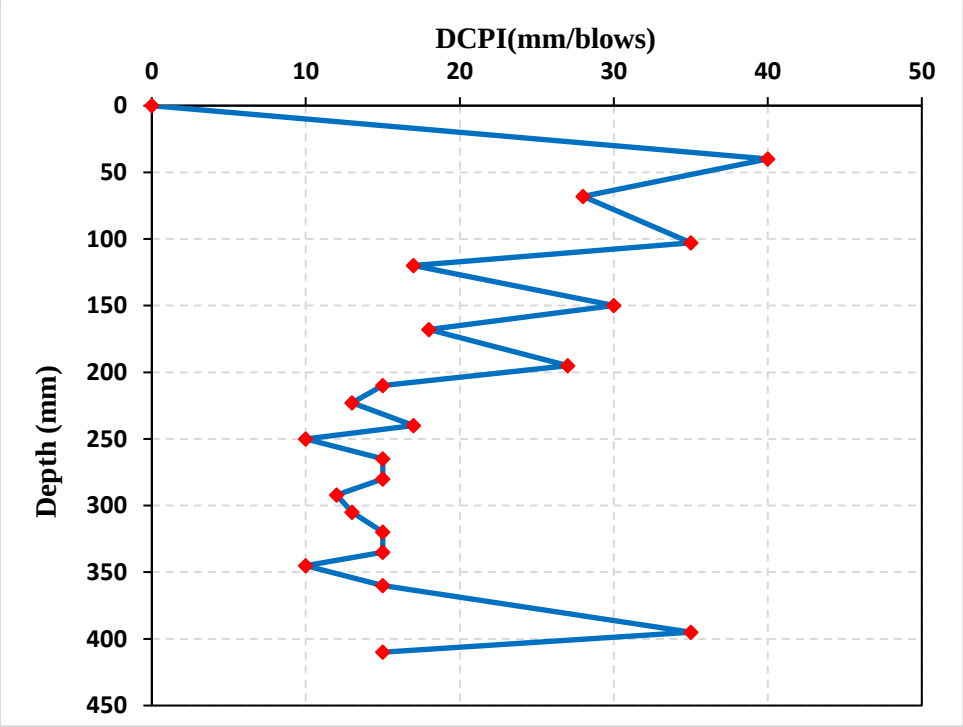

Figure (B-22) Average DCPI index curve of DCP tests(14 Nop) for (A-3) soil at Al-Intifada

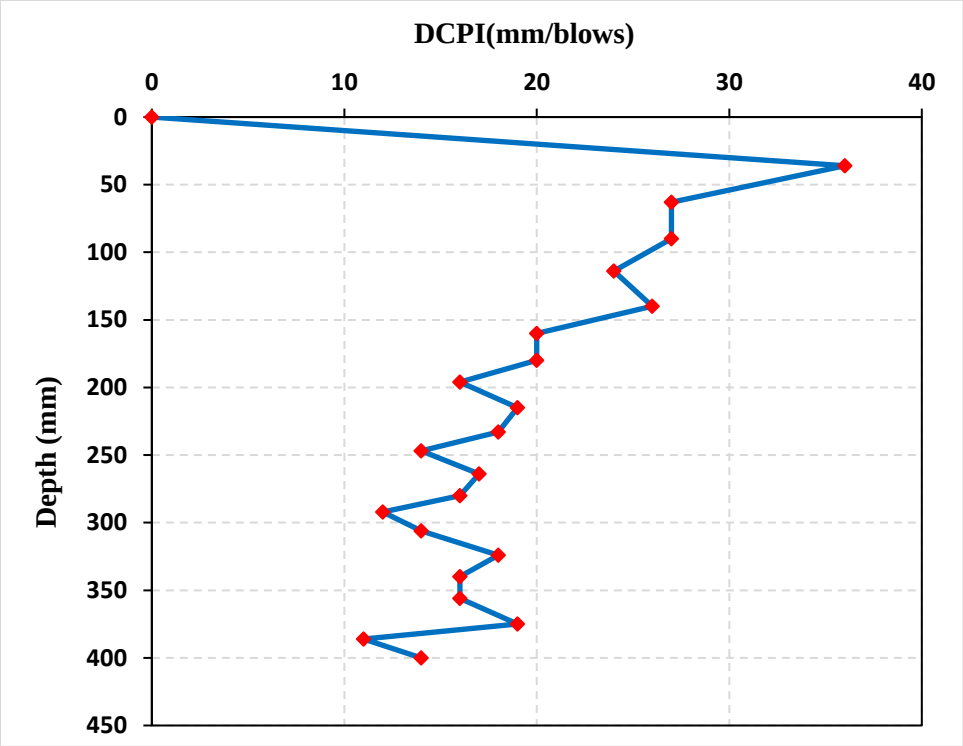

Figure (B-23) Average DCPI index curve of DCP tests(14 Nop) for (A-3) soil at Al-Intifada

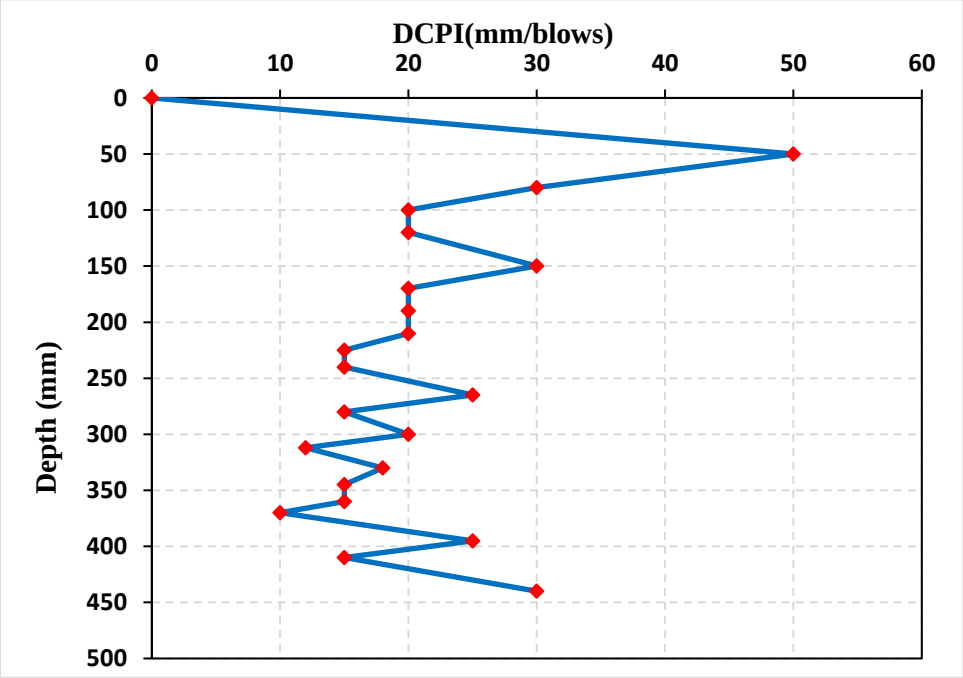

Figure (B-24) Average DCPI index curve of DCP tests(14 Nop) for (A-3) soil at Al-Intifada

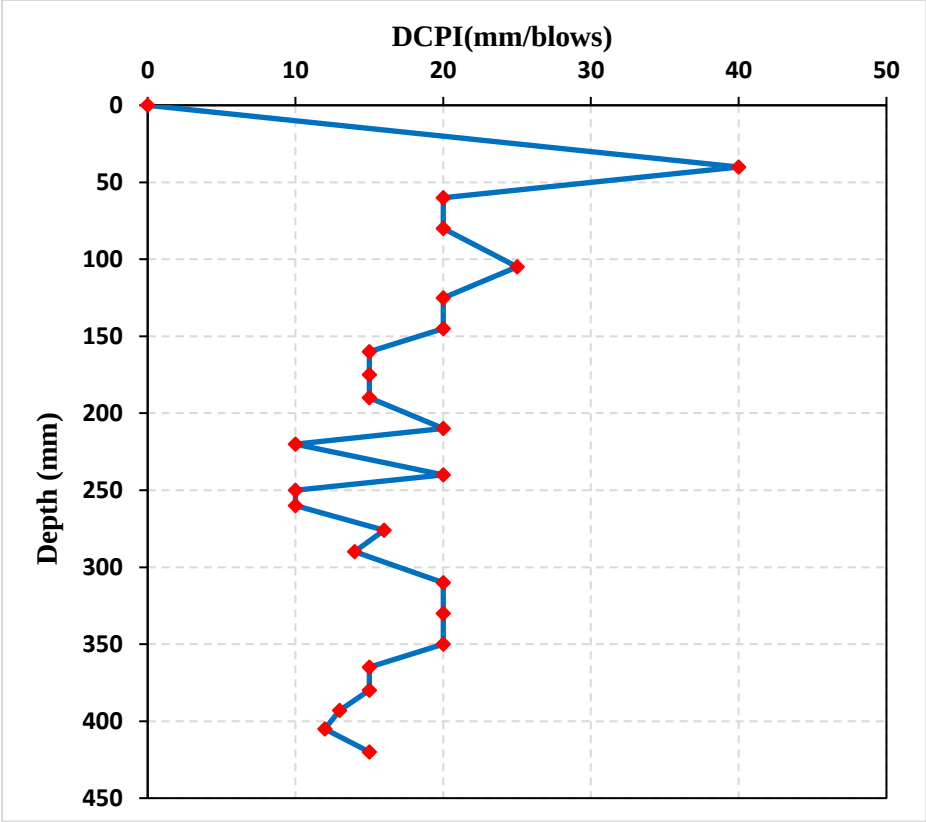

Figure (B-25) Average DCPI index curve of DCP tests(18 Nop) for (A-3) soil at Al-Intifada

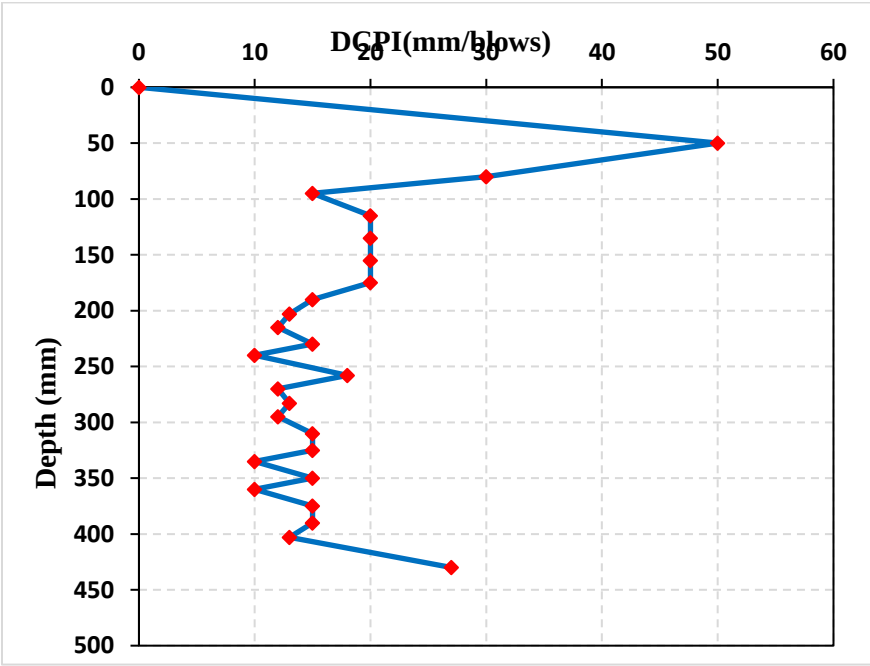

Figure (B-26) Average DCPI index curve of DCP tests(18 Nop) for (A-3) soil at Al-Intifada

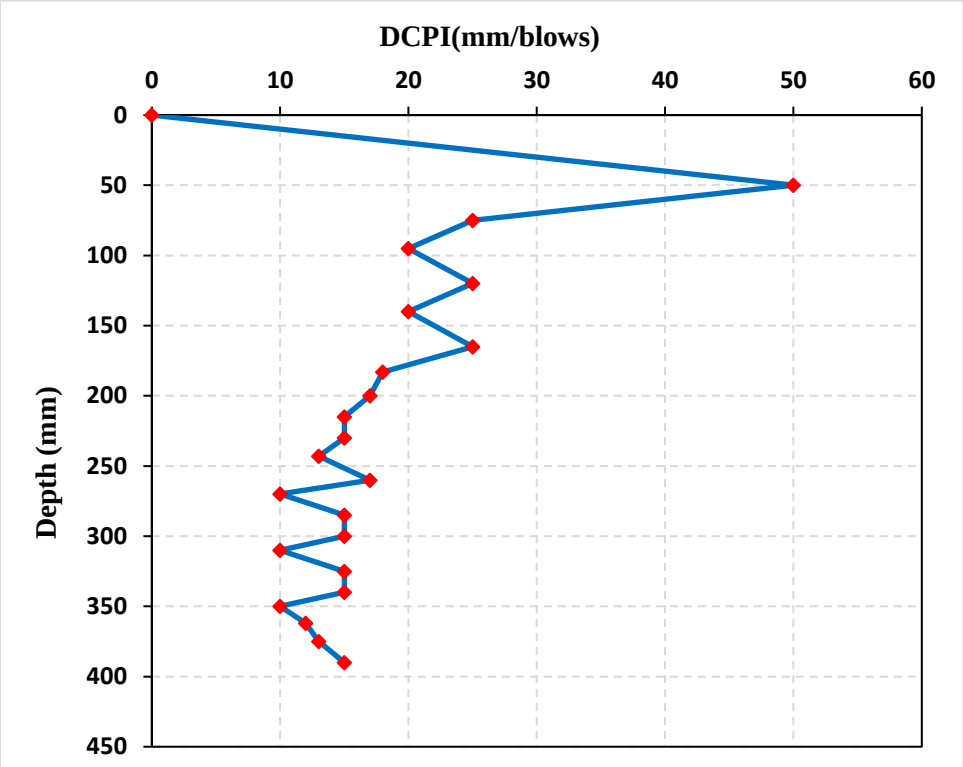

Figure (B-27) Average DCPI index curve of DCP tests(10 Nop) for (A-3) soil at Al-Intifada

الخلاصة

الرصيف الصلب عبارة عن نظام يتكون من طبقات مختلفة قادرة على مقاومة تحميل حركة المرور. ينتقل تحميل حركة المرور عبر طبقات الرصيف ثم يصل أخيرًا إلى الطبقة التحتية التي تعمل كمنصة داعمة للرصيف. تم حساب معامل تفاعل الطبقة السفلية (ks) ، الذي يميز تفاعل طبقات التربة عند تعرضها للأحمال ، باستخدام اختبار الحمل الصفيحي .(PLT) تتطلب PLT فريقًا هندسيًا متخصصًا، وتكلفة عالية ووقتًا لإجراء الاختبار. تقدم هذه الدراسة عملاً تجريبيًا ونظريًا للتنبؤ بمعامل تفاعل الطبقة التحتية للتربة الرملية من خلال تطوير نماذج إحصائية بسيطة وموثوقة بناءً على القياسات الديناميكية التي تم الحصول عليها من إجراء اختبار مقياس اختراق المخروط الديناميكي الموضعي.

ولتحقيق الهدف من هذا العمل، تم تنفيذ ثلاث تقنيات اختبار تشمل: مقياس اختراق المخروط الديناميكي(DCP) ، واختبار الحمل الصفيحي (PLT) واختبار استبدال الرمال .(SRM) تم تنفيذ هذه الاختبارات لتقييم الخصائص الهندسية الجيوتقنية للتربة الرملية الأرضية التي تم جمعها من ثلاثة مشاريع للطرق تقع في كربلاء، العراق. لتقييم تأثير عملية الحدل على أداء الدرجات الفرعية، تم أخذ ثلاثة مستويات للحدل في الاعتبار عند إعداد نموذج الاختبار المعملي باستخدام ثلاثة مستويات من الحدل(NOP) .

كانت معاملات التربة التي تم الحصول عليها من DCP هي نسبة تحمل كاليفورنيا(CBR) ، ومؤشر الاختراق (DCPI) وقدرة التحمل(q) ، في حين أن تلك التي تم تحديدها من خلال إجراء اختبار PLTتشمل: معامل تفاعل التربة، والحد الأقصى للتسوية، ومعامل مرونة يونغ. أخيرًا، تم إجراء SRM لتقييم: محتوى الرطوبة، والكثافة الجافة، ودرجة الضغط.

أظهرت نتائج العمل التجريبي أن أعلى قيمة لدرجة الحدل بلغت (98.85٪) لـ (18 NOP) وأقل قيمة (87.43٪) لـ (10 NOP) ، وتراوحت قيم ks من 135 إلى 230 كيلو باسكال. / مم ، تراوحت قيمة DCPIمن 14.5 إلى 26 مم / ضربة ، وتراوحت CBR من 8 إلى 13.5 ٪ ، وتراوحت q من 105.45 إلى 149.42 كيلو باسكال. تم تحليل هذه النتائج إحصائيًا وربطها ببعضها البعض للعثور على أفضل نموذج انحدار مناسب للتنبؤ بـks .

تم تصنيف النماذج الإحصائية إلى ثلاث مجموعات: المجموعة الأولى: نماذج تعتمد على قياسات DCP، المجموعة الثانية: نماذج تعتمد على خصائص التربة الأساسية، المجموعة الثالثة: نماذج تعتمد على DCP

وخصائص التربة الأساسية. أظهرت نتائج التحليل الإحصائي أنه يمكن التنبؤ بـ k بناءً على قياسات DCP وقياسات الخصائص الفيزيائية (DC، Cc، Cu) مع تربيع R كبير يساوي 88 ٪. أثبت اكتشاف التحليل الإحصائي أنه يمكن استخدام أجهزة DCP كأداة لا إتلافيه لتقييم معامل تفاعل الطبقة التحتية بسرعة وبدقة.

جمهورية العراق
وزارة التعليم العالي
والبحث العلمي
جامعة كربلاء
كلية الهندسة
قسم الهندسة المدنية

تقييم جهاز فحص الاختراق الديناميكي المحمول في تحديد معامل رد فعل التربة المرن للترب الرملية

رسالة مقدمة إلى

كلية الهندسة في جامعة كربلاء - قسم الهندسة المدنية كجزء من متطلبات نيل درجة الماجستير في علوم الهندسة المدنية

من قبل

ليث علي سالم

(بكالوريوس هندسة مدنية – جامعة كربلاء – 2017)

إشراف

أ.م. د. علاء محمد جواد

أ.م. د. رائد رحمان المحنة

2022 م **1443 هـ**